The valorisation of paper sludge for green composite material

by

Anderson Chimphango

Thesis presented in partial fulfilment
of the requirements for the Degree

of

MASTER OF ENGINEERING
(CHEMICAL ENGINEERING)

in the Faculty of Engineering
at Stellenbosch University

Supervisor

Prof. Johann Görgens

Co-Supervisor/s

Dr Luvuyo Tyhoda

March 2020

DECLARATION

By submitting this thesis electronically, I declare that the entirety of the work contained therein is my own, original work, that I am the sole author thereof (save to the extent explicitly otherwise stated), that reproduction and publication thereof by Stellenbosch University will not infringe any third party rights and that I have not previously in its entirety or in part submitted it for obtaining any qualification.

Date: *March 2020*

Plagiarism decleration

1. Plagiarism is the use of ideas, material and other intellectual property of another's work and to present is as my own.

2. I agree that plagiarism is a punishable offence because it constitutes theft.

3. I also understand that direct translations are plagiarism.

4. Accordingly all quotations and contributions from any source whatsoever (including the internet) have been cited fully. I understand that the reproduction of text without quotation marks (even when the source is cited) is plagiarism.

5. I declare that the work contained in this assignment, except where otherwise stated, is my original work and that I have not previously (in its entirety or in part) submitted it for grading in this module/assignment or another module/assignment.

Initials and surname: A Chimphango

Date: March 2020

Abstract

The South African pulp and paper industry generates about 500 000 wet tons of paper sludge (PS) per annum with the traditional means of waste disposal being landfilling. Increased efforts have been put forward to develop alternative use for paper sludge. Paper sludge (PS) contains short cellulose fibres that could be developed into construction material and limit the need for virgin fibres. This study investigates the feasibility of utilising PS as feedstock in the production of composite boards that are lightweight, durable, and more environmentally friendly and of comparable quality with industry wood based composites. In order to account for inevitable variability of PS, samples were collected from recycled fibre (RN-PS), corrugated recycle fibre (CR-PS) and virgin fibre (VP-PS) pulping mills in South Africa. In the study, the boards were produced by a combination of PS, magnesium-based phosphate cement, prepared with heavy magnesium oxide (MgO) and monopotassium phosphate (KH_2PO_4) as binder, and binder replacement filler, which included silica fume, fly ash and calcium carbonate. Subsequently, the physical and mechanical properties including modulus of elasticity (MOE), modulus of rupture (MOR), water absorption (WA), thickness swelling (TS) and volume swelling (VS) were determined.

A response surface methodology (RSM) was used to establish a relationship between the responses and variables, from which optimum conditions for improving board properties were predicted. For the RN-PS, the optimum process conditions were fibre: Inorganic binder ratio, 1.94; binder ratio (KH_2PO_4: MgO), 5.07; filler (% of binder), 20%; temperature 180°C. For CR-PS, fibre: Inorganic binder ratio, 1.94; binder ratio (KH_2PO_4: MgO), 5.07; filler (% of binder), 22.5%; temperature, 90°C. For VP-PS, fibre: Inorganic binder, 1.94; binder ratio (KH_2PO_4: MgO), 5.05, filler (% of binder), 15%, temperature, 25°C. Experimental testing revealed that the composite boards only met the minimum requirements for physical properties for cement bonded particleboard (EN 634-2:2007) and particle board according to the international standard (ISO 16893: (ISO 106893:2016, 2016)). The composite boards produce had medium to high density (0.98-1.01 g/cm^3) that could be used for non-structural interior finishes with no load bearing capabilities.

The optimum conditions and experimental procedure was then used to develop an economic model to simulate the manufacturing of the composite boards. Key economic indicators such as payback period (PBP), internal rate of return (IRR), and net-present value (NPV) were used to evaluate economic viability for each of the PS process, a combined scenario with all PS

feeding to a central location (Combined scenario). The results show that Combined scenario proved to be the more profitable scenario's with minimum required selling price (MRSP)'s R 157.10 /board approximately less than the average wholesale selling price of R155/board with an IRR of 20%.. Furthermore, the RN-PS scenario had the worst profitability among the PS scenarios with an MRSP of R248.4/board above the average market selling price of R155/board making it unfeasible. High OPEX cost combined with low volume throughput (9 093 m3/year) made RN-PS process economically unattractive. Sensitivy analysis showed that decreasing feedstock cost resulted in MRSP below average market except for the RN-PS scenario. It was concluded that the only the Combined scenarios was deemed to be economically viable option.

OPSOMMING

Die Suid-Afrikaanse pulp-en-papier industrie genereer omtrent 500 000 nat ton papierslyk (PS) per jaar met die tradisionele metode van afvalverwydering, wat grondopvulling is. Verhoogde pogings is voorgestel om alternatiewe gebruike van papierslyk te ontwikkel. PS bevat kort sellulose vesels wat ontwikkel kan word in konstruksiemateriaal en die noodsaaklikheid vir rou vesels beperk. Hierdie studie ondersoek die uitvoerbaarheid daarvan om PS as voermateriaal te gebruik in die produksie van saamgestelde planke wat liggewig, duursaam, meer omgewingsvriendelik is en van vergelykbare kwaliteit met industrie hout-gebaseerde samestellings. Om rekening te hou van onvermydelike veranderlikheid van PS, is steekproewe gekollekteer van herwinde vesel (RN-PS), geriffelde herwinde vesel (CR-PS) en rou vesel (VP-PS) papiermeule in Suid-Afrika. In die studie, is die planke geproduseer deur ’n kombinasie van PS, magnesium-gebaseerde fosfaatsement, voorberei met swaar magnesiumoksied (MgO) en monokaliumfosfaat (KH_2PO_40) as binder, en binder vervanging vuller, wat silikadamp, stofas en kalsiumkarbonaat insluit. Vervolgens is die fisiese en meganiese eienskappe insluitend modulus van elastisiteit (MOE), modulus van barsting (MOR), waterabsorpsie (WA), dikte swelling (TS) en volume swelling (VS) bepaal.

’n Respons oppervlak metodologie (RSM) is gebruik om ’n verhouding tussen die respons en veranderlikes te vestig, waarvan optimum kondisies vir verbetering van plankeienskappe voorspel is. Vir die RN-PS is die optimum kondisies vesel:anorganiese binderratio, 1.94; binderratio (KH_2PO_4): MgO), 5.07; vuller (% van binder) 20%; temperatuur 180 °C. Vir CR-PS: vesel:anorganiese binderratio, 1.94; binderratio, 5.07; vuller 22.5% van binder; temperatuur, 90 °C. Vir VP-PS: vesel:anorganiese binderratio, 1.94; binderratio, 5.05; vuller, 15% van binder, en temperatuur, 25 °C. Eksperimentele toetse het aangetoon dat die saamgestelde planke slegs die minimum vereistes behaal vir fisiese eienskappe van sement-verbinde-partikelplank (EN 634-2:2007) en partikelplank volgens die internasionale standaard (ISO 16893: (ISO 106893:2016, 2016)) . Die saamgestelde planke geproduseer het medium tot hoë digtheid (0.98–1.01 g/cm^3) gehad wat gebruik kan word vir nie-strukturele interieure afrondings met geen dramuurvermoë nie.

Die optimum kondisies en eksperimentele prosedure is toe gebruik om ’n ekonomiese model te onwikkel om die vervaardiging van die saamgestelde planke te simuleer. Sleutel ekonomiese indikators soos terugverdientyd (PBP), interne opbrengskoers (IRR), en netto huidige waarde (NPV) is gebruik om ekonomiese lewensvatbaarheid vir elk van die PS-prosesse te evalueer,

asook ’n gekombineerde scenario met al die PS wat na ’n sentrale plek voer (Gekombineerde scenario).

Die resultate het aangetoon dat die gekombineerde scenario bewys is om die mees winsgewende scenario’s te wees met minimum vereiste verkoopspryse (MRSP) ongeveer minder as die gemiddelde netto huidige verkoopsprys van R155/plank met IRR van 20%. Verder, die RN-PS-scenario’s het die swakste winsgewendheid gehad van al die PS scenarios met ’n MRSP meer as dubbeld die gemiddelde markverkoopsprys van R155/plank, wat dit onuitvoerbaar maak. Hoë OPEX-koste gekombineerd met lae volume deursit (9 093 m^3/jaar) maak RN-PS-proses ekonomies onaantreklik.Daar is tot die gevolgtrekking gekom dat die gekombineerde scenario’s beskou is as ekonomies lewensvatbaar.

Acknowledgments

I would like first of all thank our Heavenly Father, Lord Jesus Christ who has blessed and carried me through this journey.

I would like to thank the following people, for their contribution to this study:

- Dr Tyhoda and Prof Johann Görgens for your guidance through the project as well as the opportunity.
- Paper Manufacturers Association of South Africa (PAMSA) in conjuction with Kimberly-Clark (Pty) as the industry partner. The opinions, findings, conclusions and recommnedations made are that of the author and not necessarily attributed to the sponspors.
- Dr Amiandamhen and wood science research group for your support and assistance.
- Colleagues and friends at the Department of Process Engineering.
- Mr. Henry Solomon for your assistance in lab work.
- My dad (Samson), mom (Annie), brother (Kidney), sisters (Tawina and Madalitso), niece (Priscilla) and nephew (Jayson) for their unconditional love, encouragement, support and prayer during this period.
- To my fiancée (Ms Jacqueline Mosalisa) for all the love and support. I am forever grateful.
- To friends and members of Pinelands Presbyterian church who have prayed for and with me during this time period. Thank you for your support.

Contents

List of figures

List of tables

List of acronyms and abbreviations

Abbreviation	Abbreviated Word
$CaCO_3$	Calcium Carbonate
CCD	Central Composite Design
CR-PS	Corrugated Recycle Paper Sludge
DEA	Department of Environmental Affairs
DW	Dry weight
FTIR	Fourier transform infrared spectrometry
GDP	Gross Domestic Product
HPLC	High performance liquid chromatography
IRR	Internal rate of return
KH_2PO_4	Monopotassium Phosphate
Mar	Minimum acceptable rate of return
MgO	Magnesium Oxide
MOE	Modulus of Elasticity
MOR	Modulus of Rapture
MRSP	Minimum Required Selling Price
NPV	Net Present Value
PS	Paper Sludge
PAMSA	Paper Making Association of South Africa
PBP	Pay-Back-Period
PCA	Principle Component Analysis
RN-PS	Recycled Newsprint - Paper Sludge
RSM	Response Surface Methodology
SA	South Africa
TS	Thickness Swelling
VP-PS	Virgin Pine – Paper Sludge
VS	Volume Swelling
WA	Water Absorption
WHC	Water holding capacity
w/w	Weight per weight

Chapter 1. Introduction

1.1 **Background and context**

Rapid industrialization and urbanization are common in developing countries such as South Africa (SA), and are associated with improved living standards of people. As a result, the industry produces more industrial and domestic waste to meet the increased product demand (Bethlehem and Goldblat, 1997; Troschinetz and Mihelcic, 2009). The World Bank (2018) estimates that the current global waste generation is estimated at 2.01 billion tonnes per year of solid waste in 2016, and is predicted to increase by 70% by 2025 (World Bank, 2018). In SA, the Department of Environmental Affairs (2012)estimates that approximately 90% of the total waste produced (108 million tonnes of waste) in 2011 was being landfilled. The SA government embarked on initiatives to discourage the use of landfills by increasing legislation and landfilling taxes (Monte *et al.*, 2009). In 2017, Operation Phakisa (2017) reported that the amount of industrial waste disposed in landfills had decreased to 75% of the total waste produced (111 million tonnes) due to the government's increased initiatives..

The Department of Environmental Affairs (2012) estimates that the paper and package industry contributes approximately 35% of the total production of waste. The waste produced by the paper and package industry consist of ash, pulping wastes, wood wastes and sludge. Even though landfillings is the most common disposal methods, it presents a major concern to the environment such as release of hazardous chemical to ground water and the release of greenhouse gasses as the decay of organic waste proceeds (Monte *et al.*, 2009). In addition landfilling takes up a lot of space that is already in short supply, thus, competes with residential and recreational demands. Furthermore, operating landfills is becoming more expensive and cumbersome due to high transport costs arising from the bulkiness of PS and high moisture content and government regulations. Müller (2018) reports that as of August 2019, the DEA's waste management and classification regulation, that governs the handling of hazardous and general waste, is no longer permitting the landfilling of materials with a moisture content above 40%. The aforementioned problem have resulted in studies such as Soucy et al. (2004) and others that investigate the valorisation of PS into other industrial products, which would be a beneficial way to either reuse or recycle the PS.

Organization such as the Paper Manufacturers Association of South Africa (PAMSA) represents 90% of the paper, packaging and tissue manufacturers in SA and have made considerable effort to reduce landfilling depending on available technologies at the mill

(PAMSA, 2016). According to PAMSA (2016), companies such as Kimberly-Clark of South Africa (Pty) Ltd have reduced waste disposed via landfills by 95.6%, Sappi (Pty) Ltd have had a reduction of 12.4% of waste landfilled, while Mpact is already invested in converting PS to compost and concrete block making (Mpact, 2016; PAMSA, 2016). Alternative methods that are technically and economically sustainable for handling and disposing PS are required due to problems associated with landfilling.

In recent times, various alternative options in the handling of solid waste (such as PS) in the pulp and paper industry such as incineration, pyrolysis and bioethanol production have been investigated (Monte *et al.*, 2009; Boshoff, 2015; Williams, 2017). Incineration is advantageous since it reduces amount of material to be landfilled by burning away majority of organic matter, but in doing so, it produces dangerous air pollutants (NOx and SO_2) from direct heat source. The disadvantage of incineration is that it is an expensive process to install and operate because it requires biomass material to be dried in order to be effective and environmentally unfriendly due emission of toxic gases.. Unlike incineration, pyrolysis involves the breaking down of material via non-burning (indirect heat) of PS material, into products such as gases, tars and heavy/light oils, however, it still produces air emissions. Bio-ethanol production has also been investigated as a possible option in the handling of PS but due to high viscosity in PS, mass transfer was limited and therefore limiting the production of the bioethanol (Monte *et al.*, 2009; Boshoff, 2015; Ridout, 2016)

Developing countries such as SA are experiencing an increase in their population and urbanization. As a result, there is an increase in demand for low cost and sustainable building materials such as particle boards, fibre boards and cement boards from the construction industry (Population matters, 2013). The greater demand for raw materials in the construction industry are leading to depletion of natural resources (Ruuska and Häkkinen, 2014). As a result, there is need to move towards the valorisation of industrial waste into usable products to conserve the natural resources (Arancon *et al.*, 2013). A potential process route for valorisation of the waste would be to channel PS into wood bio-composite manufacturing.

The PS has the potential to be a valuable resource for manufacturing of composites boards, due to its fibrous nature (Geng *et al.*, 2007a; Donahue and Aro, 2010; Migneault, A Koubaa, Riedl, Hamid Nadji, *et al.*, 2011). PS composition includes organic matter in the form of degraded wood fibres, a type of lignocellulosic material that mainly contains cellulose and hemicellulose, and the inorganic materials such as kaolin, $CaCO_3$, pitch (wood resin), lignin residue and ash.

The cellulosic content mainly comprises of short fibres, and low quantities of lignin, making it a promising feedstock for recycling because of the valuable potential to utilise the lignocellulosic fraction (Liaw *et al.*, 1998; Geng *et al.*, 2007a; Kuokkanen *et al.*, 2008; Ochoa de Alda, 2008).

A major drawback of using PS is the high moisture content and the variability in composition. These variability and higher moisture content could adversely influence the feasibility of producing composite boards from PS. Therefore there is a need to consider applications for PS with varying properties, in particular, to investigate their effect on composite board performances and therefore optimize process conditions that may address the aforementioned challenges. Furthermore, there is limited information, if any, on the technical and economic feasibility of the production of composite boards from PS, and whether such boards are able to compete with traditional fibreboards or cement-bonded boards, which have been successfully applied in automotive, furniture and construction industry.

1.2 Thesis layout

The thesis is divided into four sections. Chapter 1 presents the background and context of the research. Chapter 2 reviews the literature concerning the production of bio-composite boards utilising industrial residues and the potential implication of using PS and its influence on the functional properties of the composite boards. Chapter 3 presents the experimental section of the study, which focuses on analysing the effects of the independent variables, thus, finding which of the independent variables namely the fibre/resin ratio (fibre: resin), binder ratio and the filler content would significantly influence the mechanical and physical performances of the manufactured boards such as modulus of elasticity (MOE), modulus of rapture (MOR), water absorption(WA), thickness swelling (TS), volume swelling(VS), and Density. Furthermore, the chapter looks at how the variability in the physio-chemical composition of the paper influences the functional properties of the bio-composite panels. Chapter 4 presents the techno-economic process modelling and answers the question, what is the techno-economic feasibility of manufacturing composite products from PS on an industrial scale? Chapter 5 provides a summary of the main conclusions and recommendations of the project.

Chapter 2. Literature review

2.1 **Background of paper sludge**

The pulp and paper industry is one of the largest agro processing sectors in South Africa with an estimated contribution to the country's gross domestic product (GDP) of 0.6% (R 38 Billion) in 2015 (PAMSA, 2016). The industry utilises lignocellulosic biomass such as wood and recycled fibre to produce products such as pulp, paper, tissue, boards and other cellulose-based products.

The pulp and paper industry generates different types of waste material such as lime, mud, grits, ash, residual processed wood and sludge collected from different parts of their pulp and paper manufacturing process (Monte, et al., 2008). The paper making, recycling and de-inking processes require large amounts of water and agitation, in order to pulp raw materials (softwood or hardwood) into a pulp slurry of potential fibres (Bajpai, 2011). Valuable fibres are then extracted from the slurry and sent through for further processing to make valuable commercial products. The remaining slurry containing solid waste is sent through for waste management processing, where common techniques used to purify and treat the effluent slurry, such as sedimentation, biological chemical precipitation, flotation and anaerobic treatment as reported by Hagelqvist (2013), are used to separate effluent water stream from the solid waste. The effluent stream collected is then sent for water purification processes and is either recycled back into the pulping process or appropriately disposed through the municipality water system. The solid waste collected is referred to as sludge and is typically sent to the landfill(Hagelqvist, 2013).

In the pulp and paper industry, 45 kg of primary PS is produced for every ton of product made, which equates approximately 4.5% of the product produced (Son et al., 2004). Different types of sludges are generated depending on the purification technique used. In general, pulp and paper mills first utilise physical treatment namely sedimentation, clarifiers or air flotation to remove part of the suspended solid (sludge) from the effluent stream, which is specifically referred to as Primary sludge (Soucy *et al.*, 2014). The primary sludge consist of cellulose (degraded short fibres), hemicellulose, lignin and other inorganic materials such as fines, bark, additives, lime slaker grits, wood processing residuals and furnace ash (Soucy & Migneault, 2014; Monte, et al., 2008). The remaining stream usually still needs further purification through biological or secondary treatment in order to meet government regulations before being disposed of (Ochoa de Alda, 2008). The suspended solid (sludge) released at this stage is

referred to as secondary sludge. As a result of the bacteria ability to trap water, researcher have found that secondary sludge contains less fibrous material and more water compared to primary sludge. For the purpose of this project, PS hereafter refers to primary sludge and not secondary sludge, nor a mixture of primary and secondary sludges. Primary sludge is known to have the longest fibres, which makes it an ideal candidate to convert it into usable products such as construction material (Geng *et al.*, 2007a).

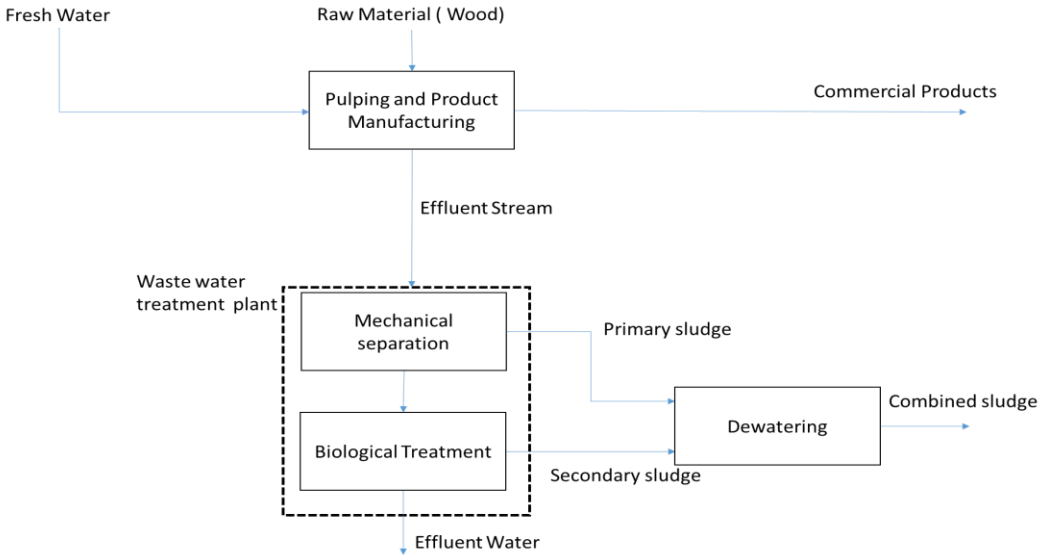

Figure 2-1: Schematic overview of primary and secondary sludge production (Adapted from Taramian et al., 2007and Migneault *et al.*, 2011)

2.2 **Characterization of paper sludge**

In this section, the characterization of PS is discussed with respect to physical and chemical properties, which is dependent on the technology used to pulp wood, the type of feed utilised and the type of effluent treatment employed before disposal of sludge (Geng et al., 2007b; Monte *et al.*, 2009). The physical and chemical characteristics of sludge have the potential to make certain PS samples more suitable for composite board production than others.

2.2.1 Pulping process

The pulping process is used to convert wood source material to cellulose rich pulp, which is one of the main component of pulp and paper products. Various pulping processes are utilised at different mills, depending on the nature of the targeted product at the mill. Mechanical methods include mechanical pulping and stone ground wood, and can sometimes be heated and called chemo-thermomechanical where chemicals are also, thermomechanical and thermo-mechanical pulps (Mabee, 2001).

The purpose of mechanical pulping (MP) is to separate fibre from raw material into individual fibres and fibre fragments, and maintain as much lignin to extract acceptable strength properties, however, this process is prone to discolouration and ageing (Bajpai, 2012). In order to improve the strength properties, heating methods are used in combination with mechanical methods, which is then commonly referred to as thermomechanical pulping (TMP) (Bajpai, 2012). TMP can be used to make newspaper and furnisher in tissue, printing and paperboards but it is only suited for softwood material rather than hardwood material. Chemical pulping methods that are also heated are referred to as chemo-thermomechanical (CTMP) and are suitable for both hardwood and softwood in producing acceptable pulp strength properties. Typical CTMP chemicals used to produce pulp with superior strength properties to MP include sodium sulphite and carbonate (Montgomery, 2005).

In recent times, purely chemical pulping methods are more efficient process routes and preferred method in industry to produce high quality pulp to make products such as white paper (Mabee, 2001). Chemical methods involve the cooking of raw material utilising chemicals such as alkaline or acids to breaking down lignin bonds and releasing fibres. Kraft pulping uses sulphate and is one of the more efficient process route for industry because it can be used in all wood-based raw materials (Mabee, 2001). Other chemical pulping processes include a sulphite process, which is commonly referred to as Neutral Sulphite Semi Chemical (NSSC). It can sometimes be combined with a mechanical method, but is considered not as strong as the Kraft process (Bajpai, 2012).

In South Africa, the majority of the pulp and paper mills operate using de-inking or re-pulping process with few exceptions opting for Kraft, NSSC and mechanical pulping, as shown in Table 2-1. The Re-pulping process consist of pulping waste paper through mechanical and chemical methods, and using recovered fibres to produce certain types of products such as boxes and tissue (Bajpai, 2012). The one major drawback of this process is need to remove coatings, laminations and even printing inks from the recycled material, to avoid damage to sensitive equipment. Deinking pulping is useful to remove printing ink from wastepaper such as newspaper in order to reuse recovered valuable fibres to make products such as paperboards (Bajpai, 2012).

Table 2-1: Paper sludge production at the different mills in South Africa according to Boshoff, 2015

Mills	Pulping process	Production of PS (dry tons per annum)	Moisture Content (%)
Kimberly-Clarke: Enstra	RP, DI	6 000	54
Nampak: Bellville	RP, DI	1 800	54
Nampak: Kliprivier	RP, DI	1 500	60
Nampak: Verulam	RP, DI	1 500	57
Sappi: Enstra	RP	7 500	71
Mondi: Richardsbay	RP, K	12 500	64
Mpact: Felixton	RP	4 000	73
Mpact: Springs	RP,DI	11 000	80
Mpact: Piet Retief	RP	500	70
Sappi: Tugela	NSSC	7 000	85
Sappi: Ngodwana	K, MP	15 000	80

Note: Pulping process: RP – Re-pulping, DI – De-inking, K- Kraft, NSSC – Neutral Sulphite Semi Chemical, MP – Mechanical pulping
Note: As of 2015, Nampak is now called Twinsaver. Sappi mills such as Saiccor and Stanger were not included in the previous study of Boshoff et al., 2015.

Sludge from re-pulping and de-inking pulp and paper mills that used recycle fibre newsprint and virgin pulp (RN-PS) produced sludge that had high ash content (approx. 60%) and therefore low cellulose fibres. Re-pulping and de-inking pulp and paper mills that used corrugated recycle fibre and virgin pulp (CR-PS) produced sludge that contained lower ash content (approx. 40%) and higher cellulose content (approx. 24%) than RN mills as a result of difference in feed materials. Mills that pulp virgin wood (VP mills) generally produced products such as dissolved pulp and chemical unbleached pulp via mechanical and Kraft pulp (Eucalyptus and Pine). The PS from VP mills generally contain the lowest ash content (approx.

20%) and highest cellulose (approx. 36%) content compared to sludge from RN mills and CR mills (Boshoff, 2015; Williams, 2017).

2.2.2 Chemical properties

Paper sludge (PS) consist of organic and inorganic components. The organic component includes lignocellulose material such as cellulose, hemicellulose and lignin. The inorganic component is made up of ash, kaolinite (clay), calcium carbonate (paper additives) and heavy metals such as Pb, Zn, and Cu from wood raw material and waste soluble ink (Kuokkanen *et al*., 2008 and Boshoff, 2015).

2.2.2.1 *Organic component*

A matrix of micro fibrils of cellulose with hemicellulose and lignin produces lignocellulose materials. The chemical composition of cellulose, hemicellulose and lignin typically found in South Africa paper and pulp mills is shown in Table 2-2.

Due to the presence of strong hydrogen bonds formed among the multiple hydroxyl groups, high structural-strength complex fibres are formed within cellulose micro fibrils (Isikgor & Becer, 2015). The strength of the fibre within the lignocellulosic material forms the backbone of the bio-composite. Along the plant cell wall, the hemicellulose component consists of a matrix of branched polysaccharides, which also forms short fibrous materials (Isikgor & Becer, 2015). The lignin component comprises of cross-linked phenolic polymers found in cell walls and acts like natural occurring binding agents between fibres (Isikgor & Becer, 2015). This has the potential to enhance the possibility of PS producing fibreboards due to the adhesive capabilities of lignin component (Migneault, Ahmed Koubaa, *et al.*, 2011).

Table 2-2: Average lignocellulosic composition of paper sludge from different mills in South Africa (Adapted from Boshoff, 2015)

Paper mills	Cellulose (%)	Hemicellulose (%)	Lignin (%)	Extractive (%)	Ash (%)
Kimberly-Clark: Enstra	19	7	10	4	60
Nampark: Bellville	21	10	7	5	57
Nampak: Kliprivier	21	10	16	6	47
Nampak: Verulam	20	8	5	3	64
Sappi: Enstra	41	8	13	8	30
Mondi: Richardsbay	25	11	19	5	40
Mpact: Felixton	38	15	19	7	21
Mpact: Springs	45	12	15	6	22
Mpact: Piet Retief	38	17	24	6	15
Sappi: Tugela	35	12	24	11	18
Sappi: Ngodwana	50	19	13	8	10

From Table 2-2 it is shown that PS from the mills using recycled printing material as feeds had the lowest amount of valuable fibres (cellulose) and the highest amounts of ash, while virgin pulp produced the highest amount of valuable fibre and the lowest amount of ash in PS (Boshoff, 2015). The low fibre content in mills that use recycled printing material could be because there is fibre degradation during the re-pulping. It is also observed that the sludge composition between different mills was significantly different (Table 2-2) and this could be attributed to the different pulping process and feeds used. Chemical pulping removes majority of the hemicellulose and lignin, and therefore produces sludge with low content of these. As is the case with sludge from re-pulping and de-inking process such Kimberly-Clark: Enstra, Nampark: Bellville, Nampak: Kliprivier and Nampak: Verulama generally have high ash content and low cellulose content as is shown in (Table 2-2). Mechanical type pulping rarely affect the composition of the lignocellulosic and therefore resulting PS having similar composition to the mills feed. This is the case with Sappi: Ngodwana, which has the highest amount of cellulosic components and closest chemical composition to virgin feed (Boshoff, 2015). It is highly advantageous to utilise PS with high levels of cellulose and low levels of ash as a feedstock for composite manufacturing, because cellulose forms the main structure of the composite and the ash may interfere with the interaction between fibre and binders.

Furthermore, natural binding abilities of lignin could also be advantageous to exploit in the making of composite boards.

2.2.2.2 *Extractives and inorganics*

Research has found that biomass contains a combination of various inorganics components in the form of crystalline and amorphous materials. These may include silicates (e.g. SiO_2, $Ca_2SiO_3Cl_2$), ox hydroxides (CuO, $Al(OH)_3$), sulphates ($CaSO_4$), phosphates ($AlPO_4$), carbonates (Na_2, $Mg(CO_3)_2$), chlorides ($CaCl_2$), and nitrates (KNO_3) to name a few (Soucy *et al.*, 2014; Boshoff, 2015). Researchers commonly refer to the total inorganic material mass as ash content, which is the solid residue that remains after combustion (Ridout, 2016).

2.2.2.3 *Inter-mill variation in sludge chemistry*

As previously indicated, the composition of PS is heavily dependent on the type of pulping process employed at the mill and type products manufactured. Previous authors such as Boshoff (2015) and Monte et al., (20009) have reported that the composition of PS varies throughout the industry as shown in Table 2-2. Further analysis also showed that even PS samples taken at the same mill but at different location, had significantly different composition.

2.2.3 Physical properties

It is important to analyse the physical characteristics of the PS in order to assess its suitable application for the production of bio-composites. Paper sludge characteristics such as appearance (colour), moisture content, coarseness, particle size distribution, fibre length distribution and surface characterisation do affect the quality of the composites and are discussed as follows:

2.2.3.1 *Appearance and composition*

Pulp and paper mill sludge is generated as viscous, wet material with a shade of light to medium grey colour. It typically contains wood fibres as the principle organic component as well as papermaking fillers (inorganic material) and other solids (dirt, glass, bacteria, metals, plastics), which can be recovered. Ochoa de Alde (2008) reported several methods that have been developed in order to recover the fibre and filler separately either via conventional route of screens and cleaners or more sophisticated methods such as wet-air oxidation.

2.2.3.2 *Moisture content*

In South African mills, the sludges are mechanically dewatered to a moisture content ranging from 50-80% (Boshoff, 2015) on site before disposal. It is necessary to reduce the moisture content in order to avoid fungal attacks that can destroy the fibre content. Many researchers have recommended a moisture content of 6-8% (oven dry weight basis) to being the ideal conditions for PS in order to be effective in the dry process of composite manufacturing (Maloney, 1986; Taramian *et al.*, 2007; Hughes, 2016).

2.2.3.3 *Fibre length distribution*

Fibre quality can be measured by the PS fibre length distribution and is good predictor of strength, stiffness and various other pulp and paper products (Kiae & Samariha, 2011). Ochoa de Alda, (2008) suggested that the potential PS to be utilised in the paper and board industry should have fibre length of at least 0.3 mm. Fibre length found in PS is significantly dependent on the pulping process employed. Table 2-3 shows the fibre lengths of PS investigated by various authors from different pulping process. Fibre lengths are both process depended and raw material dependent.

Table 2-3: Fibre lengths of biomass from literature.

Biomass	Fibre lengths (mm)	Reference
Paper Sludge from TMP	0.39	(Migneault, *et al.,* 2010)
	0.54	(Geng, *et al.,* 2006)
	0.317	(Soucy & Migneault, 2014)
Paper Sludge from CTMP	0.45	(Migneault, *et al.,* 2010)
	0.367	(Soucy & Migneault, 2014)
Paper Sludge from Kraft	1.09	(Migneault, *et al.,* 2010)
	0.875	(Soucy & Migneault, 2014)
	1.06	(Ochoa de Alda, 2008)
Paper Sludge from RP	0.9	(Ochoa de Alda, 2008)
Birch Virgin fibres	1.19	(Migneault, *et al.,* 2010)
Softwood virgin fibres	3.6	(Horn & Setterholm, 1990)
Hardwoods virgin fibres	1.2	(Horn & Setterholm, 1990)

As shown in Table 2-3, all the PS contained fibres longer than 0.3 mm, suggesting that all PS has the potential for use in paper and board industry. Kraft PS produced the highest fibre lengths compared to the other pulping techniques. This is expected since Kraft process involves the process of chemical defibrillation, which does not mechanically defibrillate the fibres and produces longer fibres such as TMP and CTMP, and feeds through virgin wood (Soucy & Migneault, 2014). In some cases, the average fibre length of Kraft was similar to birch virgin fibres, which are used for conventional medium density fibreboards (Soucy & Migneault, 2014). Mechanical pulping uses physical forces to separate the wood resulting in high yields pulp but short fibre lengths, and therefore resulting in relatively lower strength capabilities in fibreboards (Mabee, 2001).

2.2.3.4 *Water-holding capacity*

Another challenge that faces the suitability of incorporating lignocellulosic fibres such as PS in composite manufacturing is the combination of hydrophilic groups due to presence of hydroxyl groups within natural fibres, and the hydrophobic groups of matrix i.e. lignin content and hydrophobic nature of the /polymers. Mohammed et al.(2015) indicated that in the process of manufacturing composite boards from natural fibres such as bamboo and bagasse, weaker bonds can occur between hydrophilic fibre and hydrophobic cement matrices which could produce weaker physical and mechanical properties. As is the case with PS, Boshoff (2015) explained that PS from chemical pulping process such as Sappi: Ngodwana produces higher cellulose content and longer fibre lengths within PS compared to recycled fibre such as Kimberly-Clark: Enstra and mechanical pulping such as Mpact: Springs, resulting in higher hydrophilic nature and therefore higher water holding capacity. Furthermore, lignin is known to be hydrophobic and therefore reduce the water holding capacity of the tissue. Hence, it is vital to balance the addition of lignocellulosic fibres with hydrophobic binders.

2.2.3.5 *Surface characterization*

Surface characterization is usually done using Scanning Electronic Microscopy (SEM) images as shown in Huang et al., (2012), Garcia e al. (2007) and Segui et al. (2012). The SEM of the PS samples showed particles that were highly porous and clumped. The porosity of PS could lead to the formation of voids, which adversely affects the strength properties of the manufactured boards, thereby reducing their suitability for use in bio-composites.

2.3 Wood composites

Wood composites are comprised of wood-based materials glued by an adhesive. The wood composite industry is very well established and produces a wide range of wood-based composite products such as fibreboards, laminated beams and particleboards. Wood composites can be used in both structural (support structures in buildings) and non-structural applications (panels for both exterior and interior), and they remain in high demand. The industry has developed regulatory standards that assess the mechanical and physical properties of the product line. This is done to monitor product quality and maintain performance requirements (Youngquist, 1999).

Traditionally, conventional wood-based composites are made from veneers, fibres and particles. Other non-wood composites such as wood-plastic fibre and inorganic-bonded materials (gypsum, Portland cement, magnesia cement) have also gained interest in recent times for uses in automotive, construction and furniture industry (Stark, et al., 2006).

2.3.1 Overview of board manufacturing process

All wood-based products are produced in similar way as described in the following steps(Youngquist, 1999):

- Samples preparation either through drying and chipping,
- Binder application used as board adhesive resulting in matt formation,
- Pressing at specific process conditions
- Finishing of the product.

The selection of raw material, adhesives and process parameters have significant influences in the product functional performances. Particleboards are generally manufactured via dry processing with layered panels consisting mainly of wood particles and adhesive, resulting in smooth surface layer as shown in *Figure 2-2*, which shows the process route for making particleboard from cotton stalk (Shaikh, et al., 2010). Unlike the particleboards, fibreboards can be made via dry or wet process technology that exploits the strength properties of the fibre (Stark, et al., 2010). Wood plastics are manufactured through the compounded mixture consisting of lignocellulosic material in molten thermoplastic, while fibre cement boards such Portland cements fibreboards, are manufactured by creating a slurry of fibres and cement with addition of fillers in thin layers of fibre-cement formulation until the desired thickness is reached.

2.3.2 Conversion of lignocellulosic material to composites

During the process of producing composites wood products, lignocellulosic content characteristics are influenced by process conditions. Conventional particleboard making uses wood-based feedstock such as cut flakes that is cut into small pieces. In more recent times, due to economic burden of using flakes, processes have been develop using sawdust and planar shavings (Stark et al., 2011). The individual fibres present in wood particle gives the strength properties to the final product. Particleboards can be realistically produced using any source wood material as a feedstock. Common mill residues used for particleboard production include sawdust, planer shavings and chips, as shown in Figure 2-2 (Amiandamhen, et al., 2016). In South Africa, majority of companies such as PG Bison and Davidson Boards use virgin fibres as raw material in the manufacturing their boards.

However, due to potential positive economic impact, alternative resources from agricultural and industrial residue can be used to replace the solid wood particles in the manufacturing of particleboards. Previous studies have been able to show that agricultural residues such as wheat straw, sugar-cane bagasse, cornstalks and corncobs, cotton stalks, kenaf, rice husks, sunflower stalks and hulls can be used as raw materials in particleboards construction. Furthermore, various authors such as Geng *et al.*, (2006) have shown that PS has the potential to be a feedstock that could replace the solid wood particles in the particleboard formation.

It would be advantageous to establish a process route that utilises PS to produce valuable composite products. The impact of utilising PS as a complete replacement for lignocellulosic fibres in the aforementioned wood composites has not been thoroughly investigated. Instead, many researches have focused mainly on partial fibre replacement using sludge. Migneault *et al.*, (2010) investigated the partial replacement of wood using sludge from TMP process and found that the mechanical strength properties of the panel reduced with increased ratio of sludge: wood. This could be attributed to the presence of nonfibrous material such as inorganic material in the sludge reducing surface area for resin to uniformly mix. Taramian *et al.* (2007) also found similar results from NSSC and CMP sludge but found an improvement in the dimensional stability properties of the boards. Therefore, it can be difficult to predict the amount of material required and the required ranges of binding material and filler content to produce composites with comparable properties to conventional ones.

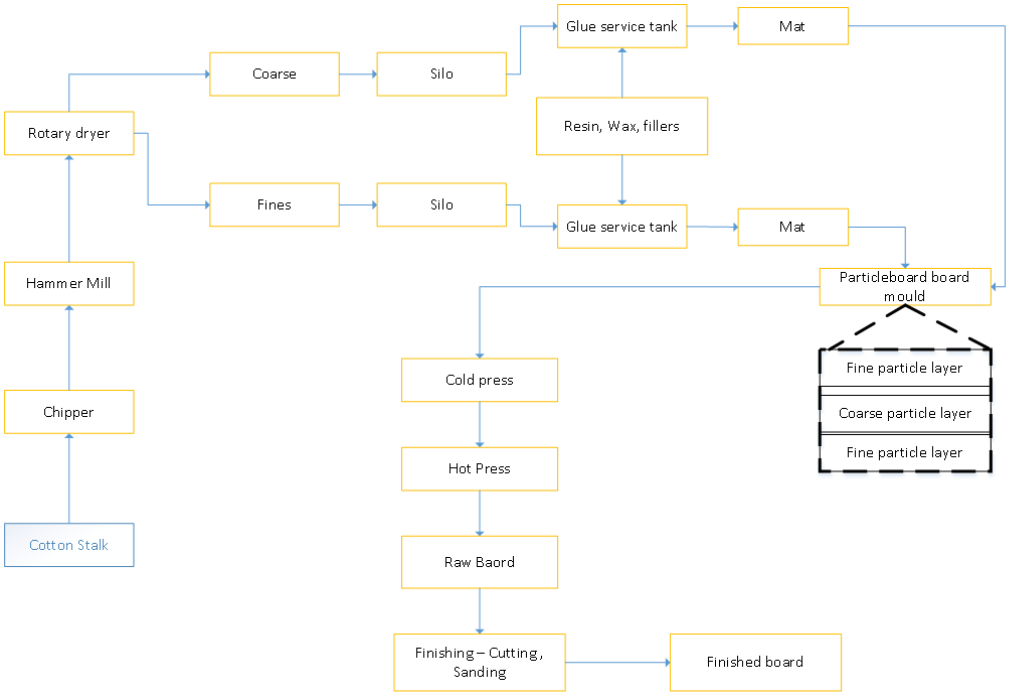

Figure 2-2: Process route for manufacturing of particleboards from cotton stalks (Shaikh, et al., 2010)

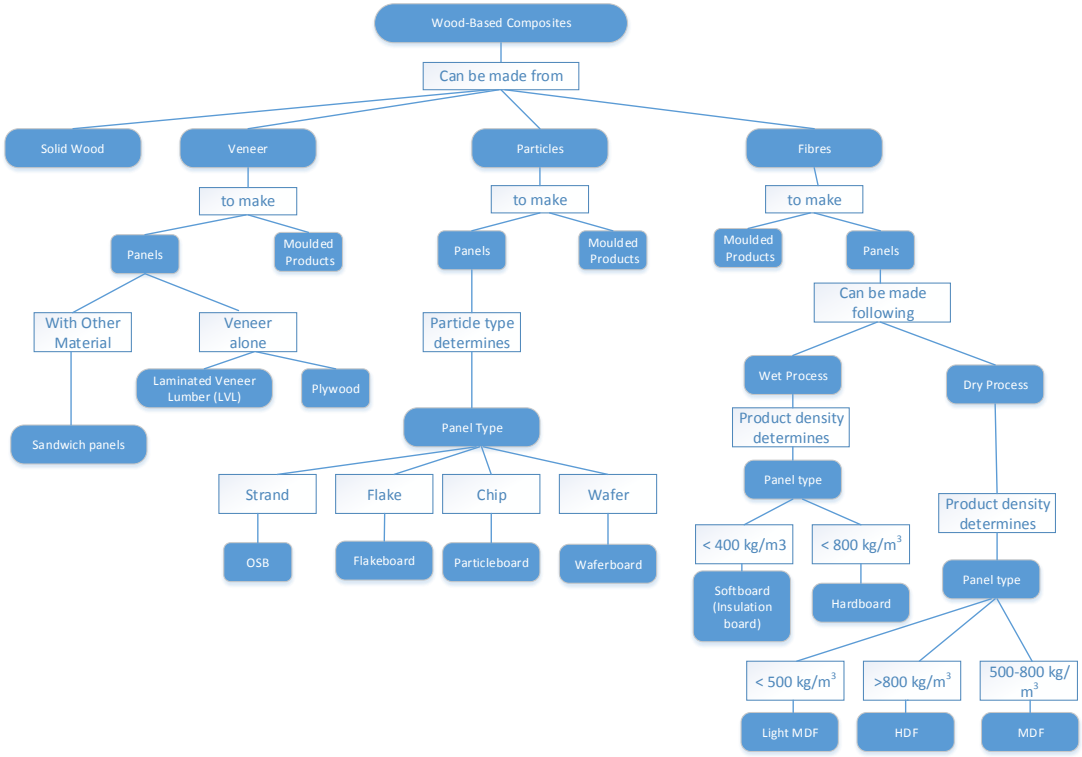

Figure 2-3: A summary of various wood based composites (Adapted from Thoema et al., 2010 and Stark et al., 2010)

In the following section, the literature review concerning the manufacturing of composites and impact of using PS in the manufacturing of composites paperboards is presented. In the board manufacturing industry the most conventional method for manufacturing composite boards is a relatively dry process using compression moulding with a mixture of raw materials and resins (Stark, et al., 2010). Particleboards are usually layered, consisting mainly of wood particles resulting in a smooth surface layer. Generally, products are finished either painting or laminating veneers to improve appearance and strength properties (Shaikh, et al., 2010). This study, similar to the other studies, the objective is to utilise agricultural and industrial waste, in this case PS, as the principle raw material in manufacturing particleboards. Unlike the previous studies, this study focuses on how to combine the PS from significantly different types of PS sourced from South African mills and phosphate binders to make the properties comparable to commercial particleboards. PS contains fibrous materials that could be exploited and used to produce composite boards but as pointed out by such as Geng et al. (2010) and Taramian et al. (2009), there are limitation to the key functional board functional properties especially the mechanical strength of the boards. The combination of very short fibrous material compared to conventional wood sources such as Eucalyptus or pine, and inorganic components found in PS have been known to limit the mechanical strength of the boards by hindering the binding mechanism of the binder.

2.3.3 Grading of products

Once the composites are made, the flexural strength and dimensional stability of the boards are tested in order to make sure they comply with product performance standards. This then determines the application that the final composite products are suitable for. The grading standards include typical flexural strength tests, such as modulus of rapture (MOR) and modulus of elasticity (MOE). MOR measures the bending strength, and refers to the highest amount of pressure or force that can be experienced by the material before it fractures (Diaz, et al., 2011). MOE is a mechanical strength parameter used to determine the stiffness and strength of the composite material (Diaz, et al., 2011). These tests usually consist of static bending tests or dynamic mechanical bending tests. Amiandamhen et al. (2016) utilised an Instron testing machine with a 5kN load cell and tested it to failure in order to calculate the MOR and MOE from standard ASTM (2006). MOR and MOE are usually reported in terms of pressure and compared to composite international performance standards as shown in the Table 2-4. This is done to determine whether the composite product has expected load-bearing capabilities. Dimensional stability test including determining the water absorption (WA),

thickness swelling (TS), volume swelling (VS) and the tests are usually done by submerging species in water for approximately 24 hrs and measuring the change in weight referred to as water absorption, the thickness and volume swelling (ASTM, 2012). This is usually done to determine whether the composite is durable enough to withstand external conditions especially when exposed to a moisture environment such as rain.

Table 2-4: Properties of composite boards made from paper sludge using optimised process conditions

Properties	Units	PB[1]	MDF[2]				MDF[3]	PB[4]	PB - ANSI A208	MDF-ANSI A 208.2-2009	Wood cement –EN 634-2
Pulping process		CMP and NSSC	TMP	CTMP	Kraft	Paper birch		RP and DI	-	-	-
Raw material composition	% of PS	15	25	25	25	V - 100%	PS-100	100	-	-	-
Resin Composition (Adhesive + filler)	%	UF - 12 NH_4CL - 2	UF - 12 Wax - 0.5 NH_4CL - 0.25				UF - 12 Wax - 0.5 NH_4CL - 0.25	KH_2PO_4- 75 MgO - 15 Fly ash - 10	-	-	
Press Temperature	°C	160	180				180	Room	-	-	-
Press Pressure	kPa	30	80				200	200	-	-	-
Press Time	min	6	5.5				5	5			
Density	kg/m^3	0.75	0.8				0.95	0.68-0.71	0.5-.8	0.6-1	1
Average moisture	%	9	3	3	3	3	5	7			
WA	%	54.7-94.11						57.15-80.83	60		
TS	%	11.62-20.31	13	12	11	9	75.2	0.22-7.66	7	14	
VS	%	-	-	-	-	-	-	1.07-9.30	-		
MOE	GPa	3.2	3.6		3.8		1.5	0.61-1.44 MPa		1.2-3.1	14.5
IB	MPa	-	1.4	1.3	1	1.6	0.25	-	0.4	0.24-0.47	
MOR	MPa	6.93-18.73	36	38	36	42	9.2	667.02 - 196.48	11-11.5	12.4-30	9

Key

Properties	PB- Particleboard, MDF - Medium density boards, WP - Wood Plastic
Resin	UF - Urea Formaldehyde, MDI - Methylene diphynyl diisocyanate, NH4Cl-Ammonium chloride
Raw material	PS - Paper sludge, V - Virgin fibre, DPS - De inking paper sludge
References	1- Taramain et al., (2007), 2- Migneault *et al.,* (2010), 3- Geng et al., (2007), 4- Amiandamhen et al.,(2016), 5 - Soucy & Migneault., (2014)
Standards	Particleboard standard - ANSI A 208.1-2009, MDF standard - ANSI A 208.2-2009 for 115 grade interior application , Wood cement –EN 634-2: British standard for cement bonded particleboard

2.3.4 Resin

The conditioned wood particles are thoroughly mixed with the resin to ensure that there is even distribution of adhesives on the wood particle before a matt is formed. This matt is then typically pressed through a board press machine as in Figure 2-2. The resin/adhesive forms part of the binding system of the final product that surrounds and supports the particles. The particles mixed with adhesive are then compacted using heat and pressure using presser-forming boards. The boards are subsequently cured, conditioned and sent to finishing operations such as trimming into standard sizes and finishing to form the final product.

The wood product industry has generally enjoyed the benefits of low-cost petroleum based adhesives such as phenol-formaldehyde (PF), urea-formaldehyde (UF) and methylene diphenyl diisocyanate (MDI). The disadvantage of these adhesives is that they are thermosetting or heat-curing resins, which require high temperature and long press time. In recent years, there has been a renewed interest in other binding systems such as Portland cement and chemically bonded phosphate ceramic (CBPC) consisting of metal oxide and acid phosphate salts. In particular, CBPC such as magnesium based cement has been gaining more interest due to its superior mechanical strength and faster setting time compared to Portland cement (Amiandamhen, 2017). The magnesium based cement is made of acid base reaction between magnesium oxide (MgO) and potassium dihydrogen phosphate (KH_2PO_4, KDP) (Wagh, 2013). With the addition of water, this reaction forms magnesium potassium phosphate binder MgKPO4.6H2O as shown in Equation **Error! Reference source not found.**, which is elatively a strong insoluble salt with high crystallinity when compared to Portland cements (Wagh, 2013; Amiandamhen, 2017).

$$MgO + KH_2PO_4 + 5H_2O \rightarrow MgKPO_4.6H_2O \quad (1)$$

The mechanical strength of magnesium potassium phosphate cement (MKPC) is provided by the main product magnesium potassium phosphate hexahydrate ($MgKPO_4.6H_2O$) or k-struvite from Eq (1). It is also known that at high temperatures, MgO becomes highly crystallised, which bonds very well with intermediate acid solution (water and KDP) and forms strong cement binding material. Furthermore, after the hardening of the cement binder two compounds exist in the product cement, i.e. unreacted crystalline MgO and struvite of potassium (Ding *et al.*, 2012). The struvite exist as both in crystal form and in an amorphous phase. The presence of both the crystal phase (unreacted MgO and struvite), which makes up the cement framework and amorphous phase in the cement binder, significantly contribute to

the higher flexural strength properties of the composites than is found in Portland cements(Ding *et al.*, 2012) . The kinetics and performance of MKPC have been reported to be influenced by various factors including magnesia reactivity, binder ratio (KH_2PO_4: MgO), filler ratio (% of binder) and water-to-binder ratio and retarders (Chau *et al.*, 2011; Le Rouzic *et al.*, 2017).

The binder ratio of KDP: MgO has significant influence on the generation of the main cements product k-struvite (Chau, Qiao and Li, 2011; Hou *et al.*, 2016). This has a significant implication on the compressive strength and physical properties of the board. Amiandamhen et al. (2016) found that for boards made with paper sludge bonded by MKPC with fly ash, an optimum binder ratio of two produced maximum performance. Previous authors have looked at varying different systems but with varying results from literature. It is therefore difficult to predict the amount of material required and the required ranges of binding material and filler content to produce composites with comparable properties to conventional Ones. For the purpose of this study, the resin system that would be applied is the phosphate-based resin, which is relatively in its infancy stage for commercial application.

It is common knowledge that increasing the binder content significantly improves the MOE, MOR, IB and density, while WA and TS, VS declines (Shaikh, et al., 2010). Therefore, it is critical to optimise the processing conditions such as binder ratio in order to attain the desired quality. Amiandamhen et al., (2016) proposed the following optimised process conditions for fibre content, binding ratio and filler of phosphate based cement boards using ratios shown in Table 2-5

Table 2-5: Experimental process conditions for Amiandamhen et al., (2016)

	Ratios		
	Low	Middle	High
Binder ratio(KH_2PO_4 : MgO)	1	2	3
Filler: Fly ash (% of binder)	0	10%	20%
Fibre content (fibre: resin)	2	2.5	3

This was done to ensure good bonding environment between the binding material and fibre source. The majority of the overall cost of the producing composite board is significantly dependent on the amount of binding material utilised. The versatility of phosphate-based cement allows the possibility of adding fillers to the binding system both to improve the strength properties of the resin and by creating a strong bond between fly ash and $MgKPO_4.6H_2O$, (Amiandamhen, 2017). Furthermore, phosphate based cements are known to

be more environmentally friendly than other resin types such as Portland cement (Amiandamhen, 2017).

Geng et al., (2007a) investigated the suitability of utilising a combination of de-inking PS and primary sludge from a thermomechanical pulping mill, as a partial replacement of fibres in the manufacturing of medium density fibre boards (MDF) while using (UF) resin as a binder. It was found that the increased use of PS resulted in decrease in mechanical properties because of fibre lengths and ash content. The authors were able to replace 70% of the natural fibre with PS and produce panel properties that met the requirements for MDF (ANSI A208.2-2002). Taramian et al. (2007) however, found that mechanical strength was adversely influenced by the addition of PS, with only 15% PS replacement meeting MDF requirements. This trend was attributed to the presence of kaolin and Calcium carbonate within the inorganic component of PS, and thus inhibiting the binding of matt with UF resin. On the contrary, they found that dimensional stability properties such as thickness swelling (TS) improved with the addition of PS while water absorption was at minimum with 15% PS replacement. Migneault *et al.* (2011) showed that with 25% PS replacement of virgin fibres, all the panels met the MDF requirements and agreed that non-fibrous material within PS was also adversely affecting the final panel properties. Other researchers such as Donahue and Aro (2010) found that the overall best performing board composed of PS with binder ratio of 0.79 , while Amiandamhen el al., (2016) found an optimum fibre (PS): inorganic ratio of 2.92 with CR-PS bonded with phosphate based cement. Furthermore, they found that compressive strength of the boards increased with an increase in PS content and binder ratio.

2.3.5 Fillers

Unfortunately, even though MPKC has shown to be mechanical and physically stronger than traditional cement such as Portland cement, it cost 2-3 times more (Amiandamhen, 2017). Fillers can be introduced to partially replace MKPC, which could enhance the performance of the board and reduce cost. The usage of high amounts of cement to produce high flexural strength has the risk to experience shrinkage and cracking. Amiandamhen (2017) suggested the use of fillers in order to increase the strength capability of the resin system. It is important that the choice of filler is not too costly because it the driving force in choosing the process routes and techniques. Therefore, utilising other industrial residue such as kaolinite, calcium carbonate and silicon fume that could be used to enhance the adhesive abilities of the resin (Mantia & Morreale, 2011) should also be assessed. The addition of fillers such as fly ash (FA), silica fume (SF) and calcium carbonate ($CaCO_3$) to cement, has been known to reduce costs

and enhance the durability of the composite boards making them eco-technically advantageous (Donahue and Aro, 2010; Antoni, Chandra and Hardjito, 2015). Previous research included FA, which mainly consists of alumina-silicate and could only replace up to 40% of MKPC system before adversely influencing the performance of the boards (Li and Chen, 2013; Wagh, 2013; Amiandamhen *et al.*, 2016). Chen et al., 2012) investigated the effects of adding FA and SF (which are both pozzolanic materials) to MKPC system. They found out that FA and SF could improve the denseness of the crystal structure and therefore improved the water resistance of MKPC. The fineness of SF enabled it to fill the void spaces of the MIPC, thereby improving the pore structure which therefore improves the compressive strength and water resistance (Zheng *et al.*, 2016). The use of $CaCO_3$ has also been investigated as possible filler to partially replace cement. Previous authors have noted that due to the nature of $CaCO_3$ to fill the gaps between the particles and therefore increase density, it improves the compressive and physical properties of cement (Antoni *et al.*, 2015). However, the research into the effects of pozzolan material such as FA and SF, and on $CaCO_3$ on wood based (i.e. paper sludge) composite boards bonded with MKPC system is not comprehensive.

.Fillers are often used to partially replace the binder in order to reduce the cost of the binder. Amiandamhen et al., (2016) added 10% of fly ash to the phosphate binder. The researchers found that even though filler content improved the functional properties of the board, too much filler (fly ash), eventually resulted in reduction of strength properties due to reduced binder content. As a result, it is critical to find an optimum range of filler addition. The composite product still maintained dimensional stability properties comparable to low density particleboard and Portland cements, but was not able to produce boards with comparable strength properties (Amiandamhen *et al.*, 2016). The researchers also observed a decrease in flexural strength with an increase in partial replacement of binder with fly ash, which could be explained by the reduced binder supporting individual fibres (Amiandamhen *et al.*, 2016). As a result, it is critical to find an optimum range of filler addition. The impact of the partial replacement of binding material has not been investigated by any researches. It would be interesting to evaluate the effect of adding ‘green’ fillers such as fly ash, silicon fume kaolin, sand, which maintain or increase the strength properties of the boards but also reduce the cost of production. Adding relatively cheap fillers such as fly ash not only improves functional properties, but also reduces cost of production (Amiandamhen, 2017).

Some researchers found that the dimensional stability properties meet the standards for low density particleboards, while the strength properties did not meet the required standard of MOE

9 MPa for low density particleboards and 14.5 GPa for Portland cemented boards (BS EN 634-2:2007, 2007). This suggested that not enough binding material was used in order to improve the bonding between the fibres, resulting in boards that have no load bearing capabilities and could therefore could be used as partitions or slidings.

2.4 Gap in literature

As of late, the cost of waste handling sludge has increased and pressure to discover alternative handling methods has also increased. Notwithstanding, it is hard to either develop handling methods in light of the fact that different procedures expect sludge to be dried which is very costly or expect sludge to be washed to lessen inorganic substance. Lamentably, due to ever-tight economy and limit funding source, it is critical to develop alternative handling methods that is both technically feasible and economically viable to be investor friendly. Numerous researchers have already implied the potential of utilizing PS as a feedstock to use to create composite boards such as medium density fibreboards or particleboards (Geng et al., 2007). Not only does our investigation look at technical feasibility of using PS from significantly different pulp and paper mills within the South African industry, but also looks at the economic implication of manufacturing plant on an industrial scale production of economically viable biocomposite of acceptable standard for techno-economic feasible study.

The overall research goal of the study was to assess the feasibility of utilising various types of PS as feedstock in the manufacturing of bio composite boards with acceptable functional properties. The experiments was designed to utilize as much PS as possible and find optimum process conditions. To better understand the cement-fibre interaction and mechanism, the optimisation of process conditions and statistical analysis was performed on the mechanical and physical performances of the composite boards manufactured

Firstly, the focal point of the study was to survey the impact of key physio-chemical properties of PS on the functional properties of the composite board product. Three different kinds of PS were considered. Laboratory board making process was designed statistically and optimal key process conditions were developed, to produce boards with comparable functional properties and quality to the conventional cement-bonded composites. Secondly, the study also focused on using the optimum process conditions to develop an economic model. The techno-economic model included considered possible process routes, equipment and material cost so as to evaluate the monetary suitability of producing bio-composite panels utilising PS as feedstock on an industrial scale. .

2.5 Research questions, aims and objectives

2.5.1 Key questions

1. Can properties equivalent to conventionally manufactured boards such as modulus of elasticity (MOE), Modulus of rupture (MOR), water absorption (WA), thickness swelling (TS), volume swelling (VS) and density be achieved using PS from south African mills?
2. How does significantly different PS samples influence the functional properties of the bio-composite panels?
3. What is the techno-economic feasibility of manufacturing composite products from PS on an industrial scale?

2.5.2 Aims and objectives

The general aim of this study was two-fold: firstly, to investigate the feasibility of producing bio-composites panels (particleboards) using PS from three distinctively different types of pulp and paper mill sources in South African, which inherently has variable composition. Secondly, to develop economic models in order to assess the economic feasibility up scaling the production of the bio composite boards onto an industrial scale from the discounted cash flow analysis.

The specific objectives of the investigation are:

1. To characterize the physio-chemical properties of PS that would influence the functional properties of composite boards.

   The selection of PS was based on the type of mills, chemical composition of PS, and the raw materials utilised in pulp and paper production. Three significantly different types of PS samples were selected based on their variation in process parameters and composition. PS selected from Kimberly-Clark (Enstra) comes from a tissue paper mill that generally producers PS with high ash content. PS from Mpact (springs) comes from a corrugated recycle mill, which produces a PS that usually contains less ash than Kimberly-Clark but more than Sappi. PS from Sappi (Ngodwana) comes from a virgin pulp paper mill that produces PS with low ash content. This was done to assess whether composite boards could be made from varying composition of fillers and ash content. **(Chapter 3)**
2. To assess and determine the technical feasibility of producing composite boards, from various PS available from local pulp and paper mills in South Africa, with functional properties meeting commercial standards.

The laboratory boards consisted of PS, binder of monopotassium phosphate and magnesium, filler content of calcium carbonate, fly ash and silicon fume, and varying board press temperature from 25°C to 180°C. The board's physical and mechanical properties such as density, modulus of rapture, modulus of elasticity, water absorption, thickness swelling and volume swelling was tested. These properties will then compared to each other and board standard to determine acceptable quality had been meet and also determine possible application **(Chapter 3).**

3. To optimise key experimental process conditions during the manufacturing of board products in order to maximise functional properties.

Laboratory board making process was designed statistically and optimal key process conditions were developed to produce boards with comparable functional properties and quality to the conventional cement-bonded composites. **(Chapter 3)**

4. To assess the economic feasibility of utilising PS as feedstock for manufacturing bio-composite boards on an industrial scale.

From the optimum process conditions, the techno-economic model was develop to investigate the profitability of the different scenarios. The model was designed that all the PS produced from the mills is utilised to make board. The economic study was based on the equipment and material requirement and the minimum required selling price was determined to assess the profitability and viability of the different process routes. **(Chapter 4)**

2.6 Scope

The scope of the research project was:

- The project will only focus on PS as a feedstock for wood based composite cement bonded board products
- The economic analysis will only focus on the feasibility of producing composite products in the South African industry by considering economic indicators such as the NPV, IRR, and payback period.

2.7 Research approach

The first phase of the study involved collection of PS samples from three types of mills in South Africa followed by an assessment of their physio-chemical characteristics. The PS was processed for the production of composite boards using a board press machine. The boards were then tested for mechanical and physical performances such as MOE, MOR, WA, TS, VS, Density were measured. The data was then optimised to investigate whether it was possible to attain board properties comparable to conventional board properties based on applicable standards. The second phase of the study evaluated the techno-economic feasibility of manufacturing composite products from PS on an industrial scale. This was achieved by modelling the manufacturing process and therefore developing an economic model.

Chapter 3. Analysis of composite boards produced from paper sludge

3.1 **Materials**

3.1.1 Residue

Three different types of paper sludge (PS) samples were selected based on their variation in process parameters and composition for the experiments. Table 3-1 describes PS selected from Kimberly-Clark (Enstra), Mpact (Springs) and Sappi (Ngodwana), and their process description. The selection of PS was based on the type of mills, previous reported chemical composition of PS, and the raw materials utilised in pulp and paper production. In addition the PS specifically used in this study were selected based on their variations in process parameters, as described in Table 3-1, and composition described in a previous study by Boshoff et al. (Boshoff, 2015). In the study, the PS samples were classified based on their primary feed at the mills and shown in Table 3-1, thus RN-PS for Recycled newsprint, CR-PS for corrugated recycle and VP-PS for virgin wood

Table 3-1: Pulp and Paper mills selected parameters (Adapted from Boshoff, 2015)

	Kimberly-Clark South Africa (Pty) Ltd: Enstra	Mpact Paper Ltd: Springs	Sappi South Africa Ltd: Ngodwana
Pulping process	De-inking, Re-pulping	De-inking, Re-pulping	Kraft, Mechanical Pulping
Primary products	Tissue Paper	White-lined carton board, laminated board and speciality coated board	Kraft liner board, chemical unbleached pulp, mechanical and dissolved pulp
Primary Feed	Recycle fibre; Newsprint, Printing and writing; Virgin pulp	Corrugated recycle; Recycled fibre; Virgin pulp;	Virgin wood, Eucalyptus and Pine
Paper sludge classification	RN – PS	CR – PS	VP - PS

Note: RN-PS is Recycled Newsprint, CR-PS is Corrugated recycle and VP-PS is virgin wood paper sludge

The as-received wet PS samples were dried under atmospheric conditions in order to reduce moisture content to avoid rotting. The dried PS was milled to create homogenous feedstock and reduce the clumped samples, using a Retsch hammer mill fitted with 2 mm sieving slice. The resulting sludge samples were then conditioned at 20°C and 65% relative humidity (RH) for 96 hrs in order to allow binding mechanism to cure and for stabilizing the board's moisture content.

3.1.2 Magnesium oxide

In this study, the MgO used was in the form of MAGOXBPPO, a commercial magnesium sourced from Kimix, South Africa and had the following characteristics via X-ray Fluorescence (XRF): CaO ≤ 0.09%, MgO ≤ 100%, TiO_2 ≤ 0.02; loss on ignition < 0.64 % ; assay 96% min; arsenic < 0.003%;; calcium <1.1%; iron <0.05%; acid insoluble substances <0.1%; free alkali and soluble salts <2.0%, heavy metals <0.002% (Amiandamhen *et al.*, 2016).

3.1.3 Monopotassium phosphate

The monopotassium phosphate (KDP) used in this study was bought from Kimix, South Africa and had the following analysis: assay 100%; arsenic < 0.0003%, lead < 0.00005%, KH_2PO_4 > 98%, P_2O_5 > 51.2%, K_2O > 33.5%, chloride < 0.2%.

3.1.4 Fillers

The fillers used in this study included calcium carbonate, silica fume and fly ash. The calcium carbonate was supplied by Kimix, South Africa and had the following composition: Assay > 99.5%, chloride < 0.001%, $CaCO_3$ > 98%. Silica fume is a highly pozzolanic material and was supplied by Mapei, South Africa with silica sand < 0.1%. The fly ash was a class C fly ash obtained from Ulula Ash Kriel power plant in the form of powdery residue and had the following composition: SiO_2 < 60%, Al_2O_3 < 35%. CaO < 10%, MgO < 5%, Fe_2O_3 < 5%, TiO_2 < 5%.

3.2 Methods

3.2.1 Physio-chemical characterisation of sludges

The moisture content for the dried PS samples was determined based on TAPPI T264 cm-07 standard for the preparation of wood for chemical analysis. Moisture content was determined by weighing approximately 2 g of sample on a tared weighing glass or bottle. The sample was then oven-dried for approx. 2 h at 105 °C ± 3° and subsequently cooled in a desiccator. The sample was returned to the oven for approx. 1 h, cooled and weighed. The procedure was repeated until constant weight was recorded. The moisture content was calculated using Equation 2.

$$\text{Moisture content (\%)} = \frac{\text{Weight}_{\text{wet sample}} - (\text{Weight}_{\text{dry sample+ glass}} - \text{Weight}_{\text{glass}})}{\text{Weight}_{\text{dry sample}}} \times 100 \quad (2)$$

Bulk density of the PS was measured using PS samples that had been dried in the oven for 24 h, and poured into a 25 ml cylinder. The bulk density was determined by weighing the sample in the cylinder and taken note of the volume of the sample in the cylinder. For consistency, the bulk density measurement was done in triplicates and was calculated using Equation 3.

$$\text{Bulk density } \left(\frac{\text{g}}{\text{m}^3}\right) = \frac{\text{Weight}_{\text{dry paper sludge in beaker}}(\text{g})}{\text{Volume}_{\text{taken up by the sample}}(\text{m}^3)} \quad (3)$$

The average fibre length (in mm) was analysed using the Tappi standard for fibre length of pulp by projection based on TAPPI T-223 (Tappi, 2006).

The lignocellulosic chemical composition of all the PS samples were done to determine ash content, extractive content, acid-insoluble lignin content and sugar content (glucose, cellobiose, xylose and arabinose) Total ash content was determined gravimetrically after combustion of sample at 575 °C ± 25 °C in a muffle furnace for minimum of 4 h according to TAPPI T211 (2004). According to National Renewable Energy Laboratory (NREL), the total extractive content was determined via Soxhlet extraction method(Sluiter *et al.*, 2005, 2012; Sluiter, Hames, *et al.*, 2008; Sluiter, Ruiz, *et al.*, 2008).. According to NREL method, the acid-insoluble lignin was determined by adding 0.3g of material and diluting with 3ml of 72% sulphuric acid in a test tube. The test tube was then incubated in a water bath at 30 ± 3° C for about 30 - 45 min followed by autoclaving for an hour at 121 °C. The autoclaving was done after diluting the sample to obtain acid concentration of 4 wt. %. The hydrolysed sample was then filtered through a crucible and washed with 250 ml boiling water. A sample of the solution was taken to measure acid soluble lignin by spectrophotometry at 205 nm. The cake was dried

in an oven at 105 ^{o}C for 24 h to determine the mass of acid insoluble lignin gravimetrically. The structural carbohydrates were determined by standard procedures for structural carbohydrates and lignin in biomass (Sluiter, Ruiz, *et al.*, 2008; Sluiter *et al.*, 2012). In summary, the procedure involved hydrolysing a sample 0.3 ± 0.1 g using sulphuric acid (72 wt.%) and incubating this in a water bath and the sugars were measured using HPLC.. A more detailed procedure for carbohydrates and lignin is detailed by Sluiter et al. (Sluiter, Ruiz, *et al.*, 2008; Sluiter *et al.*, 2012). The mineral composition (oxides) analysis of the PS was measured using PANalytical via X-ray Fluorescence (XRF) analysis.

3.2.2 Board formation

The prepared the PS samples were prepared, mixed with magnesium based binder and filler based on mixing proportions shown in Table 3-2. All boards were made with a target density of 1 g/cm^{3}the dry-mixture was then physically stirred thoroughly. A pre-determined amount of water was added to the dry mixture until a homogenous mortar was obtained. The amount of water added was based on formulation described by Sotannde et al. (2012) as shown in equation 4.

$$W = B + (FSP - MC) \times F \quad (4)$$

W= amount of water (ml), B = inorganic components (g), FSP = fibre saturation point (%), MC = moisture content (%) and F = biomass fibre (g)

. The mixture was placed in a mould approximately 218 x 77 x 40 mm to produce the boards. A 27 mm steel bar was pressed on the boards to get a final thickness of 13 mm, which in the process squeezed out excess water and reduced the presence of voids and air spaces in between the fibres. The mould was then transferred to laboratory press machine and pressed at 200 kPa, and predetermined temperature for 10 min. The method followed was based on previous studies done by Amiandamhen et al. (2016). After fabrication, the mould was removed from the press and each of the boards demoulded. The manufactured boards were then placed in a conditioning room at 20°C and 65% RH for 96 h to allow for the boards to cure before physical and mechanical testing was carried out. The boards were made to a moisture target of 5% after being cured.

3.2.3 Experimental design

The experimental design via a central composite design (CCD) was implemented to simultaneously optimise the input process conditions in order to maximise the mechanical and

physical properties of the boards from each PS sample. The following process parameters namely fibre ratio (fibre: binder) on mass bases, binder ratio ($KH_2PO_{4:\ MgO}$) on mass bases, filler content (fly ash, calcium carbonate, silicon fume) measure % of binder and pressing temperature were considered to have significant influence on the functional board properties. The process parameters were set up in the ranges similar to previous research done by Amiandamhen et al., (2016) as shown in Table 3-2. Even though Amiandamhen et al. (2016) did not meet the mechanical strength standard, the study did not include temperature. It is expected to see an improvement in board strength properties. Another reason to investigate the process conditions is that different type of PS was utilised. The study did already illustrate the inherent potential of utilising certain biomass to produce light weight composite material.

Table 3-2: Preliminary experiment process parameter set up

Variables	Low	Medium	High
Fibre ratio (fibre: binder) on mass basis	3	4	5
Binder ratio (KH_2PO_4:Mgo) on mass basis	2	3	4
Filler content (% of binder) on mass basis	0	10	20
Temperature (°C)	25	100	160

The response surface method (RSM) was then used to predict the relationship between experimental variables (fibre ratio, filler content, binder ratio and temperature) and responses variables. The response variables included modulus of elasticity (MOE), modulus of rapture (MOR), water absorption (WA), thickness swelling (TS) and volume swelling (VS) the experimental variables were then optimised to obtain responses comparable with cement-bonded particleboards. The number of experiments (N) required for the development of CCD was defined by Equation 5.

$$N = 2^{k-p} + 2K + C_p \quad (5)$$

Where k = number of factors, C_a = number of centre points, fractionalization element p=0 for a full design. The design included a total of 26 runs, including 24 experiments and 2 centre points. In order to establish an optimum process conditions, a second-order response surface model was developed incorporating response surface methodology as described by Montgomery (2015). It was expected that at 95% confidence level, the fibre ratio (fibre: binder), filler content, binder ratio (KH_2PO_4: MgO) and temperature would significantly influence board properties based on previous studies (Amiandamhen, 2017). Therefore, it was

vital to optimise these variables in order to produce boards with desirable properties. The independent variables are represented as x_1, x_2 x_3 (i-iii), x_4 respectively as shown in Table 3-3. The variables were coded at three distinct levels -1, 0, 1 representing low, middle and high levels respectively.

Table 3-3: Independent variable and their three levels ($CaCO_3$ – Calcium carbonate, FA – Fly ash, SF – Silica Fume)

Variables	Factors	Coded levels		
		Low(-1)	Medium(0)	High (1)
Binder ratio (KH_2PO_4:MgO)	x1	-1	0	1
Fibre ratio (fibre: binder)	x2	-1	0	1
Filler	x3			
$CaCO_3$	x3 (i)	-1	0	1
FA	x3 (ii)	-1	0	1
SF	x3 (iii)	-1	0	1
Temperature	x4	-1	0	1

Once the experimental variables had been optimised, the desirability function was used to maximise each of the response variables in order to achieve the maximum board properties along with the commercial standards.

3.2.4 Testing board properties

All the boards produced according to the experimental design were tested for physical and mechanical properties. The densities of the boards were established to compare with target density. The boards were cut into test specimens using a concrete blade angle grinder. The test specimen's flexural strength were analysed using an Instron testing machine fitted with a 5 kN load cell according to ASTM D1037-06a. The test assessed the modulus of rupture (MOR) which described the flexural strength, and apparent modulus of elasticity (MOE), which were calculated according to ASTM (ASTM, 2012).

The dimensional stability properties, which include water absorption (WA) and thickness/volume (TS, VS), were then be determined by soaking the board in water for 24 hrs. Subsequently, the boards were drained for approximately 10 min and wiped with a soft cloth to remove the surface water (BS EN 635). The boards were then weighed and the dimensions of the boards re-measured. The WA was expressed as percentage increase of weight after submersion. While the TS and VS were expressed as percentage increase in thickness and volume of the boards respectively.

3.2.5 Statistical design

The data collected from the experiments were statistically analysed using STATISTICA (version 5). The significance of the interactions and effects of each independent variable were analysed and described using the analysis of variance (ANOVA). Response surface plots (RSM) were used to describe the relationship between response and independent variable, especially where there was a significant effect (p<0.05) per type of filler. A second order polynomial regression model shown in Equation6, was established to describe the empirical relationship between input and response (Montgomery, 2005; Amiandamhen *et al.*, 2016). A regression analysis was done in order to establish how good the proposed model predicts experimental data.

$$y = x_0 + ax_1 + bx_2 + cx_3 + dx_4 + a(Q)x_1 + b(Q)x_2 + \mathrm{c(Q)}x_3 + \mathrm{d(Q)}x_4 + abx_1x_2 + acx_1x_3 + adx_1x_4 + bcx_2x_3 + bdx_2x_4 + cdx_3x_4 \quad (6)$$

where y = predicted response, x_0 = intercept; a , b , c , d = linear coefficients, a(Q), b(Q), c(Q), d(Q) = quadratic coefficients; ab, ac, ad, bc, bd, cd = interaction; x_1 =fibre ratio, x_2 = binder ratio, x_3 = filler ratio, x_4 = temperature.

Optimum process conditions were established using desirability profiles available in Statistica V5. Significant models were established to predict response variables using optimum independent variables. A validation experiment, using the predicted optimum operating conditions in order to compare the predicted and observed response was performed. Two-way ANOVA statistical analysis was used to determine whether the main effects (different type of PS and different fillers) and interaction effects were statistically significant. The Tukey-Kramer test was used as a post-hoc test to understand pair-wise significance using the minimum significant difference method.

3.2.6 Cementing and analysis of bonding mechanism

The hydration products were characterised via Bruker Single-crystal X-ray Diffractometer (XRD) to analyse the products crystal structure generated by the formation of struvite crystal. The analysis was done under atmospheric conditions with scanning range of 0 to 70 degree (2θ). The samples analysed were selected based on the strongest, medium and weakest board samples in each of the three PS types. The crystallinity of the board's samples was characterised by comparing crystalline behaviour of the raw materials used in the manufacturing of the board's sample.

To further understand the reaction mechanism and obtain information on the changes in functional groups within sludge material, Fourier-transform infrared spectroscopy (FTIR) was used. The FTIR analysis was performed using the Nicolet iS10 FTIR equipment attached with attenuated total reflectance (ATR) unit.

3.3 Results and discussion

3.3.1 Physical characteristics of paper sludge

There were differences in the physical characteristics among the PS samples investigated. The major differences prominent were the bulk density, moisture content, fibre length, as shown in Table 3-4. The average bulk density (BD) of RN-PS, CR-PS and VP-PS were 150 g/cm^3, 120 g/cm^3 and 60 g/cm^3 respectively (Table 3-4). RN-PS had a higher bulk density compared to CR-PS and VP-PS because of a combination of having the highest amounts of more dense inorganic material such as ash and low amounts of less dense fibrous material within the PS (Table 3-4). Whereas, for VP-PS the low bulk density of VP-PS is a result of having the highest amounts of less dense fibrous material within PS and the lowest amounts of more dense inorganic material. Consequently, the VP-PS with low bulky density is therefore likely to produce boards that are lighter than boards made with RN-PS and CR-PS. It is hypothesed that fibre lengths play a vital role in the viability of using PS to produce boards. Fibre length analysis (Table 3-4) shows that in some cases, PS from Kraft mills (VP-PS) had fibre lengths comparable to natural resource wood such as Eucalyptus (0.9 – 1mm), virgin Birchwood (1.19 mm), *Pinus* (1.9 – 2.2 mm) and soft wood *Pinus patula* fibres (3.6mm) (Ochoa de Alda, 2008). This is very advantageous in the board manufacturing industry. In contrast, PS from recycled mill (RN-PS) displayed fibre lengths that were significantly shorter than non- recycled mills such as CR-PS, VP-PS. This is to be expected since recycled mills (RN-PS) contains a large amount of ash and fibres in the sludge, which are mechanically disintegrated during the recycling process.

Table 3-4: Physical Characterization of Paper sludge samples collected

	Birch virgin fibres [1]	Soft wood virgin[2]	RN-PS	CR-PS	VP-PS
Moisture content (%)	NA	NA	2.11 ± 0.01	3.93 ± 0.04	5.72 ± 0.02
Bulk density after drying (g/cm^3)	30.2	25.5	150.56 ±0.08	120.24 ± 0.04	60.23 ± 0.06
Fibre length (mm)	1.19	3.6	0.15 ± 0.01	0.86 ±0.02	1.01 ± 0.02

Paper sludge: RN - PS = Recycle newsprint sludge from Kimberly-Clark (Pty), CR-PS = Corrugated recycle pulp paper sludge from Mpact (Pty), and VP-PS = Virgin pulp from Sappi (Pty). 1 - (Migneault *et al.*, 2010), 2 - (Horn and Setterholm, 1990)

The results suggest that Kraft mills (VP-PS) seems to be the best candidate for fibreboards because it has the longest average fibre length despite the lower bulk density. VP-PS is generated from virgin pulp and it does not involve any process that could result in shortening of the fibres. Migneault *et al.*, (2010) also found that VP-PS was best suited to produce medium density fibreboards because of the average fibre length.

3.3.2 Paper sludge chemical characteristics

There were variations in the chemical composition in particular the ash, hemicelluloses, lignin, extractives and other chemical components present in the three types of PS (*Table 3-5*). The PS form Kraft mill, VP-PS, had the highest cellulose content (47.22 %w/w) compared to CR-PS (27.85 %w/w) and RN-PS (12.84 %w/w) (*Table 3-5*). These results are expected since Kraft mills use chemical pulping techniques that aim to produce fibres with high content of cellulose. A high cellulose content indicates the presence of high amounts of cellulose fibres within the PS, which is desirable to produce good quality low-density particleboard manufacturing. Therefore, based on the fibre length analysis (*Table 3-4*) and the high cellulose content (*Table 3-5*), the combined results suggest that the VP-PS would be suitable for low-density particleboards production. However, a high cellulose content also indicates the ability to hold water due to its fibrous structure and hygroscopic nature depending on the type of PS, which can potentially affect the physical properties of the composite boards produced.

Table 3-5: Chemical characterization of paper sludge samples collected

	Birch virgin fibres [1]	Soft wood Virgin[2]	RN-PS	CR-PS	VP-PS
Cellulose (% w/w)	-	-	12.84 ± 0.16	27.85 ± 0.04	47.22 ± 0.14
Hemicellulose (%w/w)	-	-	4.11 ± 0.05	8.53 ± 0.08	9.21 ± 0.03
Lignin (% w/w)	18	28.5	7.37 ± 0.05	18.28 ± 0.03	18.49 ± 0.05
Extractives (% w/w)	5	6.3	3.23 ± 0.09	5.31 ± 0.10	6.46 ± 0.14
Ash content (%w/w)	0.3	0.3	64.40 ± 0.05	29.90 ± 0.02	8.11 ± 0.03

Paper sludge: RN - PS = Recycle newsprint sludge from Kimberly-Clark (Pty), CR-PS = Corrugated recycle pulp paper sludge from Mpact (Pty), and VP-PS = Virgin pulp from Sappi (Pty). 1 - (Migneault *et al.*, 2010), 2 - (Horn and Setterholm, 1990)

The PS from VP-PS had a lignin content (18.49 %w/w) that was comparable to CR-PS (18.28 %w/w), but higher than RN-PS (7.37 %w/w). These results were comparable to previous studies done by Williams (2017) who found lignin composition of 19% w/w for VP-PS and 20 % w/w for CR-PS and 9.89% w/w for RN-PS. Other studies such as those conducted by Migneault et al.(2010) Boshoff et al. (2015) reported similar results. The Kraft pulping process is designed to chemically remove lignin, and therefore it produces sludge that is high in cellulose and very low lignin content. However, VP-PS (Kraft sludge) as seen in Table 3-5 contains a significant amount of lignin. This is not uncommon as previous authors have attributed the results to the presence of materials such as shives, which contain lignin and these can be found in Kraft sludge (Migneault *et al.*, 2010). Later investigations by Williams (2017) and Migneault et al. (2011) have attributed the relatively high lignin content in VP-PS to an over estimation of the lignin amount as a result of the use of the NREL analysis method, which is designed for wood and pulp and not waste material such as PS that have high ash content (Geng *et al.*, 2007a). In comparison with more traditional feedstock such as Birch virgin fibres sourced from mechanical pulping as seen in Table 3-5, both VP-PS and CR-PS had lignin content very similar to natural feedstock. This could be advantageous because lignin is known to have natural adhesive capabilities relatively similar to more traditional feedstock, which could be advantageous to composite board production (Abdullah *et al.*, 2015).

All the PS samples had significantly higher ash content than the Birch virgin fibres (*Table 3-5*). Notably, the highest ash content was found in RN-PS (64.40 %w/w) compared to CR-PS (29.9 %w/w) and VP-PS (8.11 %w/w). Low ash content sludge such as VP-PS usually originates

from Kraft mills, where papermaking fillers are not generally added during the pulping process. While high ash content sludge, generally above 30%, general originates from recycled mills such as RN-PS where papermaking fillers utilized during the pulp and paper making process (Boshoff, 2015; Ridout, 2016; Williams, 2017; Bester, 2018). In order to understand what the composition of inorganic component in PS samples, XRF analysis was done and results presented in *Table 3-6*.

Table 3-6: The inorganic composition of paper sludge samples collected from the mills from XRF analysis

	Inorganic content (wt. %)										
	Al_2O_3	CaO	Cr_2O_3	Fe_2O_3	K_2O	MgO	MnO	Na_2O	P_2O_5	SiO_2	TiO_2
RN-PS	1.42	32.67	-	0.23	0.02	0.63	0.01	0.03	0.05	2.43	0.08
CR-PS	3.43	9.15	-	0.25	0.07	0.47	0.01	0.07	0.09	5.21	0.48
VP-PS	1.1	0.6	-	0.25	0.12	0.13	0.01	0.85	0.05	2.58	0.06

Paper sludge: RN - PS = Recycle newsprint sludge from Kimberly-Clark (Pty), CR-PS = Corrugated recycle pulp paper sludge from Mpact (Pty), and VP-PS = Virgin pulp from Sappi (Pty).

Majority of the ash is made up of non-woody material such as fillers removed during the pulp and paper process. The XRF analysis shows that the ash content is mainly comprised of calcium oxide (CaO), which is in significant amounts in RN-PS. According to Ridout et al, (2016) the CaO found in ash from Kimberley-Clark (RN-PS) mainly occurred in the form of calcium carbonate ($CaCO_3$) attributed to the fillers added during paper production, prior to fibre recycling. The higher the ash content, the lower the fibrous content within the PS, which mainly is the cellulose fibres needed for the integrity of the particleboard (Table 3-5). Consequently, PS with high ash content may not favour low-density particleboard manufacturing but may be useful for making medium to high-density boards. On the contrary, the ash content could possibly act as a filler to enhance the performance of the boards.

In addition to the carbohydrate composition, the three PS showed variation in the functional groups based on FTIR spectra. The FTIR spectra of the raw PS from the different pulp and paper mills were compared in the wavelength ranges between 4000 and 650 cm^{-1} (Fig 3-1). The PS originates from woody materials, thus there are distinct absorbance peaks identified in accordance with typical wood and pulp spectra (Popescu *et al.*, 2007; Bouafif *et al.*, 2008; Migneault *et al.*, 2011).

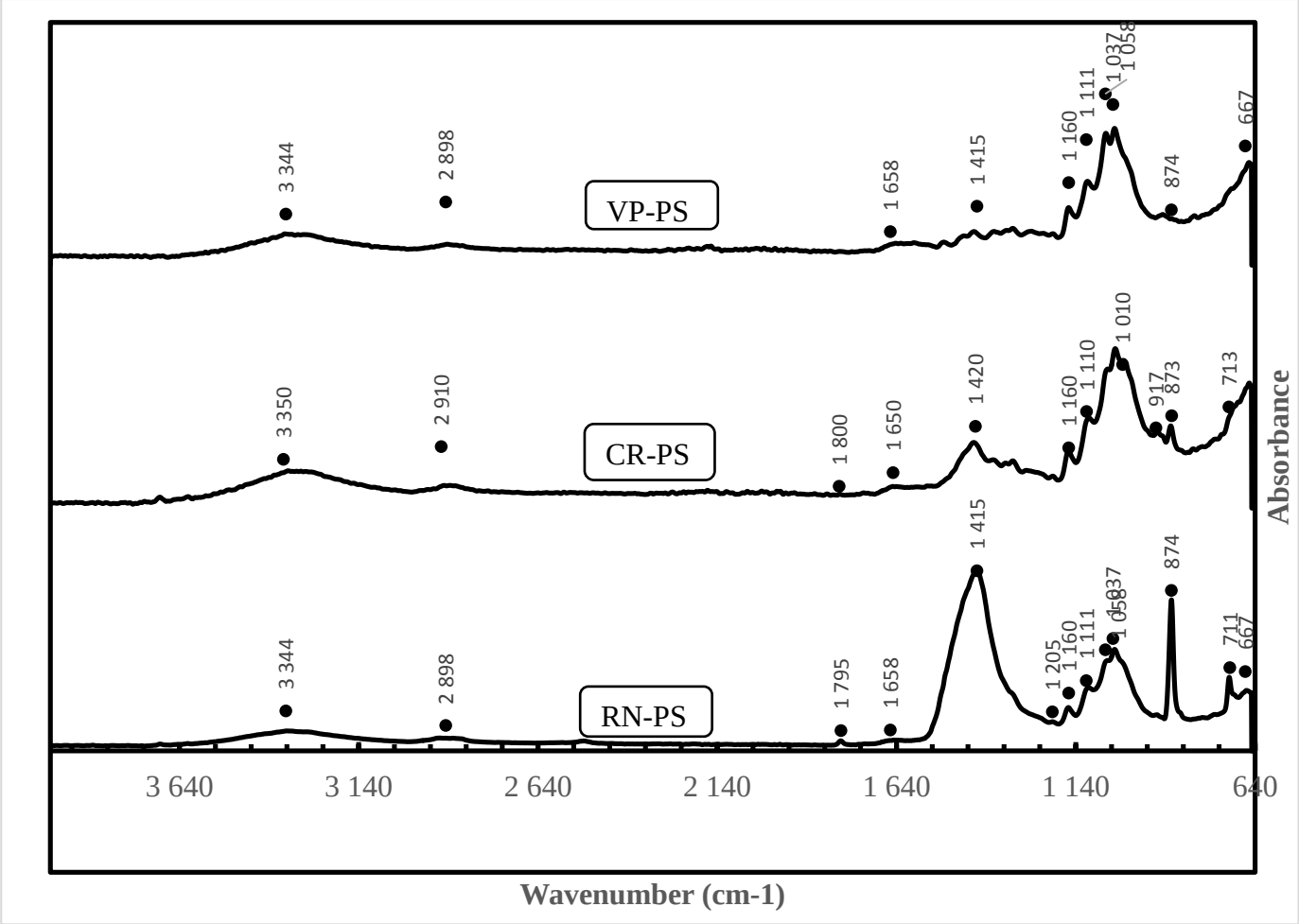

Figure 3-1: FTIR spectra of paper sludge sourced from pulp and paper mills showing the prominent peaks at characteristic wavelengths numbers.

(In the Figure VP-PS =Virgin Pulp paper sludge sourced from Sappi: Ndogwana mill, CR-PS = Corrugated recycle paper sludge source from Mpact: Springs mill, RN-PS =Recycled Newspaper print paper sludge sourced from Kimberly-Clark: Springs mill)

The spectra show distinct bands attributed to intermolecular O-H and N-H bond stretching centred at 3344 cm^{-1} and relatively broad and small peak appeared at 2898 cm^{-1} attributed to methyl/methylene bonds from C-H stretching bands as shown in Fig 3-1. These bands generally originate from a contribution of lignocellulosic components in the PS. It is therefore difficult to observe any significant difference between the PS samples within this region. However, between 2000 and 600 cm^{-1} there are distinct differences observed from the PS samples. Table 3-7 describes the distinct peaks as seen in Figure 3-1and assigns functional groups to specified regions on the FTIR spectrum (Shi *et al.*, 2011).

Table 3-7: The characterisation of major bands from FTIR spectra peaks of the three different paper sludges studied

Wavenumber (cm^{-1})					
RN-PS	CR-PS	VP-PS	Typical Regions (cm^{-1})	Band assignment	Polymer
3344	3350	3344	O-H (alcohols): 3650- 3200 O-H (carboxylic acid): 3300-2500	OH- groups including absorbed water, aliphatic alcohols found in carbohydrates and lignin, aromatic alcohols in lignin and extractives and carboxylic acids in extractives [b]	Lignin [f]
2898	2910	2898	C-H (symmetric): 2938 – 2920 C-H (asymmetric): 2840 - 2835	Present in aromatic methoxyl groups and in methylene/methyl side chains [a]	Lignin [f]
1795	1800	NA	C=O (conjugated): 1770-1760 C=O (unconjugated): 1740 - 1720	Assumed to be carbonyl bands of acetyl groups in hemicellulose and carbonyl aldehyde in lignin and extractives. [a]	Hemicellulose [f]
1658	1650	1658	H_2O:1650-1640	Assigned to water in lignin or cellulose [a]	Lignin [f]
1415	1420	~1415	C-H (Aromatic): 1430-1422	C-H asymmetric deformation in lignin [d and c]	Lignin [f]
1205	NA	NA	OH (plane): 1205 - 1200	O-H plane found in cellulose [a]	Cellulose, Hemicellulose [f]
~1160	~1160	~1160	C-O-C (in cellulose): 1162-1125	C-O-C bonds in cellulose or asymmetric stretching found in cellulose and hemicellulose [a and d]	Cellulose, Hemicellulose [f]
1110	1110	1111	C-H: 1128-1110	Aromatic C-H band stretchers	
~1037	~1010	~1036	C-O: 1015-1060	C-O-C, C=C and C-C-O stretching found in cellulose, hemicellulose and lignin [d] and C-O stretches found in cellulose, hemicellulose and lignin [c]	Cellulose, Hemicellulose, Lignin [f]
874	873	874		Glycosidic linkages found in hemicellulose [d] or C-O bend of carbohydrates [e]	Hemicellulose [f]

Adapted from a = (Popescu *et al.*, 2007); b = (Bouafif *et al.*, 2008); c = (Shi *et al.*, 2011); d =(Yang *et al.*, 2015); e=(Reig *et al.*, 2002), f = (Carrillo *et al.*, 2004)

According to Figure 3-1, there are significant differences in the relative intensities of the spectrum at 1415 cm^{-1} assigned to aliphatic C-H bands and aromatic skeleton in lignin vibrations. It was observed that RN-PS in this region has a very sharp and the highest intensity peak compared to CR-PS and VP-PS. Other lignin peaks (1795, 1658, 1415, and 1267 cm^{-1}) were observed in RN-PS but are weaker for CR-PS and even weaker or non-existent for VP-PS. The lack of presence of lignin peaks in VP-PS is expected since the sample originates from Kraft pulp mills that aim to remove lignin content during the production stages (Migneault *et al*., 2011). As previously mentioned, this contradicts with the NREL chemical composition analysis that showed 19% of lignin content for VP-PS (as shown in Table 3-5). However, this has also been previously reported by Migneault *et al.* (2011) that determined that similar acid extraction methods detailed by the NREL method, may be over estimating the presence of lignin (Jackson and Line, 1997).

3.3.3 Board properties

3.3.3.1 *Board density*

A summary of the average board densities obtained with PS blending is presented in Figure 3-2. The British standard for cement bonded boards require the density to be at least 1 g/cm^3. RN-PS boards were the only boards to meet the minimum requirement at an average of 1.07 g/cm^3 for all three fillers calcium carbonate ($CaCO_3$), fly ash (FA), and silicon fume (SF). The boards made from CR-PS (0.97 g/cm^3) and VP-PS (0.58 g/cm^3) did not meet the minimum requirement for cement bonded particle boards, but were rather classified as low and medium density boards according to the American standard (ANSI A208.2-2009) for particle boards (ANSI A208.2-2009, 1999).

Statistical analysis showed that there was significant ($p<0.05$) difference in board density among all three types of boards, i.e. paper sludge type had significant influence on the density. The difference could be attributed to the difference between the bulk densities of the paper sludges, with RN-PS (150.56 ± 0.08 cm^3) having the highest bulk density compared to CR-PS (120 ± 0.04 g/cm^3) and VP-PS (60.23 ± 0.06 g/cm^3) as shown in Table 3-4, which produce the board with highest density. Migneault et al., (2010) reported that the bulk density of material would have significant influence on the density of the board. However, the statistical analysis showed that there was no significant differences between the types of filler utilised.

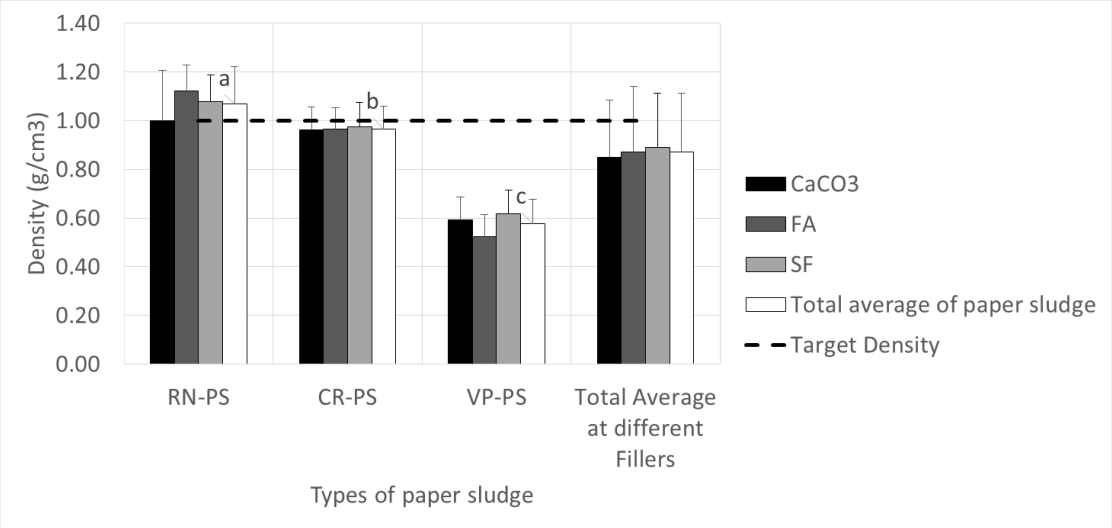

Figure 3-2: Density of the boards.

(Bars with different letters are significantly different ($p<0.05$) from each other after analysis of variance (ANOVA) and pairwise mean comparison by Tunkey's Honestly Significant Difference (HSD) method. Pair-wise comparison was done both the different types paper sludge combination labels as a-b-c and different filler combination labelled as A-B-C.)

The effects of the process conditions (binder ratio, fibre ratio, filler content, temperature) on board density was analysed using fitted response model, surface plots and Pareto charts. From the ANOVA table (Appendix A: **Error! Reference source not found.** and **Error! Reference urce not found.**), surface plots and Pareto chart (Figure 3-3), filler content and fibre ratio had the most significant influence ($p<0.05$) on board density for RN-PS boards. The results show that at a constant filler loading, the board's density continues to decrease with an increasing fibre ratio and because both linear and quadratic filler effect are significant, the density decreases up until a fibre ratio of five. As the fibre ratio increases, the board is loaded with more fibre and less binder which is much denser than fibre. Increase fibre ratio increases void spaces and therefore the boards are lighter reducing density up until a fibre ratio of 5. Beyond this point, it is believed that void spaces within the boards become filled up and thus increasing the weight, which increases the density.

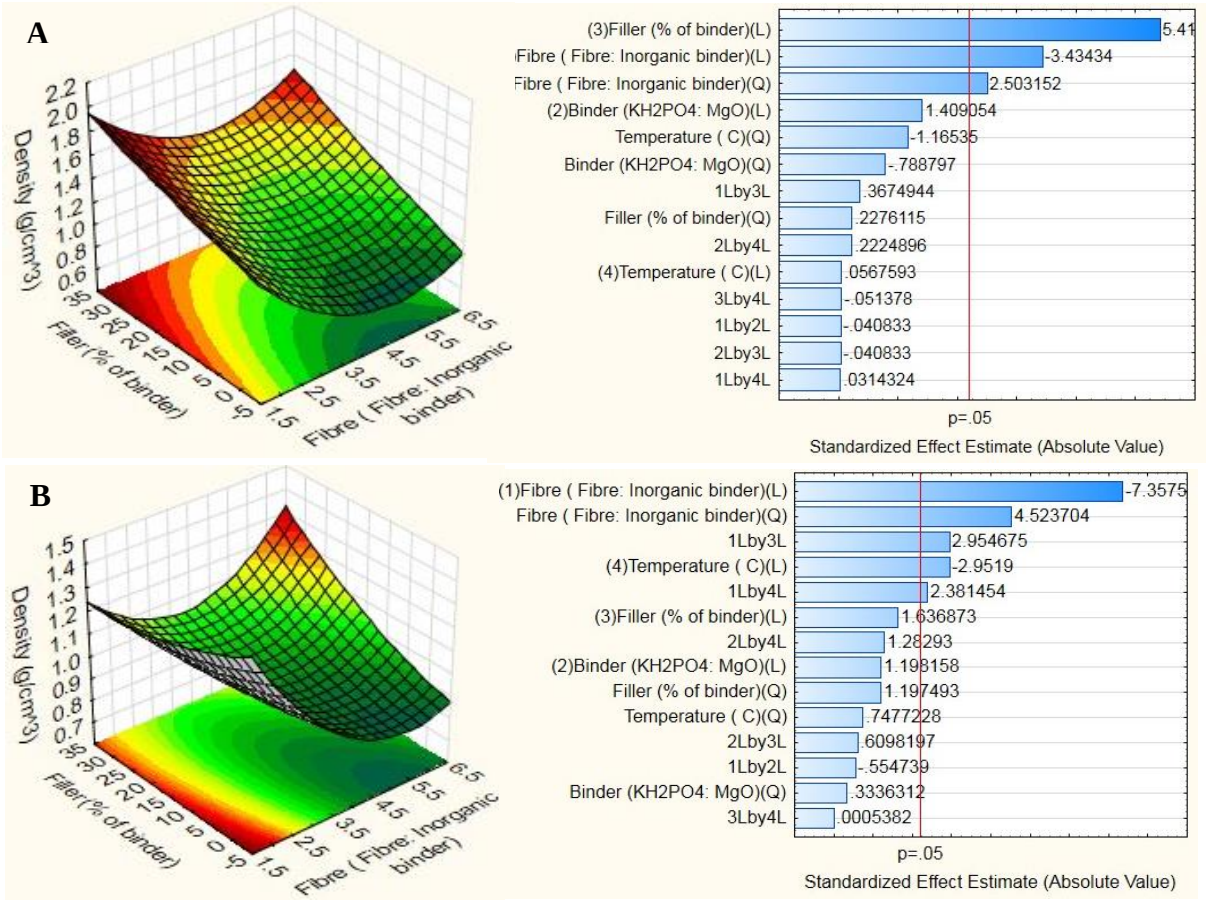

Figure 3-3: Surface plots of density for A) RN-PS with CaCO3 and B) CR-PS with CaCO3

The results in Figure 3-3 (A) show that at a constant fibre ratio, density increases with increasing filler loading. This suggest that because of the fineness of the filler such as $CaCO_3$, it fills up void spaces within the cementing crystal structure, thereby improving the particle packing and thus increasing the density of the boards (Antoni *et al.*, 2015). Similar trends in the RSM plots and Pareto analysis (Figure 3-3 B) and effects was observed for CR-PS cement bonded board, which showed fibre ratio had the most significantly ($p<0.05$) influence on the density. Similar trends were observed for fly ash and silicon fume (illustration in Appendix section)

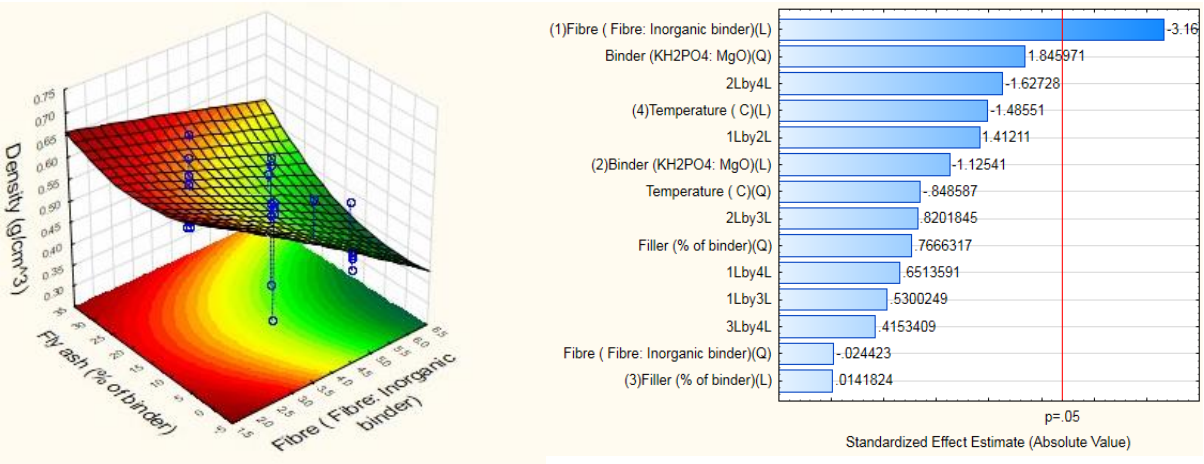

Figure 3-4: A) Response Surface Plots and B) Pareto analysis for density with VP-PS boards loaded with SF

For VP-PS with SF boards Figure 3-4 ANOVA analysis (**Error! Reference source not found.**) nd Pareto chart also showed that fibre ratio had the most significant ($p<0.05$) influence on density. The RSM plot shows that if the fibre ratio increases to 10% filler content, the density of the board's decreases. This suggest that at high fibre ratio, the boards contained less phosphate cement binder, which is much denser than cellulose fibres. Donahue and Aro (Donahue and Aro, 2010) observed a similar relationship, confirming why VP-PS boards had the lowest average board density.

3.3.3.2 *Mechanical properties*

The modulus of elasticity (MOE) and modulus of rapture (MOR) of the composite boards are shown in Figure 3-5 and Figure 3-6 respectably. The produced boards did not meet the requirements for cement bonded boards at 1 g/cm^3 with MOE of 4000 MPa and MOR of 9 GPa (EN 634-2) for particle board, according to the international standard with MOE of 2 200 MPa and MOR of 15 MPa (ISO 16893: 2016). The results showed a superior MOE ranging from 200 to 800 MPa contrasted with Amiandamhen et al., (2017) study with MOE of 67.02–196.48 MPa. MOR results ranged from 0.15 to 1.5 MPa, which was very similar to Amiandamhen et al., (2017) study of 0.61 to 1.44 MPa. Overall, it appears that the inclusion of different types of PS and increased pressing temperature in this study compared to Amiandamhen et al., (2017) where only CR-PS was used and pressing at room temperature, had a positive influence on the mechanical properties.

The results also show that the addition of PS in MKP cement and filler has a negative influence on the mechanical strength properties of the MKP cement bonded boards, compared to

traditional cement bonded board with no PS (Geng *et al.*, 2007a; Migneault *et al.*, 2010). This observation was also supported by Amiandamhen et al., (2017), who observed lower MOE of 67.02–196.48 MPa and MOR of 0.61 to 1.44 MPa compared to results. The researchers reported the possibility that in order to meet the required standard, an increase in binder ratio and decrease in fibre ratio would increase better bonding and therefore increase strength properties.

Statistical analysis (shown in Figure 3-5 and Figure 3-6) indicated that there was significant ($p<0.05$) difference between the different types of paper sludge with RN-PS boards producing superior MOE and MOR, compared to CR-PS and VP-PS boards. Previous reports by Migneault et al., (2010) found that mechanical panel properties were strongly negatively influenced by the ash content within PS. Migneault et al., (2010), additionally reported that an increase in ash content (non-fibrous material) within the paper sludge reduces the fibrous material and thus less woody material available for bonding. RN-PS contains the highest amount of ash content (63%), which could adversely influence the adhesive nature of the cement paste. However, these results (Figure 3-5 and Figure 3-6) suggest that paper sludge with high ash content and low fibre (RN-PS) were actually stronger than PS with low ash content and higher fibre content (VP-PS). This could be due to the fact that since the ash within RN-PS contains highest amounts $CaCO_3$ (XRF analysis of the PS in Table 3-6), it could be possibly reacting with KDP to form phosphate cements, and acting as an active filler. It is also possible that the ash content within the PS could be beneficial to the mechanical properties by either acting as an inert filler to improve particle packing and therefore improve compressive strength (Aminadamhen et al., 2016).

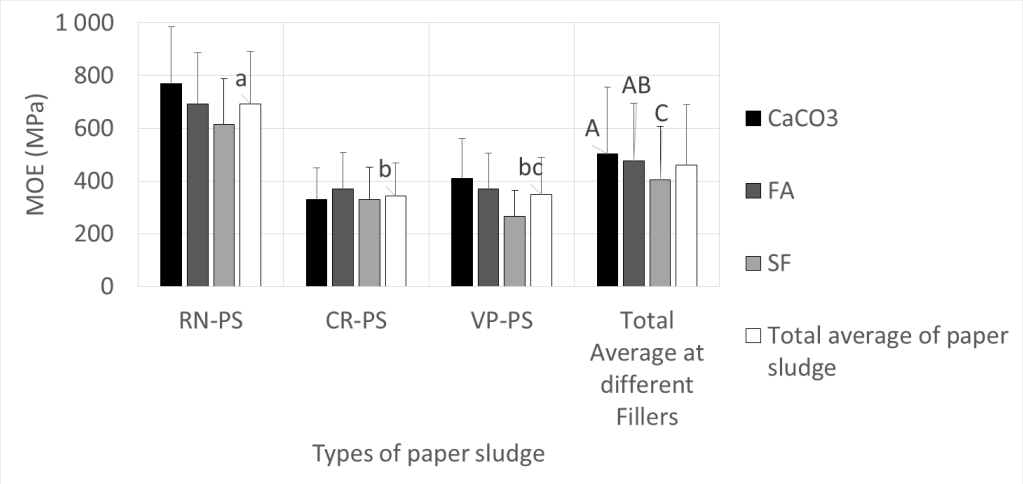

Figure 3-5: The boards Modulus of Elasticity (MOE). Bars are averages ± SD.

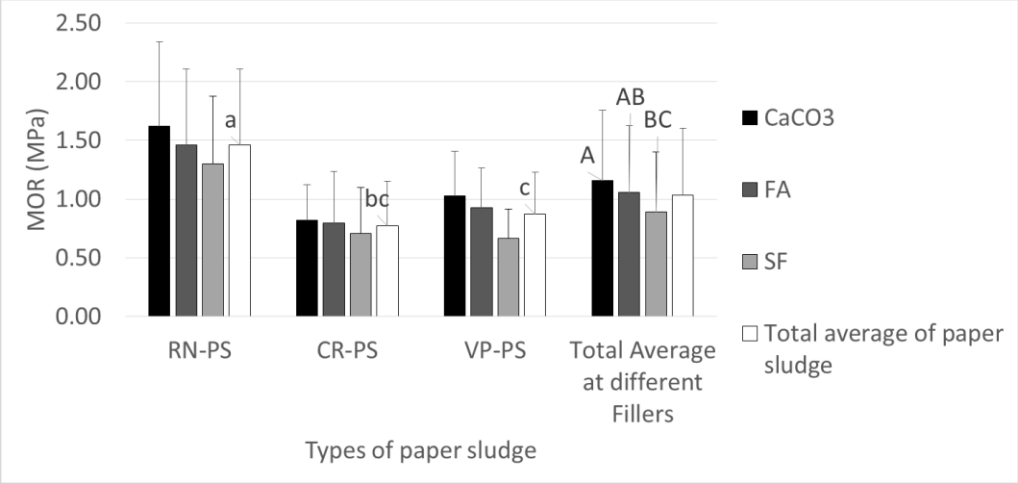

Figure 3-6: The boards Modulus of Rapture (MOR) on the right.

Further analysis also showed that there was statistical significant differences with regards to the performance of the different types of fillers (Figure 3-5 and Figure 3-6). The results showed that boards loaded with $CaCO_3$ as a filler produced the highest overall bending strength compared to fly ash and silica fume. This suggest that the presence of high levels of calcium within the $CaCO_3$ compared to FA and SF, produces the highest strengths to the boards. Similar observations were made by Wagh (Singh and Wagh, 1998), who reported superior mechanical and physical properties with class C fly ash that contained higher levels of calcium carbonate and low level of carbons when compared to class F fly ash. The presence of calcium carbonate seemed to participate in the setting reaction in a similar manner to MgO and forms calcium phosphate cements, which contribute to the strength of the boards (Singh and Wagh, 1998). This would agree with experimental results with RN-PS loaded with $CaCO_3$, which produces the highest strength with both RN-PS and $CaCO_3$ containing the highest content of calcium (Table 3-6). This was further explored when comparing the XRD of various samples with various fillers in the subsequent sections.

XRD analysis is shown in Figure 3-7, which illustrates the diffraction peaks comparing different fillers ($CaCO_3$, FA, and SF), MKP cements and cement bonded boards with RN-PS. The XRD profiles (as shown in Figure 3-7) show that $CaCO_3$ had the most intense and sharpest peaks with the greatest peak area, which suggests better crystal structure and minimal macrostrain defects within the crystal structure compared to FA and SF (Barnes et al., 2019). SF had a single broadened peak that indicate an amorphous phase and non-uniform crystal structure, with the presence of defects in the crystal structure. Ding et al. (Ding *et al.*, 2012) identified using XRD analysis, the presence of MKP and unreacted MgO in both amorphous

and crystalline phases. The combination of both phases indicates the formation of continuous crystalline structures and absence of voids in the grains as seen in XRD (Figure 3-7) and is supported by other previous studies (Ding and Li, 2005; Ding *et al.*, 2018). This combination implies greater strength properties due to the formation of continuous and stable continuous crystalline structures (Chau *et al.*, 2011). The mechanical superior performance and denser board property (as seen in Table 3-8) of RN-PS with $CaCO_3$ imply that there was much better particle packing compared to FA and SF.

From the XRD analysis (Figure 3-7), all the investigated board samples had variation in the crystal characteristics for all the combination of filler (FA, $CaCO_3$, and SF), raw material and pure MKPC. Xu et al., (2015) explained that better mechanical performances can be largely attributed to the formation of MKPC main products such as k-struvite (as seen in Figure 3-7). It is clearly from the figure that boards made with RN-PS and filled with $CaCO_3$ had the most similar crystal structure and shape to MKPC crystal. This further confirmed that the inclusion of RN-PS filled with $CaCO_3$ had the least interference in the formation crystal structure of k-struvite crystal and therefore provided the highest flexural strength. This was evident in XRD spectra that showed that RN-PS with $CaCO_3$ had the most similar MKPC crystal peaks characteristic. Thus producing the strongest boards within the highest flexural strength closest to pure MKPC as seen in Table 3-8.

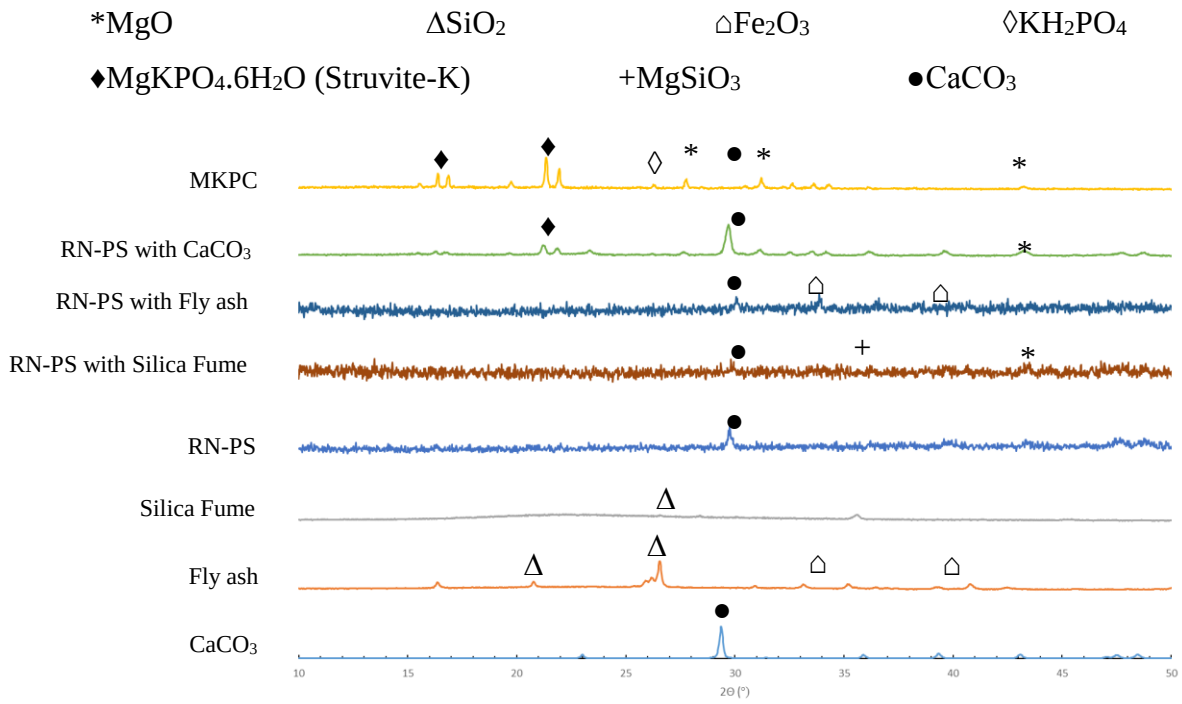

Figure 3-7: XRD spectra of RN-PS with different fillers (k-struvite products are identified from comparing with literature and previous studies on MKPC (Ding *et al.*, 2012; Yue *et al.*, 2014; Le Rouzic *et al.*, 2017)*)*

Statistical models represented by polynomial equations were plotted (Figure 3-8,

Figure 3-9, Figure 3-11 and Figure 3-12), which show the relationship among the independent variables (fibre ratio, binder ratio, filler, temperature) and response variables (MOE and MOR). The effects of the process conditions on MOE and MOR was also further analysed using ANOVA (shown in Appendices A: **Error! Reference source not found.**, **Error! Reference urce not found.**, **Error! Reference source not found.** and **Error! Reference source not found.**), which showed that binder ratio and fibre ratio had significant ($p<0.05$) influence on the MOE for RN-PS loaded with $CaCO_3$. RSM plot shows (Figure 3-5) that an increasing binder ratio has a positive effect on the resulted mechanical strength. This was in agreement with previous investigations that found positive correlation increasing between binder ratio and MOE or/and MOR (P. K. Donahue and Aro, 2010; Amiandamhen et al., 2016). Increasing the binder ratio, (KH_2PO_4:MgO) increases the amount of K-struvite product due to the fact that KH_2PO_4 is the limiting reagent (Xu *et al.*, 2015). Thus more KH2PO4 results in the formation of more MKPC products and results in better adhesive strength. Xu et al., (2015) reported that at higher binder ratio, there is a possibility of growth of main k-struvite product as well as the growth of other crystal formations resulting in better mechanical performance(Singh and

Wagh, 1998). Sigh and Wagh, (1998) further reports that better mechanical performances of MKPC composite with calcium carbonate could be due to the combination of magnesium phosphate cements forming, and the possible reactions between phosphates and calcium to form calcium phosphate cements. However, when comparing the XRD's (Figure 3-7) of pure MKPC cement to RN-PS made with $CaCO_3$, no additional distinctive peaks is evident in the composite to conclude the presence of calcium phosphate cement products. The flexural strength test results suggest that superior flexural strength of RN-PS with $CaCO_3$ compared to with FA and SF could be due to additional product formation. The products could be difficult to identify from XRD due to being in the amorphous phase or have distinct peaks overlapped by other products.

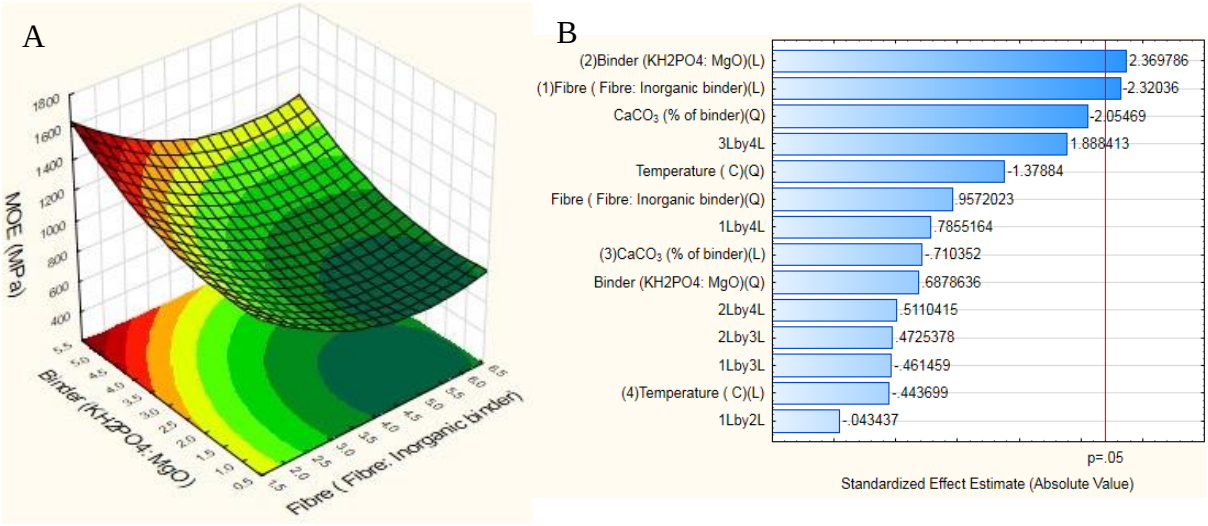

Figure 3-8: Response surface plot and Pareto chart showing the effect of variables on the MOE of RN-PS boards using CaCO3 as filler

In terms of MOR, the RSM plot and Pareto chart shown in

Figure 3-9 show that temperature, fibre ratio, filler content and binder had significant influence ($p<0.05$) on the MOR. The data suggest that there is an optimum filler loading 15% and temperature of 100^{o}C that produces the highest possible MOR. This is due to the ability of $CaCO_3$ to increase the early strength of the cement by increasing the acceleration effect and high rate of hydration (Singh and Wagh, 1998).

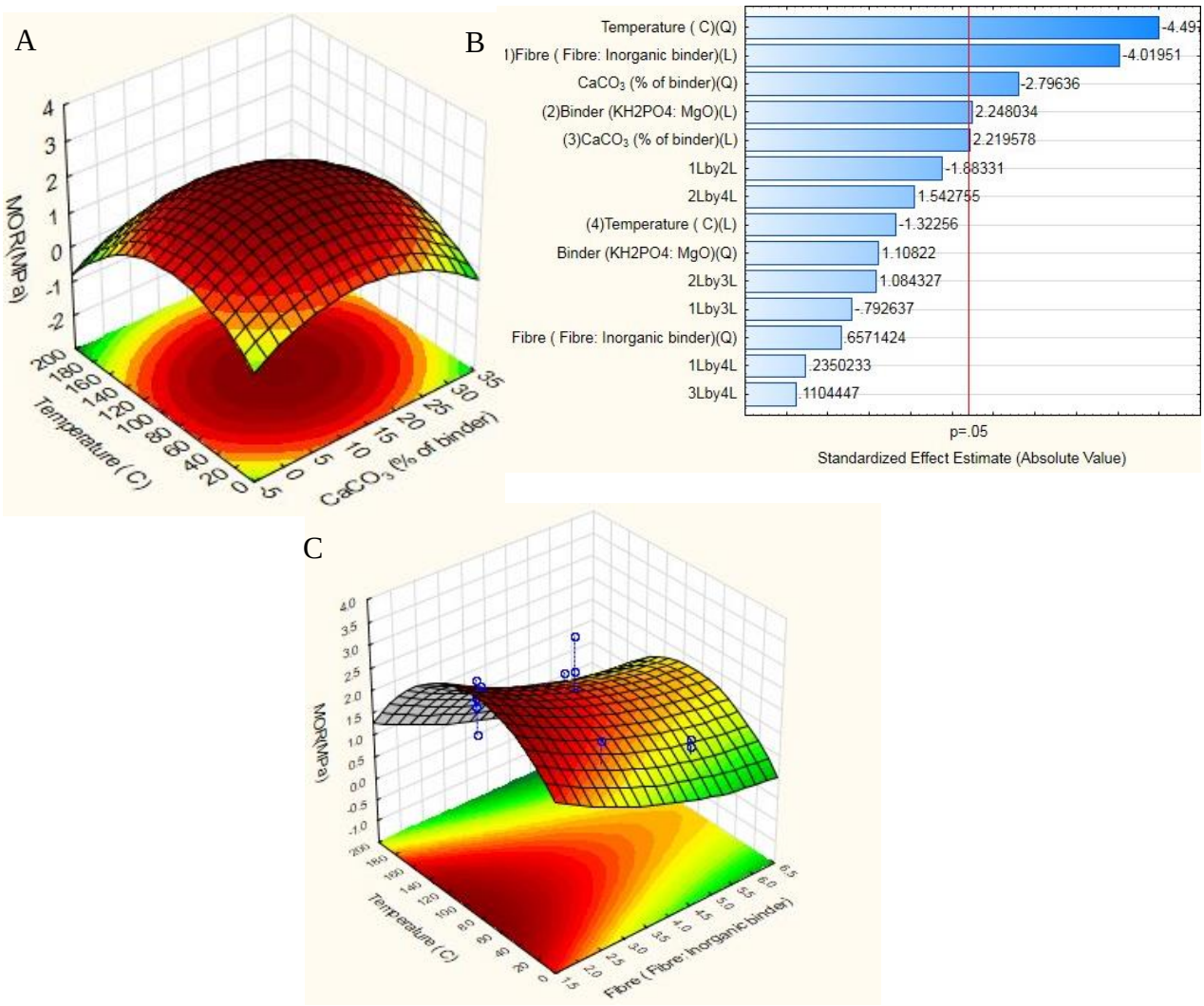

Figure 3-9: RSM plots and Pareto chart of MOR for RN-PS: CaCO3 boards

The surface plots of the models predicting MOR from RN-PS boards loaded with fly ash and the associated Pareto analysis, are shown in

Figure 3-9. From the Pareto analysis (

Figure 3-9, B) it can be seen that pressing temperature and fibre ratio had the most significant ($p<0.05$) influence on MOR. The linear fibre ratio effect was a significant influence on MOR such that as the fibre ratio decreases, the MOR decreases (

Figure 3-9, C). This should be expected since increasing fibre decreases binder component, making the board weaker. The quadratic temperature dominates the linear effect when the model predicts that when temperature increases, MOR increases up until a certain point. RSM plots (

Figure 3-9, A) trends show that maximum MOR of 3 MPa is achieved at temperature of approximately 100 °C and minimum fibre ratio of 1.5. In this instance, beyond a certain temperature the environment is not conducive to produce maximum performing boards. This could be that at extremely high temperatures, the board become brittle due to the spring back effect suggesting that the binder is not set.

Figure 3-10 displays the XRD diffraction diagram of boards that were made of similar conditions but different temperatures. When analysing XRD (Figure 3-10), it is evident that RN-PS boards formed at 100 °C had similar crystal shape to higher strength MKPC crystal shape when compared to RN-PS boards produced at 25 ^{o}C. Figure 3-10 revealed more evidence of k-struvite crystals in boards produced at 100 °C compared to those produced at 25°C especially around 20 degree (2Theta) with taller and sharper peaks(Vickers et al., 2019) than the others. The evidence of more k-struvite crystals results in much better physical and mechanical strength(Donahue and Aro, 2010; Ding *et al.*, 2012; Amiandamhen, 2017).

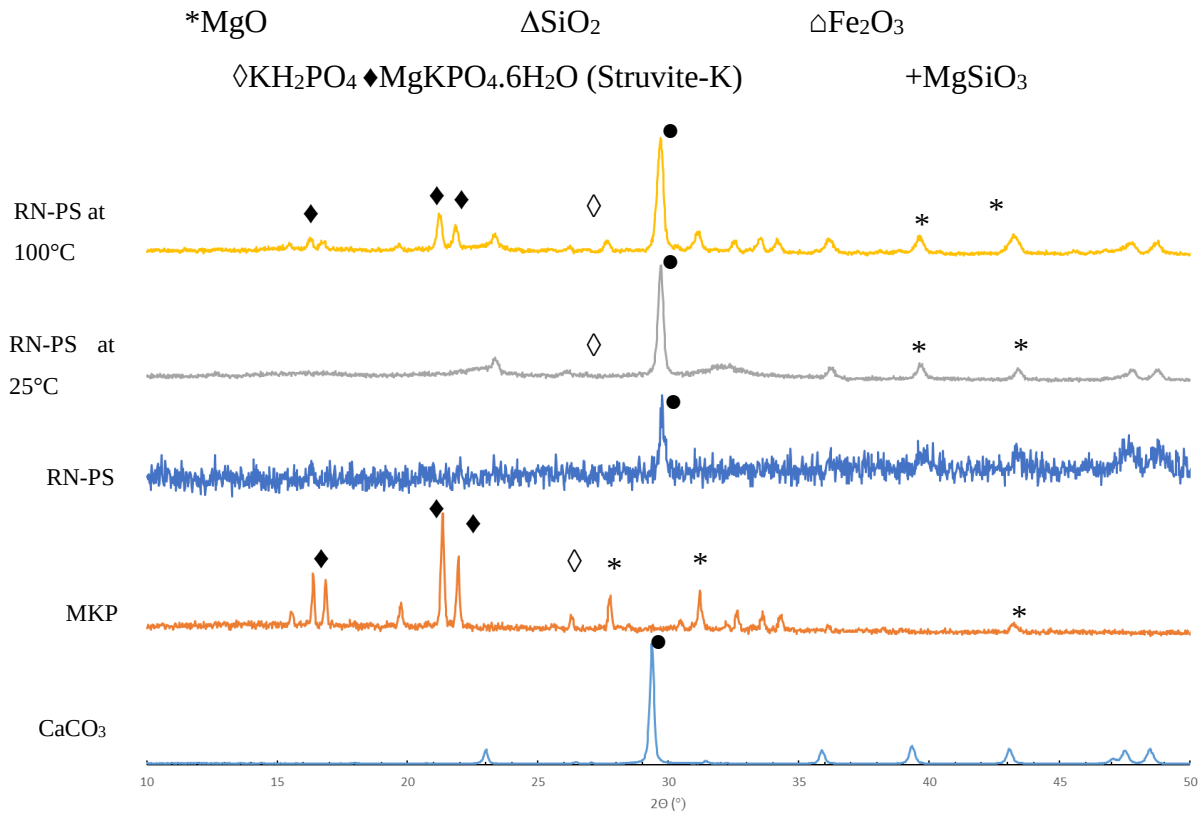

Figure 3-10: XRD spectra of RN-PS at different temperature

Pressing temperature also played a vital role in the development of inter-fibre bonding. The results show that high temperature increase flexural strength of the boards (Figure 3-6). Zhou

et al., (2011) found that pressing temperature had indeed a significant role in compressive strength of bio composite. Comparing to past investigations done by Amiandamhen et al., (2016), the investigated composite boards had superior mechanical strength properties where similar type of PS-cement was utilized and the only difference was the board pressing temperature. Elevated temperature showed on average an improvement from 131.8 MPa to 600MPa (as shown in Table 3-8. Previous research have reported that compressive strength is heavily dependent on the presence of lignin content present in biomass due to its natural adhesive ability (Zhou *et al.*, 2011). The lignin content are significantly different for each sample and High pressing temperatures soften the ligno-cellulosic structure, creating better lignin distribution, and therefore enhancing better bonding between fibres. Results in Table 3-5 all showed presence of lignin within the PS used in this investigation. Furthermore, pressing at high temperatures for RN-PS physically soften/loosens the hard dried PS similar to small stones, allowing for better mixing with the binder and board pressing resulting in stronger boards. Unlike VP-PS, after being dried were still physically "fluffy" fibres and therefore no physical benefit for pressing at high temperature.

RSM plot shows that maximum MOR is achieved at fly ash replacement of 15% and high binder ratio (

Figure 3-9); any higher loading of fly ash results in decrease in mechanical strength. Other studies have also reported similar conclusion that fly ash is beneficial to improve the mechanical performance but beyond a certain loading, performance is affected (Donahue and Aro, 2010; Amiandamhen *et al.*, 2016). There have been different reports for the optimum ratio of fly ash in phosphate based cements with Amiandamhen et al. (Amiandamhen *et al.*, 2016) showing that 20% fly ash could be added, while Donahue and Aro (Donahue and Aro, 2010) found that 40- 45% replacement of binder had a positive influence on MOR. The difference could be the fact that the PS investigated in this study had already higher ash content and therefore, required less FA as a filler to be added to replace MKPC.

Fly ash is made up of components such as SiO_2, Al_2O_3 and CaO that when interacted with KDP, could produce compounds such as potassium alumina silicate hydrates, calcium phosphate and aluminium phosphate in the composite product which could have beneficial influence on mechanical performance (Xu *et al.*, 2015). In particular, the CaO contained within fly ash has been known to produce amorphous calcium phosphate. Even though, XRD analysis in Figure 3-7shows very little evidence of additional peaks between RN-PS with fly ash

compared to raw RN-PS and fly ash. Other main solids could overlap the characteristic peaks of additional cement products(Xu *et al.*, 2015).

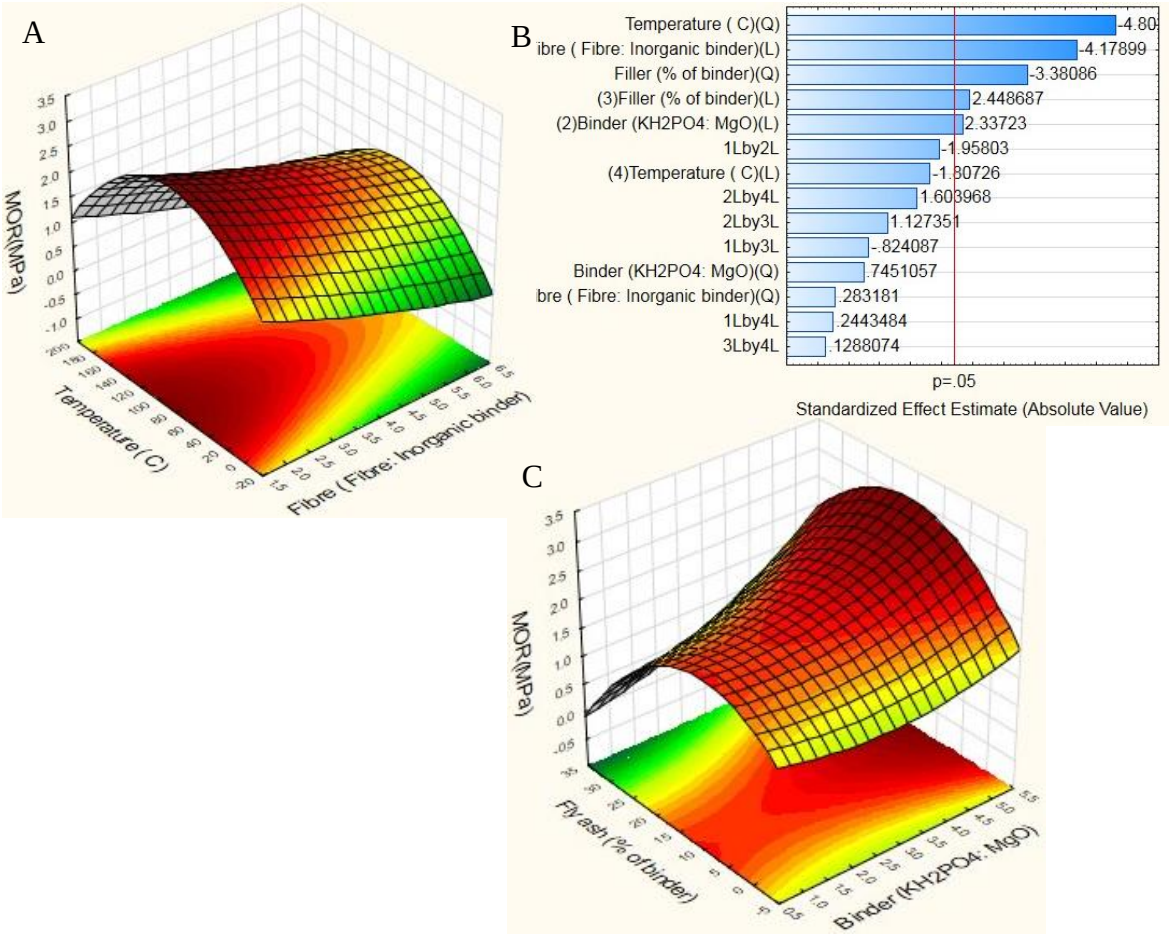

Figure 3-11: Response surface plot and Pareto chart showing the effect of variables on the MOR for RN-PS with Fly ash

For composite boards loaded with silica fume, ANOVA analysis found that temperature, fibre ratio and silica fume (% of binder) had a significant influence on the MOR. RSM plot shows that maximum MOR is achieved with a combination of the temperature of 100°C, high binder ratio of five and silica replacement of 15%. From the XRD analysis (shown in Figure 3-7) and previous research (Zheng *et al.*, 2016), silica fume is known to contain SiO_2. Mechanical strength test (shown in Table 3-8) has shown that the addition of silica fume produces the weakest boards. The addition of silica fume to the system could be having a chemical effect on the PS-cement bonded boards and resulting of silica inhibiting the formation of k-struvite and instead MgO reacting with SiO_2 to form weaker $MgSiO_3$ (as shown in Figure 3-7) during the hydration reaction compared to main product of k-struvite (Zheng *et al.*, 2016).

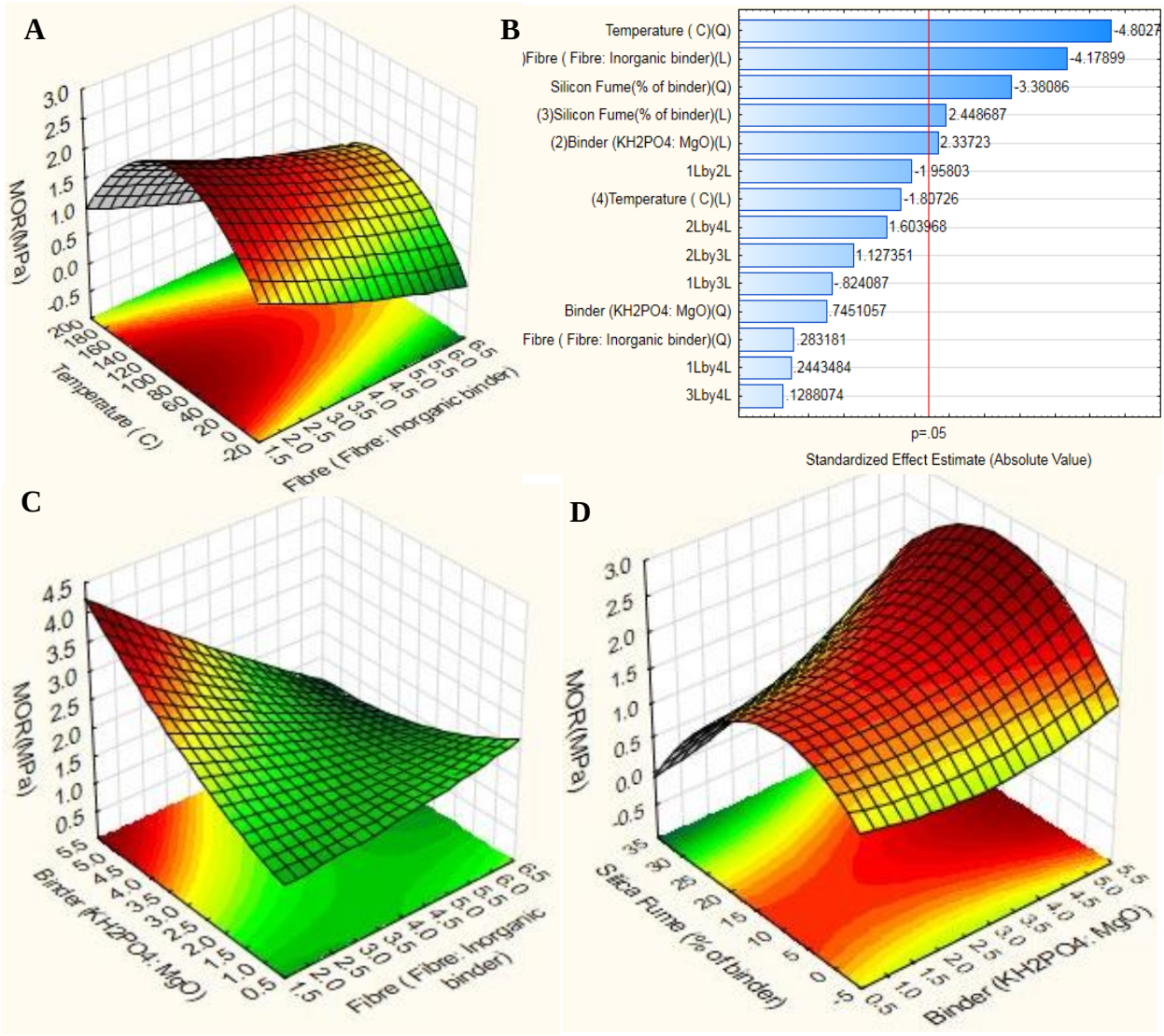

Figure 3-12: Response surface plot and Pareto chart showing the effect of variables on the MOR for RN-PS with Silica Fume

Thus, from the mechanical properties it is clear that the boards were not able to meet the specification. Results show that PS with high ash content such as RN-PS had superior performance compared to the other types of PS. In addition, the results show that among the PS candidates tested, composites with $CaCO_3$ seems to be the best performing candidates for the bio-composite production. As previously discussed, the interaction between $CaCO_3$, PS and KDP seems to be beneficial to the mechanical strength properties. Similarly, other investigations have found that $CaCO_3$ leads to better overall mechanical performance because of the additional strength provided by phosphate cements (Xu *et al.*, 2015).

3.3.3.3 *Physical properties*

Physical properties such water absorption (WA), thickness swelling (TS) and volume swelling (VS) determine the suitability utilising board composites under humid conditions and has influence on the mechanical strength properties (Ashori et al., 2012). These properties namely, WA, TS and VS are heavily dependent on the water-holding capacity (WHC) of the composite samples. The WHC is directly related to the combination of hydrophilic nature of fibres in PS and hydrophobic nature of the matrix and phosphate cement. Cement-bonded particle boards are known to be highly resistant to absorbing moisture (damp proof) and have excellent drying capabilities but are not completely water resistant (ITT, 2019). The inclusion of PS which contains hydrophobic nature from cellulose content increases the board's ability to absorb more water. Cellulose structures within paper sludge are known to trap water between the cellulose fibrils due to the large surface area that binds water (Williams, 2017). This observation was confirm by Pareto analysis and RSM (Figure 3-13, Figure 3-17 and Figure 3-15) that firstly show that fibre ratio (PS: binder) had the most significant influence on physical properties. Secondly, WA, TS and VS increase with increase in fibre ratio (increase inclusion of PS into composite sample) as a results of weaker interfacial bonds (Mohammed, 2015). The extent to which the addition of PS influenced the board's properties were different due the significant differences in the chemical and physical properties of the PS.

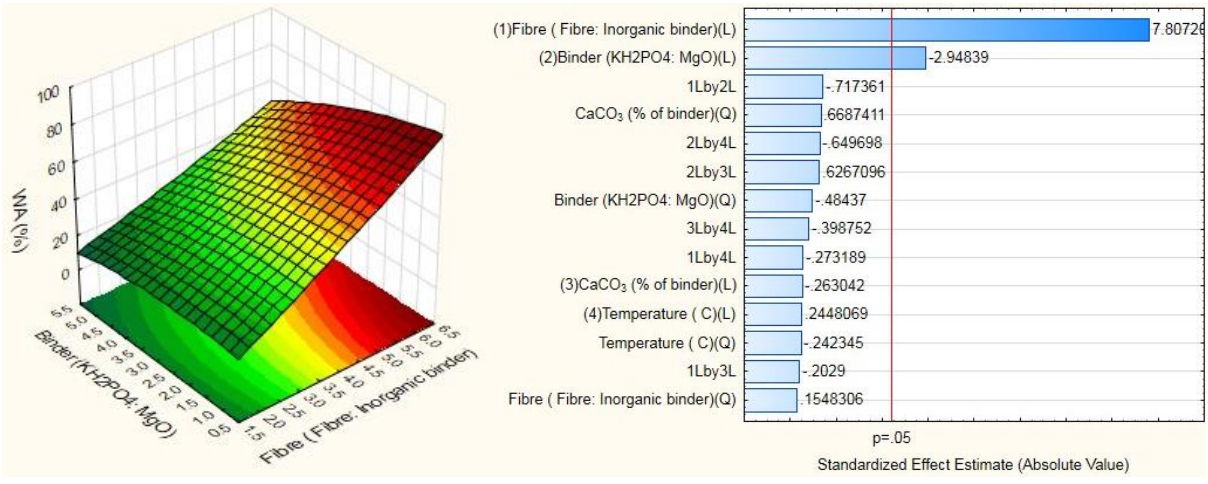

Figure 3-13: Response surface plot and Pareto chart showing the effect of variables on the WA for CR-PS with Calcium Carbonate

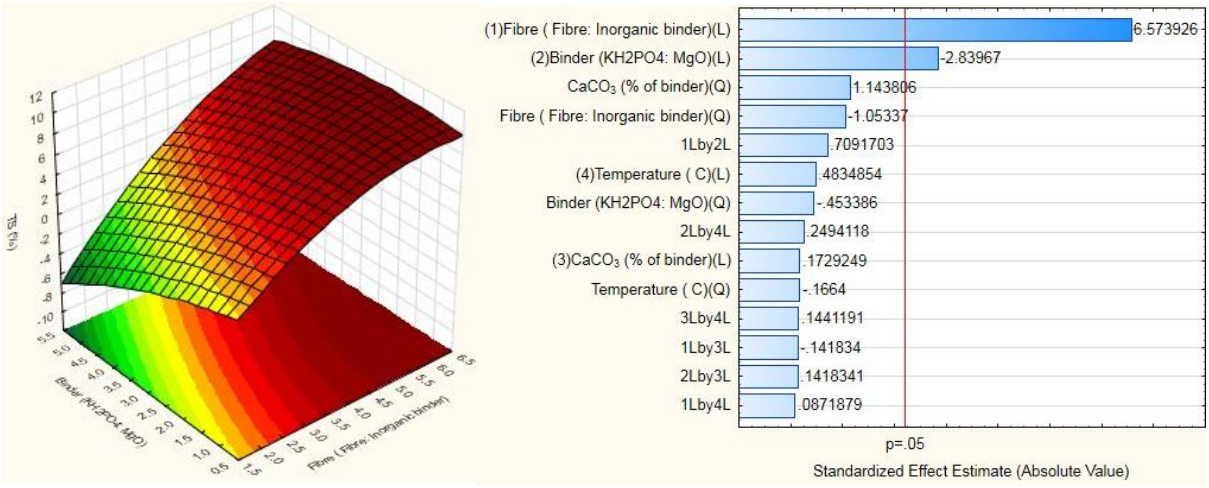

Figure 3-14: Response surface plot and Pareto chart showing the effect of variables on the TS for RN-PS with $CaCO_3$

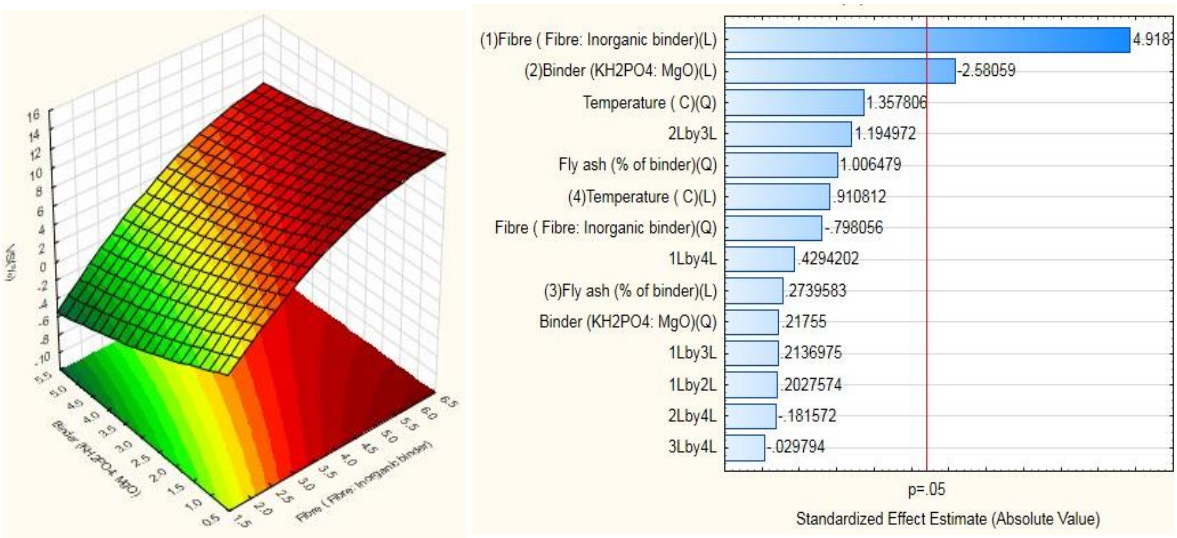

Figure 3-15: Response surface plot and Pareto chart showing the effect of variables on the VS for VP-PS with Fly ash

The experimental results for WA, TS and VS are shown in Figure 3-16, Figure 3-17 and Figure 3-18 , respectively. The results clearly show that on average VP-PS had the highest WA, TS and VS, and was statistically ($p<0.05$) different from RN-PS and CR-PS. Our results are consistent with previous results that show that the inclusion of VP-PS which contained the longest fibre lengths due to chemical pulping process and high cellulosic content had the highest WHC and thus absorbed the most water (Williams, 2017). While, because of the reduced cellulose content and hydrophobic nature of fillers and ink particle (ash content) which are found in larger properties in RN-PS (as seen in Table 3-4 and Table 3-5) had the lowest WA, TS and VS.

According to the ASTM D1037-99 particleboard standard for general use, the maximum WA should be less than 60%. On average, all the boards exhibited lower WA than the allowable maximum of 60% as seen in Figure 3-16. Based on EN634-2 standard for cement bonded particleboards which required maximum WA of 25%, none of the board samples were able to meet that standard. In terms of TS, board sample were able to meet the maximum allowable TS of 25% for ASTM D1037-99, 19% for ISO 16893:2016 standard, 15% for the British standard EN-634-2, at 14% for EN-317 board standard. They did not meet the TS standard allowable standard of 8%, for MDF made for interior use such is home decking,

As previously stated, statistical analysis showed that physical properties were significantly influenced by fibre ratio and binder ratio. Therefore to minimize physical properties such WA, TS and VS, the fibre ratio needs to be lowered, and increase in binder ratio as is seen in Figure 3-13, Figure 3-14 and Figure 3-15. This concurs well with Amiandamhen et al., (2016) and findings by several other previous researchers corroborated the initial finding that low cement: wood ratio (high fibre ratio), increases the likelihood of wood particles not being encapsulated by hydrophobic cement and therefore are exposed to more water, which increased the WA(. Donahue and Aro, 2010).

The aforementioned observations can be linked back to the findings on density and mechanical strength (Frybort et al., 2008). By increasing binder ratio, one increases density by increasing the compactibility and minimizing porosity thus, reducing WA by limiting exposure of fibre to moisture. This links back to mechanical performance, where increasing binder ratio, positively influences MOE and MOR and thus, making the board mechanically stronger. Taking all the observation into consideration, one can conclude that even though the boards were not able to meet the mechanical strength requirements, they were able to meet the physical property standard for particleboard used for general application with minimal load bearing requirement.

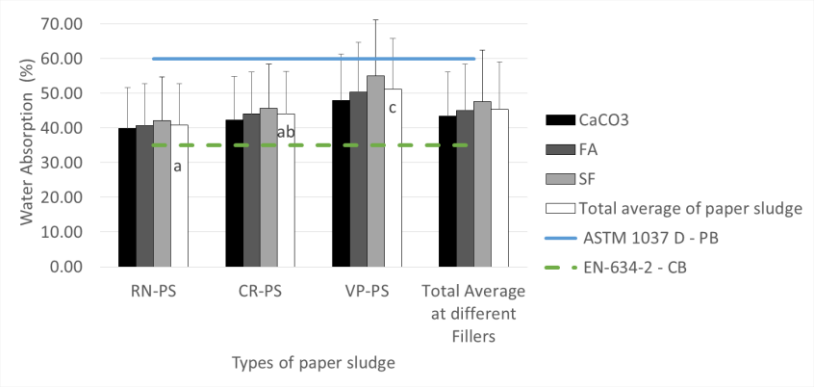

Figure 3-16: Water Absorption (WA) of the boards. Bars are averages ± SD.

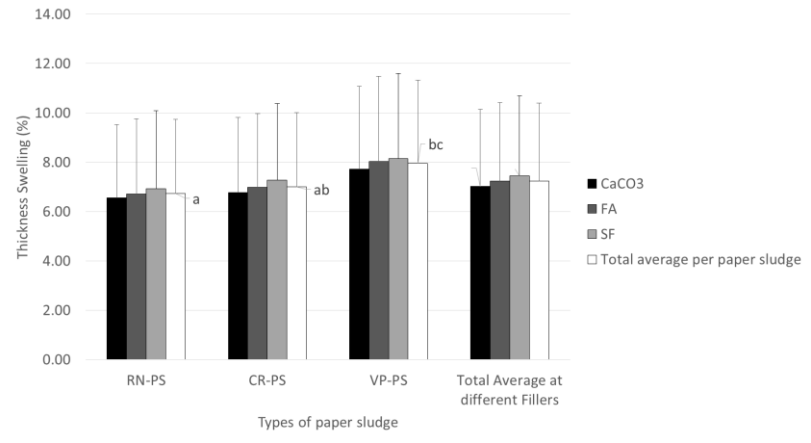

Figure 3-17: The boards Thickness Swelling (TS). Bars are averages ± SD.

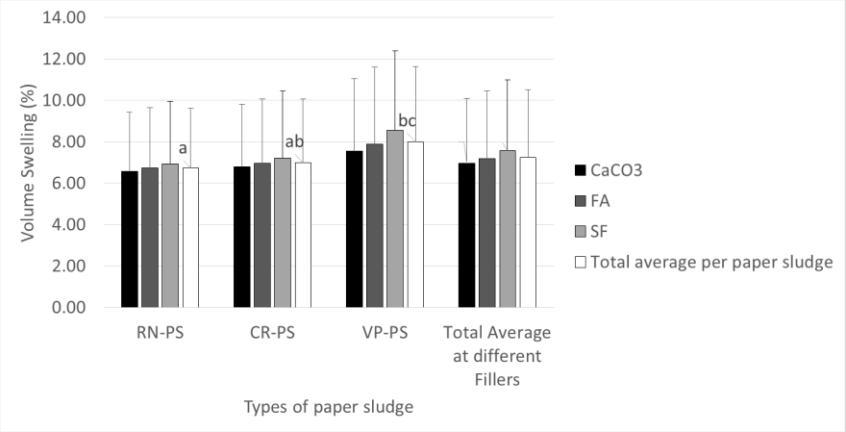

Figure 3-18: The boards Volume Swelling (VS). Bars are averages ± SD.

Table 3-8: Physical and mechanical properties of measured boards

Filler	$CaCO_3$			FA			SF			Standard (EN-634-2-2007)	Standard (ISO 16893:2016)
Paper sludge type	RN-PS	CR-PS	VP-PS	RN-PS	CR-PS	VP-PS	RN-PS	CR-PS	VP-PS		
Density (g/cm^3)	1.00	0.96	0.59	1.12	0.96	0.52	1.08	0.97	0.62	1	1
MOE (MPa)	768.69	328.42	410.52	691.82	356.56	369.47	615.72	317.34	266.84	4000	2200
MOR (MPa)	1.62	0.82	1.03	1.46	0.79	0.92	1.30	0.71	0.67	9 GPa	15
WA (%)	39.85	42.30	45.59	40.77	41.72	47.98	42.14	43.41	52.78	35	19
TS (%)	6.56	6.78	7.71	6.71	6.98	8.02	6.93	7.27	8.14	1.5	
VS (%)	6.57	6.79	7.54	6.72	6.95	7.87	6.94	7.21	8.56		

Paper sludge: RN - PS = Recycle newsprint sludge from Kimberly-Clark (Pty), CR-PS = Corrugated recycle pulp paper sludge from Mpact (Pty), and VP-PS = Virgin pulp from Sappi (Pty).

Fillers: $CaCO_3$ = Calcium Carbonate, FA = Fly ash, SF = Silicon Fume

Board properties: MOE = Modulus of Elasticity, MOR = Modulus of Rupture, WA = Water Absorption, TS = Thickness Swelling, VS = Volume Swelling

3.3.4 Optimisation

ANOVA analysis presented in (Appendix A: Table 7-6 for CR-PS, Table 7-7 for RN-PS and Table 7-8 for VP-PS) show that process conditions i.e. fibre ratio, binder ratio, filler ratio and temperature did have a significant ($p<0.05$) influence on the physical and mechanical property of the boards. Several factors had significant influence on the performance of the boards. Therefore, in order to maximise the performance, an optimisation of the process conditions is needed.

Optimisation of process parameters was carried out by using the predicted and desirability profiles of the response variables (board performance parameters) in order to maximise the performance of the boards. As previous results have stated, there are varying effects and interactions depending on type of the sludge and fillers used. For further analysis, only $CaCO_3$ filler system were considered for further analysis since it showed the most promising results as previously discussed. Optimum board performance was defined by maximizing density and mechanical properties (MOE, MOR) , and minimizing physical properties (WA, TS and VS).The board performances were weighted equally and no limits were placed on the board performance indicators to attain the maximum performing board possible. As a result, optimum process conditions could fall outside the range of investigated parameters.

Optimized board manufacturing process conditions (described in Table 3-9) indicated that a fibre ratio of 1.94, a binder ratio of 5.07, filler loading of 20% and board press temperature of 180 °C , were required for RN-PS. Under these optimum process conditions, the statistical model predicted Density of 1.6 g/cm^3, MOE of 1367 MPa, MOR of 4.92 MPa, WA of 18.86%, TS of -2.58% and VS of -0.18%. For CR-PS, optimized board manufacturing conditions indicated that a fibre ratio of 1.94, a binder ratio of 5.07, filler loading of 22.5% and board press temperature of 90 °C, was required. Under these optimum process conditions, the statistical model predicted Density of 1.27 g/cm^3, MOE of 583.9 MPa, MOR of 1.55 MPa, WA of 21.1%, TS of -2.9% and VS of 0.36%. For VP-PS, optimized board manufacturing conditions indicated that a fibre ratio of 1.94, a binder ratio of 5.05, filler loading of 15% and board press temperature of 25 °C, was required. Under these optimum process conditions, the statistical model predicted Density of 0.75 g/cm^3, MOE of 752 MPa, MOR of 2.29 MPa, WA of 16.57%, TS of -7.4% and VS of 0.09% (results shown in Table 3-10).

The analysis showed that in order to achieve optimum process condition a threshold fibre load is limited to fibre ratio of 1.942 or PS loading of 66% (w/w) for all the different type of PS,

which is lower than the reported optimum of 3.34 for 74% (w/w) PS loading for CR-PS by previous study Amiandamhen, Meincken and Tyhoda, 2016). The low fibre ratio results in more binder required but boards produced resulted in superior flexural strength from reported literature with similar board production (Amiandamhen *et al.*, 2016). Thus, the boards could be made with more PS loading, reducing the amount of the cement binder utilised.

Table 3-9: Optimised board manufacturing process conditions obtained from Central Composite Design

	Fibre (Fibre: Inorganic binder)	Binder (KH_2PO_4: MgO)	Filler (% of binder)	Temperature (°C)
RN-PS	1.94	5.07	20	180
CR-PS	1.94	5.07	22.5	90
VP-PS	1.94	5.05	15	25

An optimum binding ratio of approximately 5 is predicted to produce optimum board performance for all the types of PS, which was significantly higher than previous investigations that previously reported optimum binder ratio of 3 with natural fibres added to the system (Wagh and Jeong, 2003; Donahue and Aro, 2010). Thus, given the difference in the composition of the boards, higher binder ratio is required to maximise mechanical strength that uses a system of PS only. The inclusion of only PS into the system without natural fibres increases inorganic matter and therefore will require higher binder ratio to create better environment. Optimum press temperature was significantly different for the type of sludges. As previously explained, due to the differences in physical and chemical composition of PS, produced significantly different process conditions.

According to the process conditions, validation experiments were carried out and results are presented in Table 3-10. In general, models were suitable for variables such as density, MOE, MOR and water absorption as the they differed by less than 26% except for VP-PS with WA showing actual results being 45% greater than predicted (as shown in presented in Table 3-10). Some models did not fit well (as shown in Appendix section) with the data, which would explain major differences observed between predicted and experimental. Models for TS and VS, incorrectly predicted negative values, which is inaccurate, and therefore no desirable profiles were used for optimisation.

Based on optimum process conditions , mechanical properties (MOE and MOR) improved from average experimental results shown in Table 3-8 from 200-800 MPa to 620–1290 MPa for MOE and from 0.15 to 1.5 MPa to 1.95 – 4.92 Mpa for MOR, but did not meet the minimum required for cement-bonded boards according to the British standard. On the other hand, the results further show that the boards met the minimum requirement for physical properties such as WA , TS and VS according to the British standard (EN-632-2007) that requires Density of 1 g/cm^3, MOE of ≥ 4000 MPa, MOR of ≥9 MPa, WA of ≤ 35% and TS of ≤ 1.5% , and the particle board according to the international standard (ISO 16893:2016) that requires Density of 1 g/cm^3, MOE of ≥ 2200 MPa, MOR of ≥15 MPa, WA of ≤ 19% and TS of ≤ 19% as can be seen in Table 3-10. According to the board properties, the boards were deemed suitable for, ceilings and wall partition application with no load bearing capability according to international standard (ISO 16893:2016) since none of the mechanical strength properties meet the standard. It is clear that all the three types of sludge have shown the potential to be used for commercial use with load-bearing properties. Further modifications such as adding veneers layers, strength properties can be improved by 3-4 folds and therefore meet minimum strength requirements as shown by previous studies (Mngomezulu, 2019)

Table 3-10: Physical and Mechanical properties measure from experimental runs designed from optimised process conditions

Filler Paper sludge	CaCO3							
	RN-PS		CR-PS		VP-PS			
	Actual	Model	Actual	Model	Actual	Model	Standard (EN-634-2: 2007)	Standard (ISO 16893:2016)
Density (g/cm3)	1.5	1.6	1.23	1.27	0.74	0.75	1	1
MOE (MPa)	1290	1367.4	620	583.9	742	751.62	≥4000	≥2200
MOR (MPa)	4.12	4.92	2.1	1.55	1.95	2.29	≥9	≥15
WA (%)	23	18.86	26	21.14	30	16.57	≤35	≤19
TS (%)	1.22	-2.58	2.12	-2.94	2.54	-7.4	≤1.5	
VS (%)	1.42	-0.18	2	0.36	4	0.09		

In order to understand the chemical changes during the formulation of the product and pressing of sludge, spectra of PS sludges before hot pressing), composite board after pressing (optimum condition and weak bonded board) were compared.

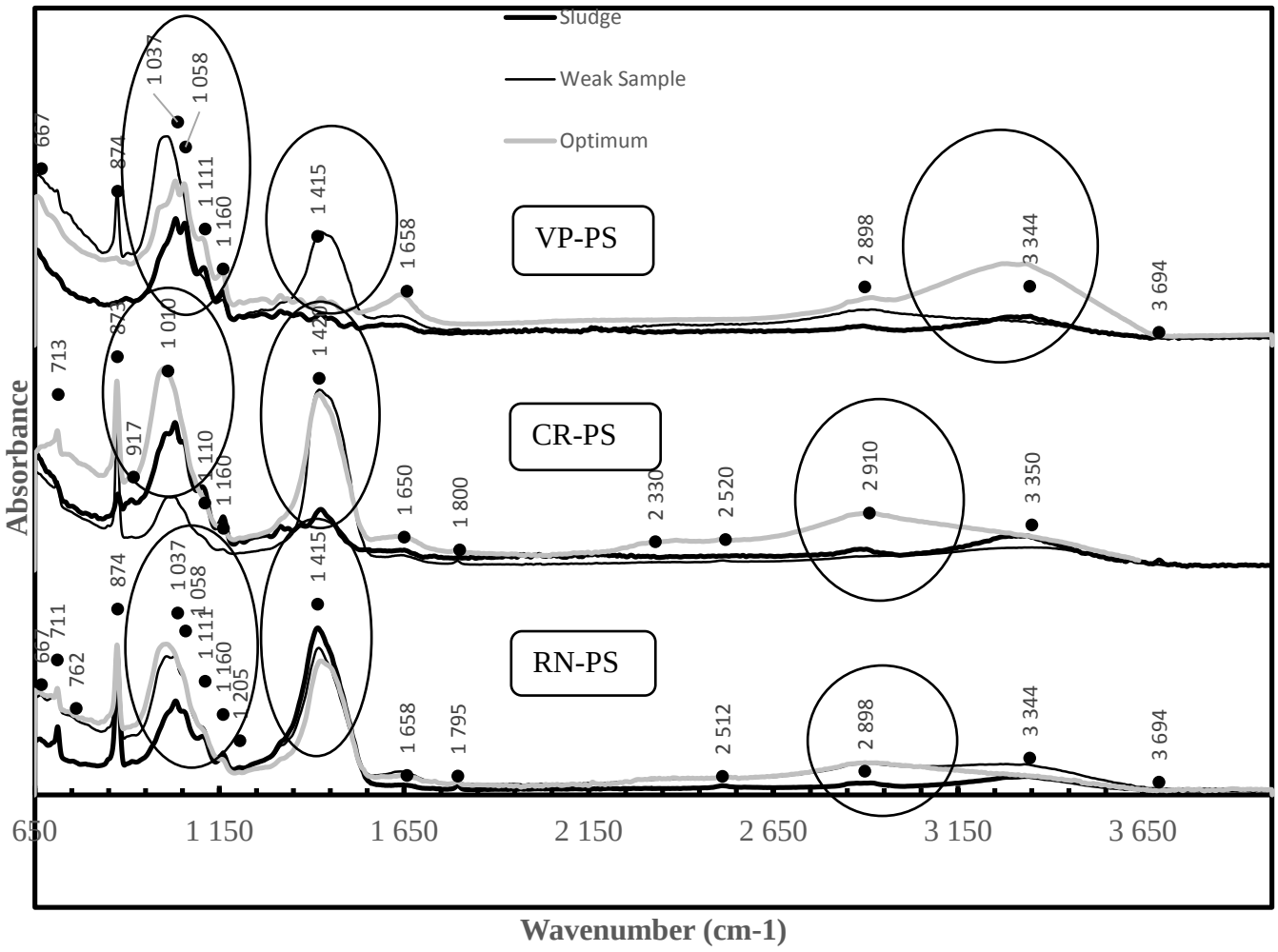

Figure 3-19: Fourier Transformed Infra-Red (FT-IR) spectra of the various samples. (In the Figure VP-PS =Virgin Pulp paper sludge sourced from Sappi: Ngodwana mill, CR-PS = Corrugated recycled paper sludge sourced from Mpact: Springs mill, RN-PS =Recycled Newspaper print paper sludge sourced from Kimberly-Clark: Springs mill)

From Figure 3-19 the biggest differences between sludge before board production and optimum condition were noted in three distinct regions namely around the 1150 cm^{-1} , 1415 $cm^{-1}$and around 3344 cm^{-1}. The differences around 1150 cm^{-1}, commonly assigned to C-H aromatic stretches, were more prominent for RN-PS board. The difference could be attributed to the formation of more new chemical bonds during the formulation and pressing of the boards. The

difference between optimum and raw PS sample around the 1415 cm^{-1} region is more prominent for CR-PS samples. This region is commonly associated with is aromatic C-H rings, which does suggest too that for CR-PS board samples, there was a production of chemical products. Differences around 3344 cm-1 between sludge and optimum condition samples for all three types of PS was noticed but it was more prominent for VP-PS. This region is commonly associated with OH- groups including absorbed water, aliphatic alcohols. According to Migneault et al., (2011), these changes could be attributed to the increase in hydrogen bond patterns. Increase presence of OH groups, increases the likelihood of hydrogen bonds, results in strong attraction to water molecules and therefore increasing the water holding capacity of the boards. The increase water holding capacity increases WA in the boards produced. This is evident with higher WA evaluated for VP-PS compared to RN-PS and CR-PS, due to the strong hydrogen bonds between water molecules.

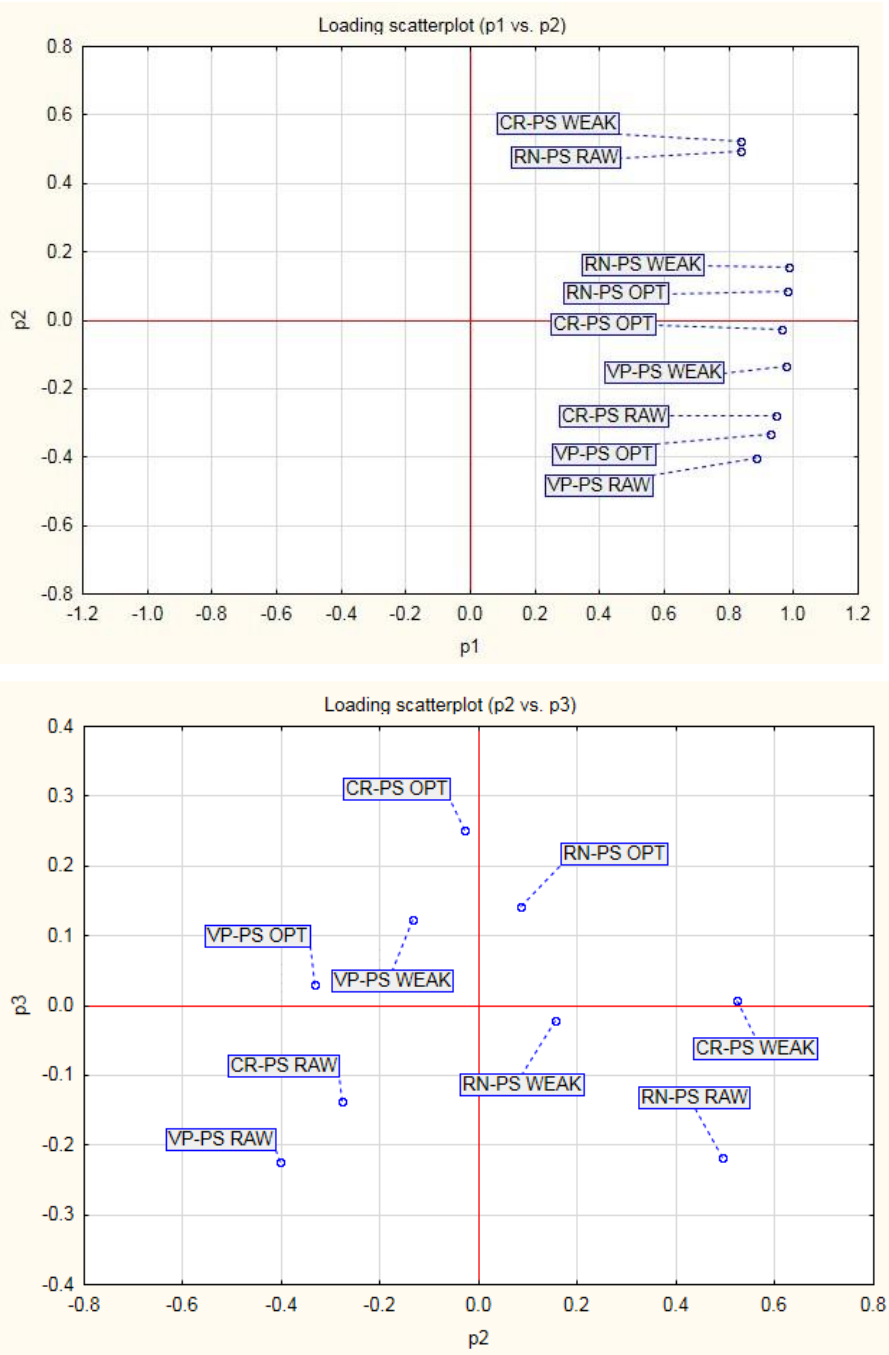

Figure 3-20: Principle Component Analysis (PCA) score plots on factors 1, factors 2 and factors 3 (PC1, PC 2 and PC3) based on the FT-IR spectra

The Principle Component Analysis (PCA) was used to decompose the FT-IR spectra data of the board samples into principle components. This method was used to correlate chemical composition and board performances. Figure 3-20 describes the scatter plots of PC2 (10.2% of variability) and PC 3 (2.4% of the variability) while PC1 (86.2% of variability). The PCA analysis showed that PC1 had no significant correlation in grouping the analysed PS and board samples. PC 2 generally separated the RN-PS samples (positive loading) from CR-PS and VP-

PS samples (negative loading). The differences could be attributed to peaks around 1415 cm^{-1} (Figure 3-19) which corresponds to C-H bands usually associated with the presence of lignin. This is odd considering that the NREL method over estimates the lignin content within PS and therefore should not be agreement with chemical composition analysis. PC3 generally clustered the optimum conditions away (positive loading) from raw PS samples and weak samples (negative loading). The differences could be correlated to spectra region around 2910 cm^{-1} for CR-PS and 3344 cm^{-1} for RN-PS and VP-PS. These regions are associated with OH- groups including absorbed water, aliphatic alcohols found in carbohydrates and lignin, aromatic alcohols in lignin and extractives and carboxylic acids in extractives in wood based material (as seen in Table 3-5). Absorbed water within PS could increase the water-holding capacity of the boards and therefore produce weaker boards. The other principle components (PC4, PC5 and PC6) all did not display any significant grouping or clustering.

3.4 Summary and conclusion

The valorisation of PS from different pulp and paper mills into composite products is a promising alternative for utilization of PS. In the study, the PS was used to produce wood composites utilizing magnesium based phosphate cement as a binder. The investigation has shown the possibility of producing medium to high-density fibreboards. The outcomes of the experiment investigation shows that it is feasible to use different types of PS, even with significant levels of fillers and contaminants, and phosphate cement and fillers. Among the fillers used, calcium carbonate had the greatest influence on the board mechanical properties compared to fly ash and silicon fume. Unexpectedly, the presence of high ash content within RN-PS did not inhibit the binding ability of the binder produced but enhanced the strength properties. As was expected, short fibrous material within PS unfavourably impacted the strength properties of the boards resulting in composite boards that did not meet the strength properties for cement-bonded boards (EN-635). The presence of PS materials however improve the physical properties of the boards namely the water absorption, thickness swelling and volume swelling by increasing the inorganic material that filled up void spaces and reducing its porosity. From the results obtained, the response variables could be modelled. Using multi-response optimisation, the optimum set of process conditions were established with highest strength properties utilising as much sludge as technically feasible.

Optimized board manufacturing process conditions indicated that a fibre ratio of 1.94, a binder ratio of 5.07, filler loading of 20% and board press temperature of 180 °C , were required for RN-PS. Under these optimum process conditions, the statistical model predicted Density of 1.6 g/cm^3, MOE of 1367 MPa, MOR of 4.92 MPa, WA of 18.86%, TS of -2.58% and VS of -0.18%. For CR-PS, optimized board manufacturing conditions indicated that a fibre ratio of 1.94, a binder ratio of 5.07, filler loading of 22.5% and board press temperature of 90 °C, was required. Under these optimum process conditions, the statistical model predicted Density of 1.27 g/cm^3, MOE of 583.9 MPa, MOR of 1.55 MPa, WA of 21.1%, TS of -2.9% and VS of 0.36%. For VP-PS, optimized board manufacturing conditions indicated that a fibre ratio of 1.94, a binder ratio of 5.05, filler loading of 15% and board press temperature of 25 °C, was required. Under these optimum process conditions, the statistical model predicted Density of 0.75 g/cm^3, MOE of 752 MPa, MOR of 2.29 MPa, WA of 16.57%, TS of -7.4% and VS of 0.09%.

Statistical analysis showed that the sludge types, temperature, filler types and their interactions significantly influenced the board's functional properties. A maximum PS loading of 66% was determined in order to produce the best quality board possible much higher than previous studies that estimated. The investigation also shows that this process route can use any type of PS, even with high levels of ash of up to 60% ash content compared to previous studies of 20%, to produce composite boards. When compared to previous studies, the investigated boards have mechanical and physical properties much superior due to the type of PS and the process conditions of temperature that enhanced the ability to utilize PS with ash content greater than 64%. The board composites were deemed suitable for ceilings and wall partition application with no load bearing capability.

Chapter 4. Techno-economic evaluation of the production of composite board from paper sludge

4.1 Introduction

Environmental concerns caused by the landfilling of paper sludge (PS), has led to an increased focus on alternative PS handling methods. In order for the potential process route to be considered, techno-economic assessment is needed to determine the financial feasibility of the proposed project. It has already been shown in chapter 3 that it is technically feasible to utilise PS as a feedstock incorporated with phosphate and magnesium based cement binder to produce composite boards. The composite boards were found to have some of the functional properties comparable to cement bonded wallboards and were more suitable for non-load bearing usage. Previous research has shown that a simple addition of veneers to the boards increases the functional properties by 3-4 folds(Mngomezulu, 2019) resulting in boards meeting strength standards for cement-bonded boards. In this section, a techno-economic model was developed to assess the feasibility of producing composite boards from PS sourced from RN-PS, CR-PS and VP-PS on an industrial scale utilising the optimum process conditions attained in chapter 3.

4.2 Literature review

It is a relatively new concept to produce composite boards from paper sludge (PS). Previous studies have only focused on the experimental part of producing composite boards using PS (Geng *et al.*, 2007a; Donahue and Aro, 2010; Migneault *et al.*, 2011) and to the best knowledge of the author, this is the first study that has looked at both the experimental and economic application in the South African environment. Furthermore, there are no existing manufacturing plants that utilise paper sludge (PS) as a feedstock to produce composite boards. It is therefore needed to review traditional particleboard process routes and manufacturing technologies that could possibly be used for the proposed composite board production.

It is envisaged that the manufacturing steps would follow similar process to existing manufacturing plants that use traditional raw materials such as wood and residues such as chips, pine or sawdust to produce wood-based products such as particle boards and medium density fibreboards (Geng, Zhang and Deng, 2007a; Amiandamhen, 2017). The motivation for this study is to propose a process route that is not energy intensive but also meets the required standards. It is therefore important to review the technologies available within the traditional particleboard or medium density fibreboard. Traditional manufacturing process of producing wood-based products consists of pre-treatment of the raw materials, binder application, board-pressing and finishing (Irle and Barbu, 2010). The greatest advantage that PS method has over traditional route is that PS method does not require any form of pre-treatment. There is no need to reduce moisture content to 7%, or any form of milling. PS can be used straight from the pulp and paper mills handling system and directly be mixed with the adhesive.

Once the adhesive has been mixed with PS, it is then sent to be pressed. In an industry setting, it is common practice to have a pre-pressing and pre-heating step. The pre-pressing step, reducers the thickness of the matt before it reaches the press and therefore reducers the amount of energy required to press. Pre-pressing also reduces the risk of air within the mat, pushing out bubbles and air pockets during the press and therefore reducing the press cycle. Because of this, prepressed and pre-heated techniques help to improve the efficiency of press and therefore increasing production (Thoemen et al., 2010). It is important that pre-pressing conditions do not allow the pre-cure of the binder thereby adversely influencing the final products functional properties (Hughes, 2016).

Preheating can be achieved via either electro-magnetic energy or using heat of condensation from high humid air, saturated steam and supersaturated steam or hot dry air. The most

common type of preheating for particleboard is using steam or hot air(Irle and Barbu, 2010). In this study, a pre-pressed stage was simulated to produce PS matt that would not only have no air pockets but also be at an appropriate thickness in the press machine.

After the matt come out of the pre-press machines, they are sent to press machines. They are two types of press machines that are commonly utilised: batch-wise in either a single or multi-opening press and in a continuous press (Thoemen et al., 2010). For this study, they are four main selection criteria for choosing the best press configuration suitable for this type of waste material and binder system. Durability of the press is one of the selection criteria as it directly impacts on the feasibility of the study. A continuous press offers a much more simplified approach with no requirement for blending, forming or pre-pressing, but offers challenges in belt control as hard objects such as metals, stones can damage very expensive belts (Thoemen et al., 2010). Continuous presses already require higher initial capital cost compared to batch system, and the additional risk of having to replace belts makes this type of press unfavourable. The next selection criteria is whether boards are pressed with equal heat transfer and pressed with equal pressure. Multi-layered daylight presses are designed to produce more than one board per press cycle. In industry, multi-daylight presses has the capacity to produce between 4 and 10 boards per cycle. Even though, the boards produced from multi-press are 5 to 7 m long and 2.5 m wide, which is not as big as the ones from single-daylight press, multiple boards produced per cycle make multi-daylight presses have a higher capacity compared to single-daylight press (Thoemen et al., 2010). Unlike single-daylight presses, unloading and loading cages are attached to multi-daylight presses to ensure negligible variations within the boards per cycle. The cages ensure that all the boards are loaded and unloaded at the same time. It is also essential that all the boards are pressed at the exact same temperatures and pressure (Thoemen et al., 2010). The last selection criteria considered was the production rate of the boards, which would affect the project's revenue. A single daylight batch presses are designed to produce a large single board up to 52m long (Thoemen et al., 2010 reference Egger (UK) Ltd in 2009). The width of the board is designed to be no more than 2.8m. This prevents steam from being trapped within the press mould that could adversely affect the curing of the binder. The main attraction to this system is that it produces large size boards. The boards would still need to be finished through trimming of the edges. However, the production rate would be drastically less than compared to multi-layered batch or continuous press.

Multi-layered press machines gives the balance of having higher production compared to single but also press with equal heat transfer and pressure to produce high quality boards.. Typical

presses in industry are heated by either steam, hot water or hot oil (Thoemen et al., 2010). Utilising hot water and hot oil is advantageous because it is easier to control and it allows the whole press plate to remain at a certain temperature and pressure.

4.3 Methods

4.3.1 Techno-economic analysis steps

In order to conduct a techno-economic analysis the following steps are shown in Figure 4-1, the first step is to review literature in order to construct a novel process flow diagram (PFD). The PFD was then used to determine material and energy balance associated with each process equipment described in PFD. The process equipments were then sized as well as their utility consumption (steam, water consumption and electricity) determined. This is then followed on by costing where the capital and operating expenses (CAPEX and OPEX, respectiviverly) are calculated and thereafter used to determine key financial indicators using discounted cash flow sheets. The key financial indicators used to analyse, includes total capital investment (TCI), the net present value (NPV), the internal rate of return (IRR), as well as pay-back period (PBP). Further analysis was done to establish the sensitivity of the economic model by changing some of the process parameters and observing changes in the key financial indicators (NPV and minimum selling price).

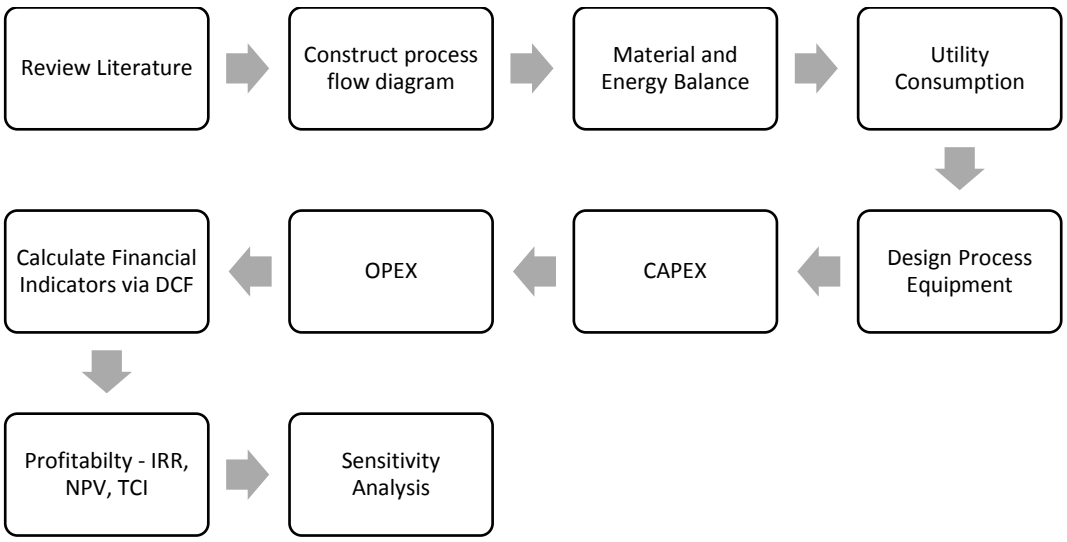

Figure 4-1: Techno-economic evaluation process

4.3.2 Software

Microsoft Excel (2013) spreadsheets are used to develop the mass and energy balance streams from literature and PFD, as well as utility consumption for each process unit was calculated.

CAPEX and OPEX were determined and therefore economic indicators were determined for each of the scenarios.

4.3.3 Process development

4.3.3.1 *Process Feed Scenarios Descriptions*

Taking into account that, there are not any existing plants in the industry utilising PS in the production of composite boards in South Africa, the techno-economic study was simulated for five different types of feed scenarios at different locations.

In the first three scenarios:

- PS from Kimberly-Clark: Enstra (RN-PS scenario) at flow rate of 6 000 dry t/yr. (50% MC) feed through proposed plant
- PS from Mpact: Springs (CR-PS scenario) at flow rate of 11 000 dry t/yr. (80% MC) feed through the proposed plant
- PS from Sappi: Ngodwana (VP-PS scenario) feed at flow rate of 15 000 dry t/yr. (80% MC)

In these three scenarios, the proposed plant is envisaged to be annexed to an existing pulp and paper mill in order to be as close as possible to the source of PS and follow the same process description as described in 4.3.3.1. The process PS feed flowrates were adopted from research done by Boshoff et al. (2015)

The fourth scenario describes PS feed from all two pulp and paper mills namely Kimberly-Clark Enstra and Mpact Springs since they are in relative proximities, feed to a manufacturing plant at a central location (Combined scenario). In this scenario, PS form all the two mills are transported to a central location and processed using the same procedure as described in the Process Description and Process Flow Diagram.

4.3.3.2 *Process Description and Process Flow Diagram*

Since there are no existing particleboard production, currently using PS as a feedstock, the process flow diagram was developed by modifying existing particleboard production process described by Midwest Research Unit (1998), Thoemen et al. (2010), Hughes (2012), and Wagh et al (2013). The general steps to produce particleboard include raw material generation, drying, blending with resin and filler, formation into matt, hot pressed and finished. The PFD of this particular particleboard production can be seen in Figure 4-2.

From the paper and pulp mills, the PS arrives with a moisture content of ≥ 50% MC, and is transported using conical screw feeder conveyor (SC-100 A/B). Specified binder amount (ratios seen in Table 4-1) made up of KH_2PO_4 (stream 5/6), MgO (stream 7/8), $CaCO_3$ as the filler (stream 9/10) and fresh water is pumped (stream 3/4) to the agitated mixer (M-100) to be mixed with PS feed from storage tank. Borax is used as a retardant to control the rate of reaction. During large scale production of cements, it is best practice to include a retardant to slow down the cement forming reaction and not set before being pressed. Borax is sent to the mixer at 10% of the binder (stream 11/12) These chemicals are mixed using agitator to ensure homogenous mixture. The exit stream from mixture is then sent to continuous matt formation unit that layers the board into single layer matt furnish with the standard board size dimensions of 1.22m x 2.44m. The furnished matt is then sent to pre-press machine (Press-100) and then multi-opening press machine with 20 plate openings (Press-101) operates at optimised temperature and pressure. The hot press machine is heated by hot oil. The matt is pressed into the desired thickness of 13 mm. After the boards are pressed into solid panels, the boards are conditioned and cooled in an air conditioned room (C-100) set at RH 65% and 20°C prior to being stacked. The panels are then sanded and trimmed (T-100) to final dimensions. The final product is then ready for packaging and shipment (Stream 20).

Table 4-1: Optimised process conditions

Scenario	Fibre (Fibre: Inorganic binder)	Binder (KH_2PO_4: MgO)	Filler (% of binder)	Temperature (°C)
RN-PS	1.94	5.07	20	180
CR-PS	1.94	5.07	22.5	90
VP-PS	1.94	5.05	15	25
Combined	1.94	5.05	20	90

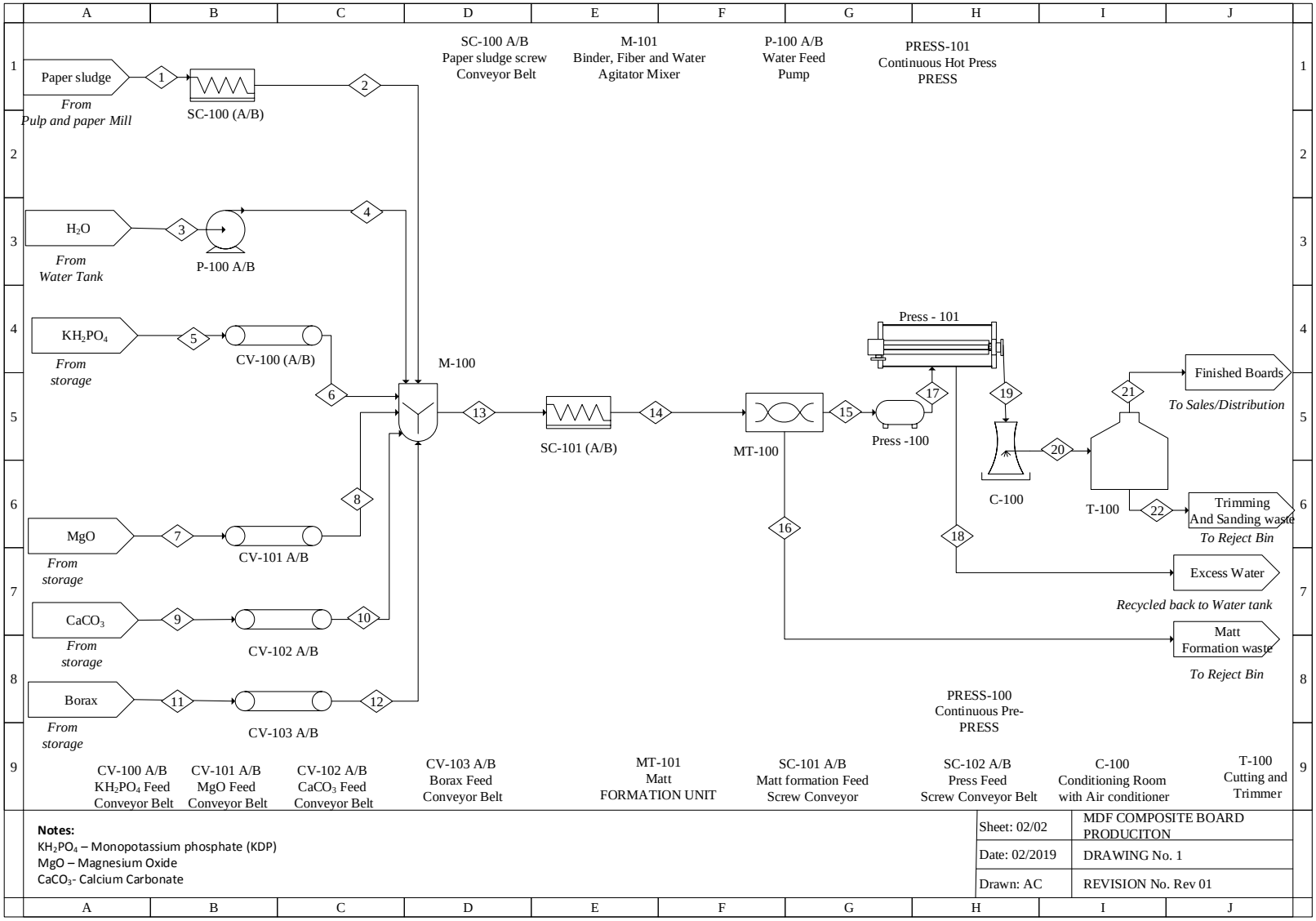

Figure 4-2: Process flow diagram for the production of particleboards from paper sludge

4.3.3.3 *Process Assumptions*

The following key assumptions were made in developing the techno-economic evaluation

- Steady state operation was assumed
- Loss due to transportation and handling or raw material 0%
- Moisture loss after matt formation is 8%
- Material loss due to sanding and cutting is 6%
- KH_2PO_4, MgO and $CaCO_3$ is assumed to be continuously replaced, as they are not sourced onsite and bought from suppliers.
- Borax is assumed to be continuously replaced.
- Loss due to matt formation is 6% (Shaik et al., 2010)
- The process water, low-pressure steam was assumed to be sourced from the pulp and paper mill except for combined scenario. Operational cost associated with these operations was included in variable cost.

4.3.4 Economic evaluation

4.3.4.1 *Capital cost estimation*

The capital cost estimation (CAPEX) following the process steps described in **Error! eference source not found.**. Process equipment purchased cost have been estimated based on various literature sources. Some of the equipment such as the water pump and storage tanks were sized according to literature heuristics costed based on characteristics size parameters and calculated based equation described by Equation 7 (Sinnott, 2005).

$$Ce = C \times S^n \quad (7)$$

Ce= purchased equipment cost based in mid-2004 ($)

S = Characteristic size parameter referenced by Sinnot et al. (2005)

C = Cost constant referenced by Sinnot et al. (2005)

n = index for the type of equipment

Some equipment purchase cost were based on base cost (Cbase) and base size parameters (Sbase) either found in literature data and vendor and applying Equation 2 described by Humbird *et al.*, (2011) to calculate purchase cost (Cnew).

$$Cnew = Cbase \times \left(\frac{S_{new}}{S_{base}}\right)^n \quad (8)$$

Cnew New purchase cost

Cbase	Base cost
Snew	New size parameter
Sbase	Base size parameter
n	Size scaling factor

Size scaling factors for various equipment's are described in Table 4-2.

Table 4-2 Scaling factors

Equipment	Exponent
Agitators	0.5
Compressors, motor driven	0.6
Distillation columns	0.6
Heat exchange	0.7
Inline mixers	0.5
Skidded equipment	0.6
Pressure Vessels	0.7
Pumps	0.8
Tanks, atmospheric	0.7
Solid handling equipment	0.8

For equipment such as the forming machine, prepress machine, belt conveyor for mat boards, loader for mat board, hot press machine, unloader for finished board, overturning machine, edge saw machine, stacking machine, sanding machine the purchase cost was sourced from specific machinery supplies selected based on meeting the required capacity of the envisaged board production plant (Alibaba, 2019).

In some cases, equipment purchase cost are based on the historical cost data that need to take into account cost are not static and change with inflation. Equation 9 is therefore used to scale up equipment cost from historic time period to the current time period (Sinnott, 2005).

$$Current\ Cost = Cost\ in\ previous\ year \times \frac{CEPCI\ (current\ year)}{CEPCI\ (past\ year)} \quad (9)$$

After the purchase cost of all the process equipment's were calculated, the installation factors needs were to be taken into account by multiplying the purchase cost (C_{ap}) by the installation factors from Humbird *et al.* (2011) This was down via Equation 10 described by Humbird *et al.* (2011).

$$\text{Installed Purchase Process Equipment Cost} = C_p \times \text{Installation factor} \quad (10)$$

For capital cost estimation, it is assumed that the capital investment required to build a facility to supply the utility has already been made (Turton et al, 2012). The new product production cost (NPP) is then calculated taking into account all the installed purchase cost. The total direct cost (TDC) is determined by taking into account NPP, warehouse cost (4% of NPP), site development (9% of NPP) and additional piping cost (4.5% of NPP). The total indirect cost is calculated by taking into account field expenses (10% of TDC), office construction (20% of TDC), contingency (10% of TDC) and other cost (10% of TDC). Fixed capital investment is then determine by adding TDC and total indirect cost. The total capital Investment (TCI) is then determined by taken into account FCI and working capital (5% of FCI).

4.3.4.2 *Operation Cost Estimation*

The following section describe the operating cost estimation (OPEX), which comprises of manufacturing, operating cost and general expenses. The NPP was envisaged to operate for 8000 hrs/year (333 days per year) based on similar plant described by the Development studies association (2008).

4.3.4.2.1 Raw Materials

The cost of raw materials were calculated based on the mass required for the year production and chemical prices. Cost of raw materials was calculated multiplying annual flowrates by the unit cost shown in Table 4-4 and illustrated in Equation 11.

$$Cost\ of Raw\ Material = Flowrate\left(\frac{kg}{hr}\right) \times Cost\left(\frac{R}{kg}\right) \times Operation\ time \quad (11)$$

Table 4-3: Unit Cost of Raw Materials used

Raw Material	Cost (R/kg)
KH_2PO_4	R 9.06[a]
MgO	R 4.85[b]
CaCO3	R 32[c]
Borax	R 10[d]

a – sourced from local company (Alibaba, 2018)

b – Sourced from local company (Alibaba, 2018)

c – Sourced from local company (Kimix chemicals & lab supplies, 2018)

d – Sourced from local company (Alibaba, 2018)

e – Sourced from local company (Alibaba, 2018)

4.3.4.2.2 Utilities

Most of the utility are being sourced from onsite generation within the plant. The associated cost of the utility are presented in *Table 4-4*. Hot oil is designed to be recycled and therefore is not continuously supplied. Sample calculation for heating requirement shown in Appendix section 7.2.1.2 for RN-PS scenario.

Table 4-4: Utility Cost Summary

Utility	Cost (R)
Electricity	R 0.84/kWh [a]
Steam	R140/ton [a]
Fresh water	R16.96/ton [a]
Residue transport	R77.46/ton [a]
Hot Oil = $14.5/GJ [b]	R204.02/GJ

a- Williams, 2017

b- Turton *et al.*, 2012

4.3.4.2.3 Labour

Labour cost presented in *Table 4-5*, was calculated based on the staff required at the proposed board manufacturing plant. The quantities were based on previous work done by Development studies association (2008) and Shaikh et al., (2010), who had a similar manufacturing process and demand to this study. Salary estimation were based on average current market value sourced from Pay scale South Africa.

Table 4-5: Staff requirement summary

Position	Required Quantity of staff For scenario	Salary R
Plant Manager	1	459 058

Plant Engineer	2	669 350
Maintenance Supervisor	1	242 844
Maintenance Tech	2	174 415
Lab Manager	1	358 936
Shift Supervisor	2	345 446
Shift Operators	6	169 418
Administrator/Finance Head	1	515 539
Accountant	2	257 483
Secretary	1	117 698
Clerks & Secretaries	2	95 048
Total Salaries	21	

It should be noted that, besides the operators and maintenance technician, all other positions would work normal working hours. Since the plant will operate for 24 hours per day, shift operators will be divided into 3 groups of 2, working 12-hour shifts and alternative days.

4.3.4.2.4 Other Operating Expenses

The other operating cost include maintenance determined as 3% of NPP, which is the total installation cost of all the process equipments. Property Insurance & Tax is determined by taking 0.7% of FCI as described by Humbird et al., (2012).

4.3.4.3 *Market Research*

4.3.4.3.1 Target market, demand and board application

The envisage project has been designed to produce board products similar to conventional particleboards, that can be used furniture wall boards, partitions, furnishings or building and construction industry for flooring with no load requirements, wall panels, false ceiling. Our main consumers for this type of product would consist of the DIY retail sector, building and construction sector and the furniture industry (KAP, 2018). The increasing demand for composite board products is heavily linked to increase in urbanization and economic climate around the target market. Companies such as PG Bison have already experience a revenue increase of 7% and built new particleboard operations in Piet Retief. This further highlights that there is ample demand in the South African market for these board types and therefore board prices increase at an inflation rate of 5.8%.

It is acknowledge that the wood board industry has taken a knock due to the recent fires in the Western Cape, which did have a negative effect on supply and demand. As previously stated, the one key advantage of the envisaged product is that the phosphate binder is known to be fire retardant, which therefore further makes this venture more favourable to potential customers. Although the strength properties of the boards did not meet mechanical board strength specification, the addition of veneers have been known to improve by four-folds and therefore will meet strength properties as illustrated by (Mngomezulu, 2019)

4.3.4.3.2 Revenue: Board Pricing

Majority of the revenue of the project is based on the sale of composite boards at a calculated selling price. The selling price of the composite board is dependent on its applications due to their mechanical and physical properties. These properties are significantly dependent on the strength of the resin system (Stark, et al., 2010). The proposed plant is envisaged to produce composite boards that are more suitable for low or non load bearing applications. In order to ensure industrial application success, it is important to sell the boards at a price that is competitive with current market. Current market prices shown in Table 4-6, show that composite boards with similar applications, range from R200 – R300 /board with a standard dimensions of 1.2m x 2.4 m with 12-13 mm thickness with an average cost of R233/board. Assuming that most retail stores add a mark-up of 50%, it would be appropriate to compare the cost price of the boards to cost price of the market values at R155 per board. The proposed plant is envisage to use similar distribution channels as current board producing markets. A minimum required selling price was determined for the different scenarios to ensure that the cash flow projection matches the assumed hurdle rate of 20%.

Disposal cost was accounted as part of the production revenue because the envisaged board production plant will save on PS disposal. Disposal cost consist of two parts, namely landfilling charge at R705/dry ton and transport cost at R174/dry ton (Robus et al., 2016).

Table 4-6: Market related prices from previous studies

Company or Manufacture	Board Type	Selling Price/board	Application
International			
Shaikh et al., (2010)	Particleboards from Cotton	0.34$/ft^2 = R 144.78/board approx. R215 with inflation	door panel inserts, partitions, wall panels, pelmets, furniture items, floor and ceiling tiles
Development Studies Associates (2008)	Particleboards from Eucalyptus	220-380 Birr/board = R150 /board	door panel inserts, partitions, wall panels, pelmets, furniture items, floor and ceiling tiles
Alibaba : China	Particleboard	US$200/cm^3 = R623	
South Africa			
Davidson (2018)	Particleboard	R 300	
Davidson (2018)	Medium Density Fibreboards	R 600	
Builders (2019)	Masonite soft board (2440 x 1220 x 13 mm)	R 215	Insulation, Pin boards Ceilings - Not moisture resistant
Builders (2019)	Post form marron glass counter top	R 900	Kitchen counter top
	PG Bison Chipboards (2750 x 1830 x 16mm)	R 455	Shelving - It offers excellent structural strength with superior screw-holding capability and machinability.
	Evowood Soft boards (2440 x 1220x 10mm)	R 200	Insulation ceiling boards, as display boards, office screens or packaging
Average for load bearing board		R 400 / board	
Average for non-loading bearing		R 233 / board	Assuming 50% mark-up therefore cost price of R 155.50

4.3.4.4 *Cash Flow sheet Assumptions*

The following assumptions presented in *Table 4-7* were made to develop the cash flow analysis. Assumptions are based on previous work (Farzard et al, 2017, Shaikh et al., (2010), Gorgens et al., 2015, Development Studies Association, 2008). The plant is envisaged to operate 8000 hrs/p.a. (90% of the year) to account for unexpected plant maintenance work and planned down time. The envisage plant construction period is expected to be completed within 1 year and operate for 15 years. The plant is expected to follow similar production plan to Development Studies Association (2008), where ramp up production capacity is followed to allow time for adjustments in logistics and markets, and machine and operator training.

The hurdle rate or return on investment was set at 20%, which consist of weighted average Cost of Capital (WACC) set at 10% based on local wood board manufacturing company and risk premium, which is associated with the envisaged project cash flow of 17% (York timber, 2018). A risk premium of 10% was selected based on taking a conservative approach takes into account that even though there is a well-established market for the production composite boards, there is many uncertainties associated with the new process and only process assumptions and estimation have been used to develop current cash flow. Process technologies and conditions are not fully understood on an industrial scale and there is no historical data to predict the success of such a project. Depreciation on assets is expected to follow a straight-line approach at an annual depreciation of 20% over a 5-year period resulting in zero salvage value. Revenue and operating cost are adjusted for inflation at 5.7% and income tax rate of 28% was taken into account throughout the projects lifespan.

Table 4-7: Key Cash Flow Calculation Assumptions

Assumption	Value
Annual operating hours	8000 h
Scrap value	0
Equity	100%
Working Capital (% of FCI)	5.00%
Depreciation method	Straight line
Salvaging value % of initial price	20%
Annual depreciation	20.00%
Salvage Value	$0
Depreciation Period (Years)	15
Construction Period (Years)	1
Ramp-up until operational at full capacity	
First year capacity	70%
Second year capacity	80%
Third year capacity	90%
Exchange rate in 2018	R14.07/$
Inflation Rate	5.7%
Cost Year for Analysis	2018
WACC	10%
Risk premium	10%
Minimum acceptable rate of return or hurdle rate	20%
Discount Rate (Internal Rate of Return [IRR])	20%
Income Tax Rate	28.%

4.3.4.5 *Profitability indicators*

The profitability indicators used to investigate the economic feasibility including payback period (PBP), net present value (NPV), minimum required selling price (MRSP), and internal rate of return (IRR). The PBP is defined as the time required after start-up to recover the fixed capital investment. The shorter the time period, the more profitable the project. The NPV is the cumulative discounted cash position of the project at the end of its lifespan. The more positive the project, the more favourable the project is to potential investors. The IRR is defined as the interest rate at the NPV is set to zero and all the cash flow has been discounted. It gives an

indication of the highest interest rate after tax that the envisage project will break even. A project is considered favourable when IRR is greater than the set hurdle rate of the project (Turton *et al.*, 2012). The MRSP was determined when the IRR matched or exceeded the set hurdle rate. For the process route to be profitable, the MRSP had to either match or be lower than the average market price for the specific type of board. .

4.4 Results and discussion

4.4.1 Plant capacity

The annual production capacities of the proposed plants and the annual feedstock throughput from the different scenarios as shown in Table 4-8, were determined from the mass and energy balances. As expected, the production capacity shows that the Combined scenario had the highest annual board production at 25 763 m^3 /year compared to VP-PS (22 732 m^3/year), CR-PS (16 670 m3/year) and RN-PS (9 093 m^3/year). This was obviously because the Combined scenario had an increased availability of PS sourcing it from RN-PS and CR-PS production plants at a feed rate of 51 dry ton/day compared to sourcing PS from a single source. Current board production plants in South Africa produce approximately 76 000 m^3/year, none of the scenarios are able to match this capacity. The aim of the envisaged projects is not to target the entire market but to focus on certain potential clients. The type of clients that would be interested in getting composite boards that are made from waste material but with comparable functional properties to current commercial boards (KAP, 2018).

Table 4-8: Plant production capacity

	Unit	Scenario 1 RN-PS	Scenario 2 CR-PS	Scenario 3 VP-PS	Scenario 4 Combined
Feedstock					
Paper sludge	Dry ton/day	18	33	45	51
Moisture Content	%	54	54	80	67
KH_2PO_4	ton/day	6	11	16	18
MgO	ton/day	1	2	3	3
$CaCO_3$	ton/day	2	4	3	5
Borax	ton/day	0.12	0.22	0.33	0.35
Water	ton/day	13	20	27	35
Product					
Finished Boards (8'x4'x13mm)	boards/year	234 965	430 770	587 413	665 735
Finished Boards	m3/year	9 093	16 670	22 732	25 763
Finished Boards	ton/day	26	47	64	73

4.4.2 CAPEX & OPEX

The capital expenditure (CAPEX) and operating expenditure (OPEX) for each PS scenario is given below with Figure 4-3. The OPEX cost had the highest contribution to the total expenses compared to CAPEX for all the scenarios. This is mostly due to the expensive nature of the variable cost, especially the raw materials such as monopotassium phosphate (KH_2PO_4) and MgO used as binder.

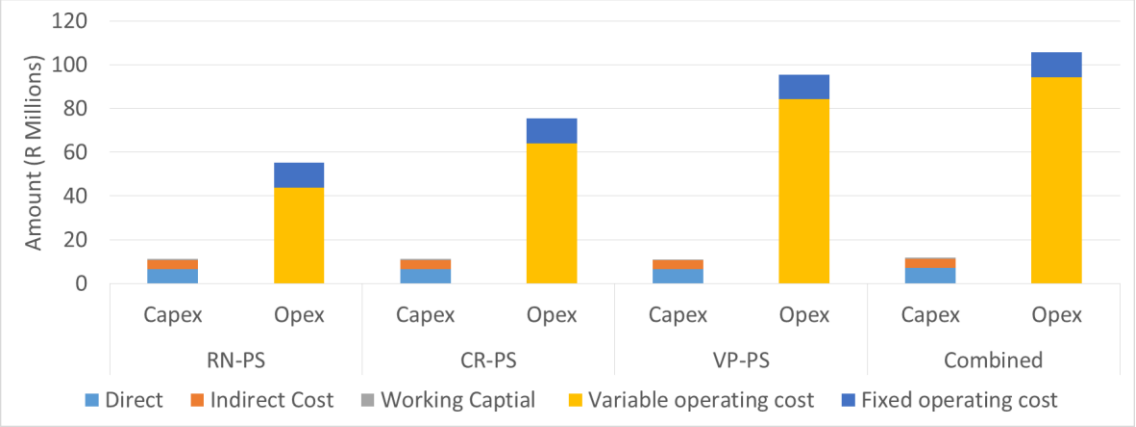

Figure 4-3: CAPEX and OPEX for all the manufacturing scenarios. Refer to 4.3.3.1 for definition/explanation of the scenarios

4.4.2.1 *Capex*

Table 4-9 displays the breakdown of the total capital investment (TCI) cost from all the production scenarios. Among the PS scenarios, the Combined scenario required the highest TCI of R 11.94 million followed by RN-PS (R 11.26 million), CR-PS (R11.12million) and VP-PS (R11.06 million). Clearly, because of a large PS feedstock flowrate in Combined scenario, larger equipment sizes is required to process the required plant capacity. Furthermore, pump cost also had a large contribution factor to the CAPEX as it included installation cost and pumping requirement from fresh water header to fresh water storage tank, and from storage tank to mixer. RN-PS had the highest pump cost mainly due to the pumping requirement to pump from water tank to mixer. .

Table 4-9: TCI Scenario Summary. Refer to 4.3.3.1 for definition/explanation of the scenarios (R million /year)

Total Capital Investment (TCI) (‘R million / year)	Scenario 1 RN-PS	Scenario 2 CR-PS	Scenario 3 VP-PS	Scenario 4 Combined
Total Installation Cost	5.70	5.64	5.60	6.05
Warehouse (4% of NPP)	0.23	0.23	0.22	0.24
Site Development (9% of NPP)	0.51	0.51	0.50	0.54
Additional Piping (4.5% of NPP)	0.26	0.25	0.25	0.27
Total Direct Cost (TDC)	6.70	6.62	6.58	7.11
Total Indirect Cost (60% of TDC)	4.02	3.97	3.95	4.27
Fixed Capital Investment (FCI)	10.72	10.59	10.53	11.37
Working Capital (5% of FCI)	0.54	0.53	0.53	0.57
Total Capital Investment (TCI)	11.26	11.12	11.06	11.94

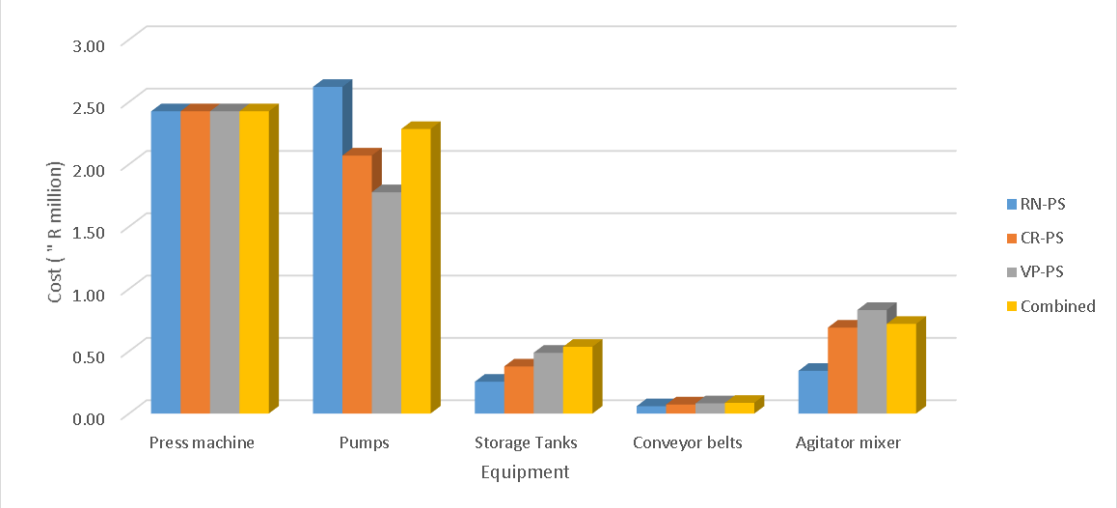

Figure 4-4: Distribution of installation cost for the manufacturing scenarios

4.4.2.2 *OPEX*

Table 4-10 displays the breakdown for total operating cost (TOC), for all the scenarios. The highest operating cost was required from combined scenario (R 105.6 million), followed by VP-PS (R 95.4 million), CR-PS (R 75.4 million) and RN-PS (R 55.2 million). As shown in Figure 4-3 and Figure 4-5, it can be seen that variable cost namely, binder cost of KH_2PO_4, MgO accounts for 95% of the TOC. Because of the quality and strength properties of phosphate binder, raw material cost are extremely high. Because of having the largest PS feedstock flowrate, the Combined scenario required highest binder flowrates (KH_2PO_4 and MgO) and consequently required the largest OPEX and thus due to the small CAPEX is unlikely that there will be any economic of scale benefits in producing larger volumes. Even though the RN-PS scenario has the highest energy requirement due to pressing at highest temperature (180 °C) per board value of 11 697 kJ/board, when compared to Combined scenario that pressed at 90°C requiring 4905 kJ/board, the overall cost are lower due to lower production rate of 234 965 boards/year requiring a total energy/year of 5 497 GJ/year compared to vs 665 735 boards/year requiring total energy of 6 531 GJ/year for Combined scenario (shown in Table 4-10 and sample calcualtions in Appendix section: Chapter 7). Therefore, because less boards/year were required to be pressed, heating requirements were less than the Combined scenario.

Table 4-10: TOC Scenario Summary. Refer to 4.3.3.1 for definition/explanation of the scenarios (R million/year)

Total Operating Cost (TOC)	Scenario 1 RN-PS	Scenario 2 CR-PS	Scenario 3 VP-PS	Scenario 4 Combined
Raw Materials				
Monopotassium Phosphate	18.73	33.26	49.71	53.02
Magnesium Oxide	1.98	3.51	5.27	5.63
Fresh Water	0.13	0.21	0.28	0.36
Calcium Carbonate	1.72	3.54	3.22	4.86
Borax	3.17	5.62	8.44	9.00
Utilities				
Electricity	17.07	17.17	17.22	17.18
Hot oil	1.11	0.85	0.00	1.31
Total Labour Cost	11.01	11.01	11.01	11.01
Maintenance (5% Of FCI)	0.17	0.17	0.17	0.18
Property Insurance and Tax (0.7% of FCI)	0.08	0.07	0.07	0.08
Production Cost	55.15	75.41	95.39	105.59

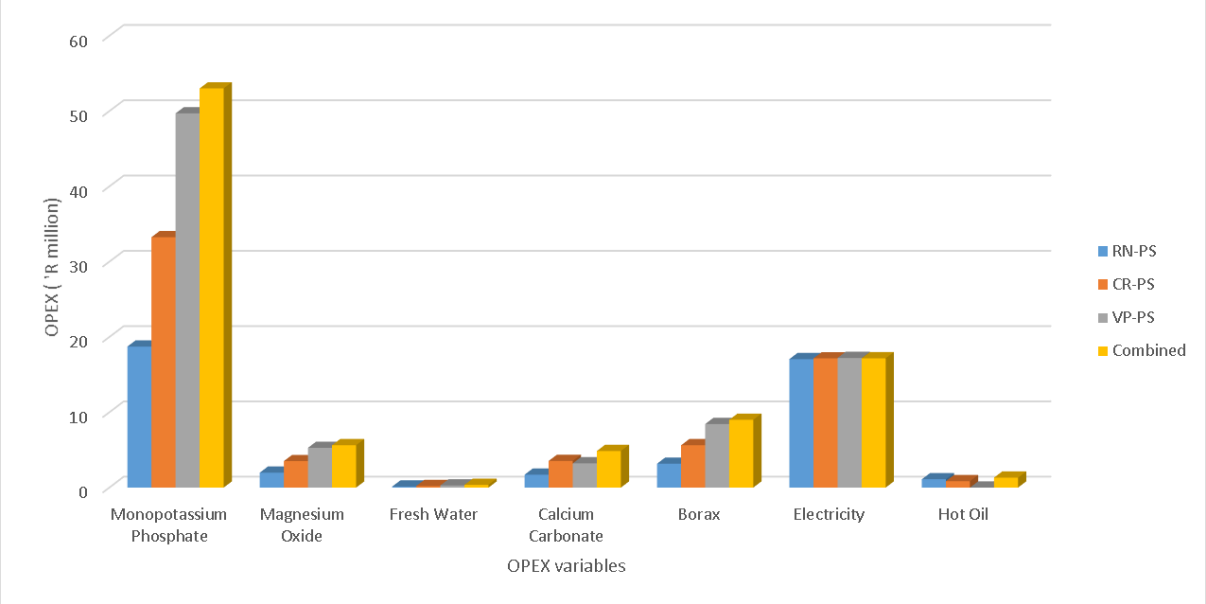

Figure 4-5: Distribution of variable operating cost distribution for all manufacturing scenarios

4.4.3 Financial performance of proposed plant

The CAPEX and OPEX were used to analyse the discounted cash flow analysis in order to determine economic performance of each of the production scenarios. Key economic indicators used to analyse techno-economic feasibility include net present value (NPV), total capital investment (TCI), minimum required selling price (MRSP) set at an internal rate of return (IRR) of 20% and payback period (PBP).

4.4.3.1 *Profitability indicators*

The minimum required selling price (MRSP) for the different scenarios were determined at minimum acceptable IRR of 20% and compared to relevant market price. Figure 4-6 shows the profitability indicators for all the scenarios comparing them to average market price of R155 per board for non-load bearing boards (as shown in Table 4-6). Combined scenario had the lowest MRSP (R157/board) at an IRR of 20% majority due to larger board production capacity overcoming the extra transport cost.

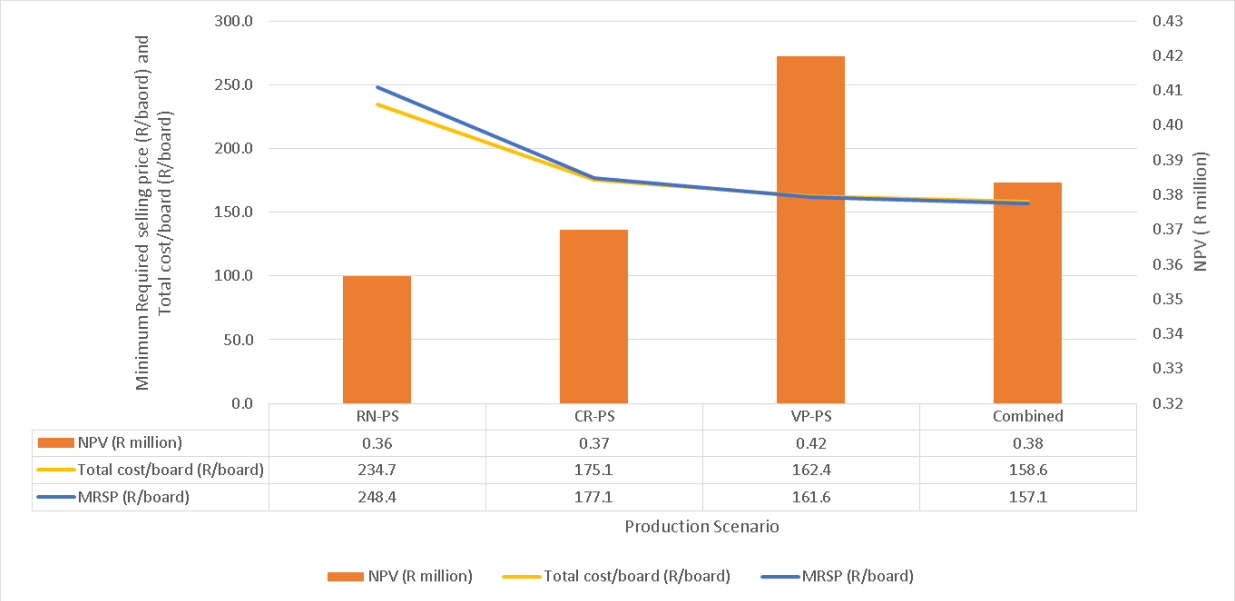

Figure 4-6: Profitability indicators for the different scenarios

RN-PS scenarios shows that it requires a MRSP of R 248 per board, almost 1.6 times the average market-selling price of the board (R155/board), which makes it unfeasible. The high MRSP for RN-PS is due to low PS production of PS, only producing 6 000 tons/day of PS, much lower than the other scenario (as seen in Table 4-8) and therefore not able to produce enough profits to overcome high OPEX. The economic model for RN-PS was not able to overcome those expenses and should not be considered by investors even though it had superior

mechanical strength properties because of high MRSP 1.6 times the average market price. In order for the RN-PS scenario to be economically feasible, PS production has to increase to 34 200 ton/day of PS, to reduce MRSP to R155 per board. For CR-PS, required a MRSP of R177 per board, which is R22 above the average market-selling price. Therefore, Combined scenario performed the best among the scenarios and is the most promising scenario.

4.4.3.2 *Cost Sensitivity analysis*

In the following section, the sensitivity of the particleboard plant profitability is analysed on the basis of minimum selling price and NPV changes due to changes in key parameters. The economic parameters were varied by ± 25% and the effects on the key parameters were observed in order to identify key parameters that have significant effect on the proposed plants profitability (as shown in Table 4-11 for VP-PS scenario). For minimum required selling price (MRSP), sensitivity analysis of the economic parameters include product rate, utility cost, working capital, feedstock cost, fixed capital investment (FCI) and feed flowrate in dry ton/year.

Table 4-11: Economic Parameters for VP-PS scenario. Refer to 4.3.3.1 for definition/explanation of the scenarios

Economic Parameters	-25%	0%	25%
Production rate (boards/day)	1322	1762	2203
Utility Cost (R million/yr.)	13	17	22
Working capital ('000 R/yr.)	395	526	658
Feedstock cost(R million/yr.)	50	67	84
FCI (R million/yr.)	8	11	13
Feed Flow rate (dry ton/year)	11250	15000	18750

Generally utility cost, feedstock cost, feed flow rate and production board rate had the greatest effect on the economic model. Fixed capital investment (FCI) and working capital had very little to no influence on MRSP because they are significantly less than OPEX. For the projected scenarios, it is important to monitor the economic climate especially since utility cost such as electricity, low-pressure steam and hot oil fluid prices are prone to fluctuate. As a result, the

economic models are extremely vulnerable to these process variables making these scenarios unfriendly to investors.

As is seen in the sensitivity analysis RN-PS (Figure 4-7) and CR-PS (Figure 4-8) still produced MRSP above the market price of R155/board, even when utility cost reduced by 25% or feed flow rate, and production rate is increased by 25%. For CR-PS, the scenario only becomes investor friendly when the feed cost is reduced by 25%, therefore reducing the MRSP to R 147/board. With regards to the VP-PS scenario, in order for the MRSP to be below the average market price R 155/board, the PS feed flow rate or board production rate had to be increased by 25% as seen in (Figure 4-9). Feed cost had the most significant influence on the profitability when decreased by 25%, MRSP drops from R 161.6/board to R 129/board which is well within the average market selling price. From the sensitivity analysis for the Combined scenario (Figure 4-10), it can be observed that the proposed the Combined scenario is the most sensitive to feedstock cost with an decrease of 25% resulting in a selling price of R126/board from R 157.10/board. All other changes show that even with an increase in PS feed flowrate or board production rate or reduction in utility cost, the system is still not investor friendly with MRSP still slightly above the average market price of R155/board.

. Overall, the combined scenario (Figure 4-9) looks to be the most attractive scenario from a techno-economic view to produce enough composite boards to overcome high operating cost. As stated in the previous chapter, all the boards made from PS were considered suitable for application that has no load bearing requirements.

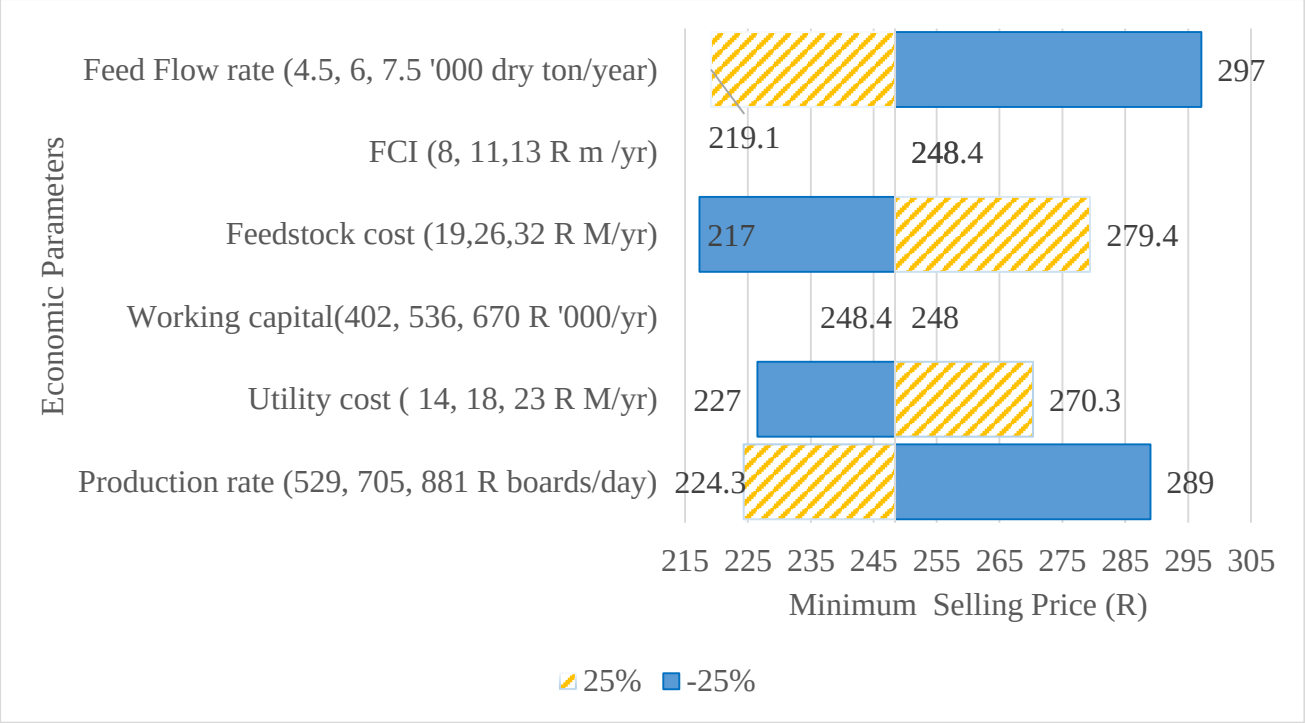

Figure 4-7: Sensitivity analysis on MRSP for RN-PS

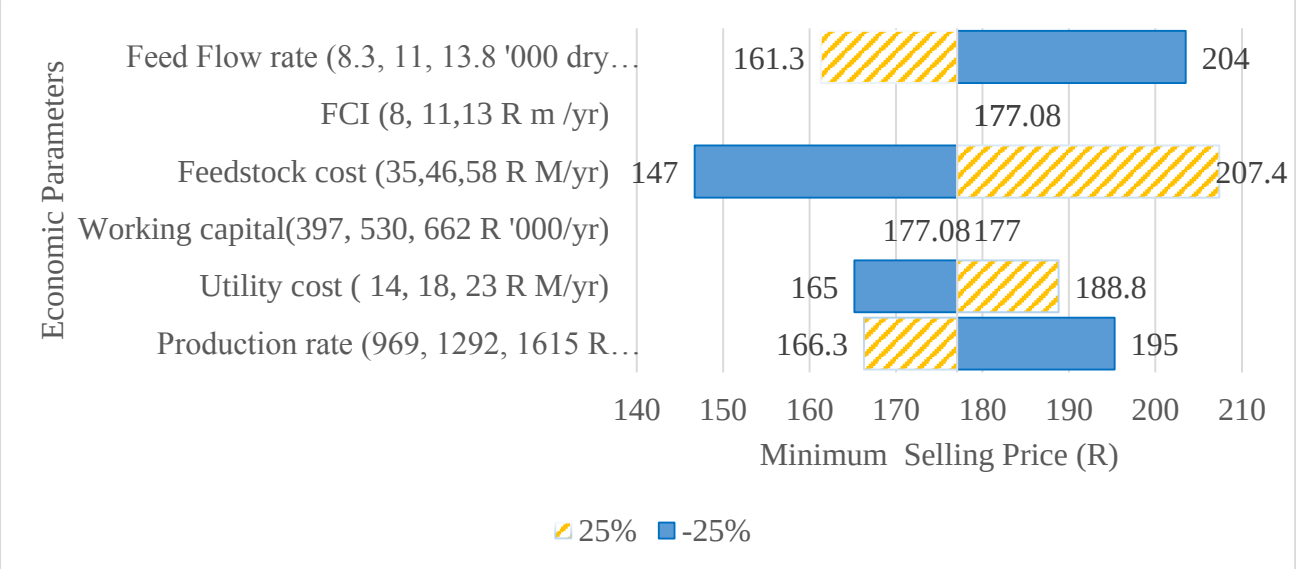

Figure 4-8: Sensitivity analysis on MRSP for CR-PS

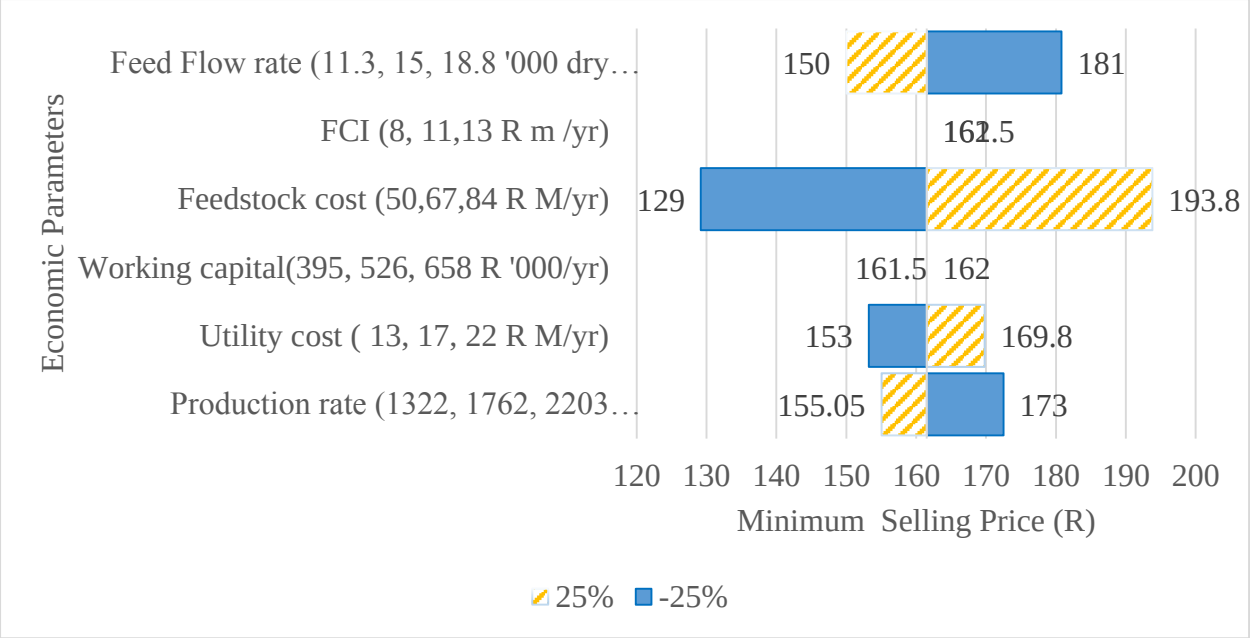

Figure 4-9: Sensitivity analysis on MRSP for VP-PS

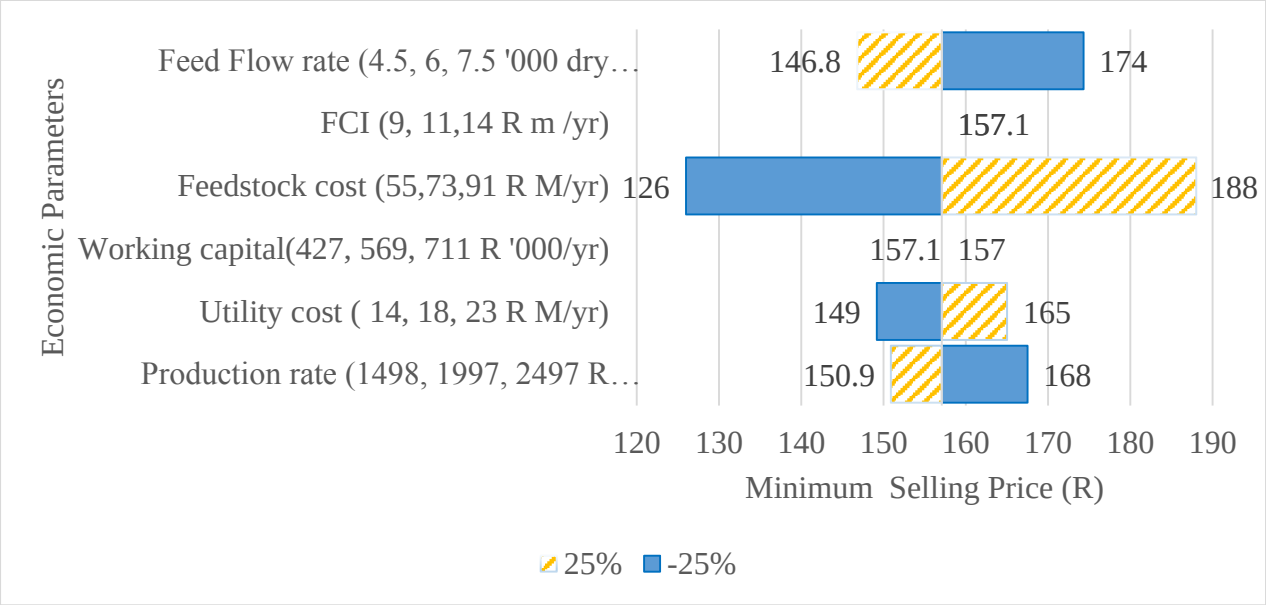

Figure 4-10: Sensitivity analysis on MRSP for Combined

4.5 Summary and conclusion

The section was intended to assess the techno-economic feasibility of utilising PS feedstock to produced composite board products on an industrial scale. Process flow diagram, mass and energy balance, CAPEX and OPEX were used to simulate the production of composite boards using PS. The economic models where designed assuming that all the PS produced at the mill was used to produce particleboard. The techno-economic analysis was based on four different scenarios and following conclusion were drawn from the study:

The results showed that despite being having superior board performances among the PS samples, the RN-PS scenario had the least profitability among the PS scenarios. A minimum required selling price (MRSP) of R 248.1 per board at minimum acceptable IRR of 20%, which was 1.6 times as much as the average selling price R155 per board. The low PS capacity of 6 000 tons/day of PS, much lower than the other scenario and producing board production volume throughput (9 093 m^3/year) made the process economically unattractive. High OPEX was mainly due to high raw material cost specifically monopotassium phosphate and borax. The raw material ratio where determined to be optimum process conditions producing maximum performing boards but negatively impacting the feasibility of RN-PS..

The Combined scenario proved to be the most profitable with a MRSP of R157.1, the closest to the average cost price of R155/board. The biggest contributing factor was that the Combined scenario had the highest production capacity of (25 763 m^3/year) much higher than the other scenarios. Even though operating the press machine at a temperature requiring heating requirement, the revenue created by selling the board production capacity was able to overcome high OPEX cost.

A sensitivity analysis on the MRSP showed that feedstock cost had the most significant influence on the profitability of the different scenario, followed by utility cost, feed flow rate and production rate. Cost of the binder accounted for majority of the OPEX and is included in utility sensitivity analysis. For RN-PS a reduction in feedstock cost by 25% and utility cost or increase in production rate did improve the economic viability but remained above the market range of R155board. For CR-PS, all other changes remained not economically viable except with feedstock cost is reduced by 25%, the MRSP is therefore reduced from R177.1/board to R146.70/board. Overall, reducing feedstock cost by 25% showed that both the VP-PS and Combined scenario profitability improved well below the average market cost price of R155/board. From a techno-economic view point, the Combined scenario looks to be the most

attractive scenario from a techno-economic view to produce enough composite boards to overcome high operating cost. Furthermore, the boards are restricted to be applied for non-loading application.

Chapter 5. Conclusion and recommendations

The use of paper sludge (PS) as a feedstock in the production of construction and building material is relatively new alternative in handling PS waste. This study had a two-folded aim, firstly to determine whether composite boards with acceptable quality could be produced from all the PS samples, and if so, what the formulation/processing requirement. Secondly, to determine whether the process requirements, together with economic study, resulted in a techno-economic viable investment.

5.1 **Conclusions**

5.1.1 Production of composite from paper sludge

Three different types of PS from pulp and paper mills in South Africa were selected based on variations in physical and chemical properties to represent the population of PS produced in South Africa. Paper sludge was collected from recycled fibres pulp and paper mill (RN-PS), corrugated recycled pulp and paper mill (CR-PS) and virgin pulp and paper mill (VP-PS). Short fibrous material within the PS adversely affected the strength properties of the boards resulting in composite boards that did not meet the strength properties for cement bonded particleboard (EN 634-2:2007) and international particleboard standard (ISO 106893:2016, 2016). Since board performances and strength properties did not meet mechanical board strength specification, it is proposed that the addition of veneers can improve strength properties of boards by four-folds, to meet strength properties. However, the PS composite boards were able to meet the physical properties namely the water absorption, thickness swelling and volume swelling. The boards made could be used as wallboards or ceiling with no load bearing application required.

5.1.2 Optimisation of process conditions

The results suggested that it is possible to utilize a variety of PS, even with high levels of fillers and contaminants, to produce composite boards with appropriate functional properties for non-loadbearing applications, through modification of process conditions. Experimental results showed that RN-PS boards were the strongest compared to CR-PS and VP-PS. Factors such as ash content actually had a positive influence on the strength and physical properties of the boards. Statistical analysis showed that the optimum process conditions for RN-PS boards were, Fibre: Inorganic binder of 1.94, binder ratio (KH_2PO_4: MgO) of 5.07, Filler (% of binder) of 20%, 180°C. For CR-PS, Fibre: Inorganic binder of 1.94, binder ratio (KH_2PO_4: MgO) of 5.07, Filler (% of binder) of 22.5%, 90°C. For VP-PS, Fibre: Inorganic binder of 1.94, binder

ratio (KH_2PO_4: MgO) of 5.05, Filler (% of binder) of 15%, 25°C. Results show that, RN-PS boards required significantly less binder than CR-PS and VP-PS. This could again be connected to the presence of high ash content within RN-PS that could be physically filling void spaces within the phosphate crystal structure. Secondly, because of the high ash content within RN-PS, phosphorous compounds could be reacting with calcium carbonate found in ash to make addition calcium phosphate cements and therefore adding strength to the boards. This was not the case for VP-PS samples that have low ash content and therefore require much more binder.

Even so, all the boards met the minimum requirements for physical properties for cement bonded particleboard (EN 634-2:2007) and particleboard according to the international standard (ISO 16893:2016) but not the strength properties. The composite boards produced had medium to high density (0.98-1.01 g/cm3) that could be used for non-structural interior finishes with no load bearing capabilities. A simple lamination of veneers has the potential to improve these strength properties beyond the minimum requirements according the cement bonded particleboard (EN 634-2:2007) and particleboard according to the international standard (ISO 16893:2016). It was concluded that all the PS samples could therefore be used to produce boards with no load bearing abilities. . A maximum PS loading of 66% was determined in order to produce the best quality board possible. Furthermore, the board's composite can still be suitable for wall ceiling, partition application with no load bearing capability.

5.1.3 Economic analysis on profitability

A techno-economic analysis was done on proposed manufacturing plants that are assumed to be located at different sites. These scenarios were then also compared to a scenario with a central location for all the PS is collected from mill as feedstock for the production of the boards. From the experimental results three different types of PS could potentially be used to produce composite boards. Therefore, the techno-economic analysis was performed for the four different scenarios for the production of the boards. The proposed plant is envisaged to be annexed to an existing pulp and paper mill in order to be as close as possible to the source of PS and follow the same process description.

When deciding on the minimum required selling price (MRSP) at a minimum acceptable IRR of 20%, it is vital that it is within the average market price of R155/board otherwise it is not considered not economically viable option. The Combined scenario proved to be the most profitable with a MRSP of R157.1, the closest to the average cost price of R155/board. The biggest contributing factor was that the combined scenario, is the highest production capacity

of (25 763 m^3/year), which is much higher than the other scenarios. This is increased capacity was due to the availability of PS. The RN-PS scenario performed the worst with MRSP of R248.4 /board, mostly due to low production capacity and therefore unable to overcome large OPEX (variable cost). All the economic scenarios showed significant influence to feedstock cost resulting in MRSP below the average market selling price except for RN-PS scenario. Even though, the boards produced do not have load-bearing properties and are traditionally sold at cost price of R155/board compared to load bearing capabilities at R266/board, the economic models shows that with high production capacity and lowering feedstock cost especially monopotassium phosphate, would make the enterprise economically viable.

5.2 **Recommendations**

Based on the results, discussion and conclusions, the following recommendations were made:

5.2.1 Improve board strength properties

Further analysis needs to be done on how to improving of the strength properties of the boards. This analysis would be test whether the addition of veneers improves the strength properties enough to meet the necessary standard. In addition the analysis could test the use of the board according to specific application chosen.

5.2.2 Investigate effects of weathering

It would be advantageous to investigate and analyse the effects of weathering on the board key properties especially for ceiling or wall applications.

5.2.3 Reduce operating cost

Majority of the operating cost consisted of raw materials with cost of monopotassium phosphate and magnesium oxide contributing the highest proportion. It could be advantageous to investigate cheaper alternative in order to improve the profitability of the process.

5.2.4 Better profitability comparison

It would be advantageous to compare the research to other cement bonded particleboards such as Portland cement bonded board, which follow different process routes. Portland cements are more commercially successful in South Africa and would be a competitor in the construction and material industry. Alternatively, to improve profitability of RN-PS, one should aim to increase production from 6 000 to 34 200 ton/day of PS to overcome high OPEX cost.

5.2.5 Investigate more board properties

With the focus of making boards that are not only durable but also fire resistant, it would be beneficial to show that the boards have been fire tested and rated. Furthermore, prove the immense benefit of utilising phosphate based cement even though they are expensive.

5.2.6 Better optimization

To optimise the performance the boards based on the economic models to achieve the cheapest/ most economic friendly process conditions.

Chapter 6. References

Abdullah, R., Ishak, C. F., Kadir, W. R. and Bakar, R. A. (2015) 'Characterization and feasibility assessment of recycled paper mill sludges for land application in relation to the environment', *International Journal of Environmental Research and Public Health*, 12, pp. 9314–9329. doi: 10.3390/ijerph120809314.

Alibaba (2019) *Alibaba - Hot press machine*. Available at: https://www.alibaba.com/product-detail/5000-200000-cbm-per-year-particle_60599705704.html?spm=a2700.7724838.2017115.10.55f673b6D158mm%0A (Accessed: 17 June 2019).

Amiandamhen, S. O. (2017) *Phosphate Bonded Wood and Fibre Composites*. Stellenbosch University.

Amiandamhen, S. O., Meincken, M. and Tyhoda, L. (2016) 'Magnesium based phosphate cement binder for composite panels: A response surface methodology for optimisation of processing variables in boards produced from agricultural and wood processing industrial residues', *Industrial Crops and Products*. Elsevier B.V., 94, pp. 746–754. doi: 10.1016/j.indcrop.2016.09.051.

ANSI A208.2-2009, T. (1999) 'No Title'.

Antoni, Chandra, L. and Hardjito, D. (2015) 'The impact of using fly ash, silica fume and calcium carbonate on the workability and compressive strength of mortar', *Procedia Engineering*. Elsevier B.V., 125, pp. 773–779. doi: 10.1016/j.proeng.2015.11.132.

Arancon, R., Lin, C., Chan, K., Kwan, T. and Luque, R. (2013) 'Advances on waste valorization: new horizons for a more sustainable society', *Energy Science & Engineering*, 1(2), pp. 53–71.

Ashori, A., Tabarsa, T. and Sepahvand, S. (2012) 'Cement-bonded composite boards made from poplar strands', *Construction and Building Materials*. doi: 10.1016/j.conbuildmat.2011.06.001.

ASTM (2012) 'Standard Test Methods for Evaluating Properties of Wood-Base Fiber and Particle Panel Materials - ASTM:D1037-12', *ASTM International*, (June), pp. 1–8. doi: 10.1520/D1037-12.1.

Bajpai, P. (2011) 'Biotechnology for pulp and paper processing', *Biotechnology for Pulp and*

References

Paper Processing, 9781461414, pp. 1–414. doi: 10.1007/978-1-4614-1409-4.

Bester, L. M. (2018) *Development and optimisation of a process for cellulose nanoparticle production from waste paper sludge with enzymatic hydrolysis as an integral part by*. Stellenbosch University.

Bethlehem, L. and Goldblat, M. (1997) *The Bottom Line: Industry and the Environment in South Africa*. Rondebosch: University of Cape Town Press and International Development Research Centre.

Boshoff, S. (2015) *Characterization and fermentation of waste paper sludge for bioethanol production*. Stellenbosch University.

Bouafif, H., Koubaa, A., Perré, P., Cloutier, A. and Riedl, B. (2008) 'Analysis of among-species variability in wood fiber surface using DRIFTS and XPS: Effects on esterification efficiency', *Journal of Wood Chemistry and Technology*, 28(4), pp. 296–315. doi: 10.1080/02773810802485139.

Carrillo, F., Colom, X., Suñol, J. ., Saurina, J., Adapa, P. K., Karunakaran, C., Tabil, L. G. and Schoenau, G. J. (2004) 'Qualitative and quantitative analysis of lignocellulosic biomass using infrared spectroscopy', *European Polymer Journal*, 40(9), pp. 1–20. doi: 10.1016/j.eurpolymj.2004.05.003.

Chau, C. K., Qiao, F. and Li, Z. (2011) 'Microstructure of magnesium potassium phosphate cement', *Construction and Building Materials*. Elsevier Ltd, 25(6), pp. 2911–2917. doi: 10.1016/j.conbuildmat.2010.12.035.

Chen, B., Yang, X. Y. and Liu, N. (2012) 'Experimental Research on the Properties of Modified MPC', *Advanced Materials Research*, 450–451, pp. 769–799. doi: https://doi.org/10.4028/www.scientific.net/AMR.450-451.796.

Department of Environmental Affairs, T. (2012) *National Waste Information Baseline Report*. Pretoria.

Ding, Z., Dong, B., Xing, F., Han, N. and Li, Z. (2012) 'Cementing mechanism of potassium phosphate based magnesium phosphate cement', *Ceramics International*. Elsevier, 38(8), pp. 6281–6288. doi: 10.1016/j.ceramint.2012.04.083.

Ding, Z., Li, Y., Lu, C. and Liu, J. (2018) 'An Investigation of Fiber Reinforced Chemically Bonded Phosphate Ceramic Composites at Room Temperature', *Materials*, 11(858), pp. 1–13.

doi: 10.3390/ma11050858.

Ding, Z. and Li, Z. (2005) 'Effect of aggregates and water contents on the properties of magnesium phospho-silicate cement', *Cement and Concrete Composites*, 27(1), pp. 11–18. doi: 10.1016/j.cemconcomp.2004.03.003.

Donahue, P. K. and Aro, M. D. (2010) 'Durable phosphate-bonded natural fiber composite products', *Construction and Building Materials*. doi: 10.1016/j.conbuildmat.2007.05.015.

Geng, X., Zhang, S. Y. and Deng, J. (2007a) 'Characteristics of Paper Mill Sludge and Its Utilization for the Manufacture of Medium Density Fiberboard', *Wood and Fiber Science*, 39(2), pp. 345–351.

Geng, X., Zhang, S. Y. and Deng, J. (2007b) 'Characteristics of Paper Mill Sludge and Its Utilization for the Manufacture of Medium Density Fiberboard', *Wood and Fiber Science*, 39(2), pp. 345–351.

Hagelqvist, A. (2013) 'Batchwise mesophilic anaerobic co-digestion of secondary sludge from pulp and paper industry and municipal sewage sludge', *Waste Management*, 33(4), pp. 820–824. doi: 10.1016/j.wasman.2012.11.002.

Horn, R. A. . and Setterholm, V. C. (1990) *Fiber morphology and new crops*. Timber Press.

Hou, D., Yan, H., Zhang, J., Wang, P. and Li, Z. (2016) 'Experimental and computational investigation of magnesium phosphate cement mortar', *Construction and Building Materials*. Elsevier Ltd, 112, pp. 331–342. doi: 10.1016/j.conbuildmat.2016.02.200.

Hughes, M. (2016) 'CHEM-E2105 Wood and Wood Products', (March).

Humbird, D., Davis, R. E., Tao, L., Kinchin, C. M., Hsu, D. D., Aden, A., Schoen, P., Lukas, J., Olthof, B., Worley, M., Sexton, D. and Dudgeon, D. (2011) 'Process Design and Economics for Biochemical Conversion of Lignocellulosic Biomass to Ethanol', *Renewable Energy*, 303(May), p. 147. doi: 10.2172/1013269.

Irle, M. and Barbu, M. C. (2010) 'Wood-Based Panel Technology', in THOEMEN, H., IRLE, M., and SERNEK, M. (eds) *Wood-Based Panels An Introduction for Specialists*. London: Brunel Unviersity, p. 283.

ISO 106893:2016, T. (2016) 'Internation Standard for wood-based panels - Particleboard- ISO 16893:2016 E', *International Standard*.

References

ITT, K. (no date) *Cement Bonded Particle Board*. Available at: http://www.iitk.ac.in/ce/test/Materials/56.html.

Jackson, M. J. and Line, M. A. (1997) 'Organic Composition of a Pulp and Paper Mill Sludge Determined by FTIR , 13 C CP MAS NMR , and Chemical Extraction Techniques', 8561(96), pp. 2354–2358. doi: 10.1021/jf960946l.

Kuokkanen, T., Nurmesniemi, H., Pöykiö, R., Kujala, K., Kaakinen, J. and Kuokkanen, M. (2008) 'Chemical and leaching properties of paper mill sludge', *Chemical Speciation and Bioavailability*, 20(2), pp. 111–122. doi: 10.3184/095422908X324480.

Li, Y. and Chen, B. (2013) 'Factors that affect the properties of magnesium phosphate cement', *Construction and Building Materials*. Elsevier Ltd, 47, pp. 977–983. doi: 10.1016/j.conbuildmat.2013.05.103.

Liaw, C. T., Chang, H. L., Hsu, W. C. and Huang, C. R. (1998) 'A novel method to reuse paper sludge and co-generation ashes from paper mill', *Journal of Hazardous Materials*, 58(1–3), pp. 93–102. doi: 10.1016/S0304-3894(97)00123-4.

Mabee, W. (2001) *Study of woody fibre in papermill sludge*. Masters, University of Toronto.

Migneault, S., Koubaa, A., Nadji, H., Riedl, B., Zhang, S. Y. and Deng, J. (2010) 'Medium-Density Fiberboard Produced Using Pulp and Paper Sludge from Different Pulping Processes', *Wood and Fiber Science*, 42(3), pp. 292–303.

Migneault, S., Koubaa, A., Riedl, B., Nadji, H., Deng, J. and Zhang, S.-Y. (2011) 'Binderless Fiberboard Made From Primary and Secondary Pulp and Paper Sludge', *Wood and Fiber Science*, 43(2), pp. 180–193.

Mngomezulu, L. B. (2019) 'Phosphate-bonded composite products : The influence of filler materials , biomass type , and processing method on panel properties By Lehlohonolo Benjamin Mngomezulu', (April).

Monte, M. C., Fuente, E., Blanco, A. and Negro, C. (2009) 'Waste management from pulp and paper production in the European Union', *Waste Management*, pp. 293–308. doi: 10.1016/j.wasman.2008.02.002.

Montgomery, D. (2005) *Design and Analysis of Experiments*. New York: John Wiley & Sons.

Mpact (2016) *Sustainability report*.

References

Müller, P. (2018) 'Carbon-content waste disposal rethought', *Creamer Media's Engineering News*. Available at: http://www.engineeringnews.co.za/print-version/carbon-content-waste-disposal-rethought-2018-05-30.

Ochoa de Alda, J. A. G. (2008) 'Feasibility of recycling pulp and paper mill sludge in the paper and board industries', *Resources, Conservation and Recycling*, 52(7), pp. 965–972. doi: 10.1016/j.resconrec.2008.02.005.

Operation Phakisa, T. (2017) *Briefing to Environmental Affairs Portfolio committee*. South Africa.

PAMSA (2016) *Paper in Perspective*.

PAMSA, T. (2016) *Industry Progress Report: Paper in Perspective*.

Popescu, C. M., Popescu, M. C., Singurel, G., Vasile, C., Argyropoulos, D. S. and Willfor, S. (2007) 'Spectral characterization of eucalyptus wood', *Applied Spectroscopy*, 61(11), pp. 1168–1177. doi: 10.1366/000370207782597076.

Population matters, T. (2013) *Population and Wellbeing*.

Reig, F., Adelantado, J. V. G. and Moreno, M. C. M. . (2002) 'FTIR quantitative analysis of calcium carbonate (calcite) and silica (quartz) mixtures using the constant ratio method. Application to geological samples', *Talanta*, 58(4), pp. 811–821. doi: 10.1016/S0039-9140(02)00372-7.

Ridout, A. J. M. J. C. (2016) *Valorisation of paper waste sludge using pyrolysis processing*. PhD, University of Stellenbosch.

Le Rouzic, M., Chaussadent, T., Platret, G. and Stefan, L. (2017) 'Mechanisms of k-struvite formation in magnesium phosphate cements', *Cement and Concrete Research*. Elsevier Ltd, 91, pp. 117–122. doi: 10.1016/j.cemconres.2016.11.008.

Ruuska, A. and Häkkinen, T. (2014) 'Material Efficiency of Building Construction', *Buildings*, 4(3), pp. 266–294. doi: 10.3390/buildings4030266.

Shi, J., Xing, D. and Li, J. (2011) 'FTIR studies of the changes in wood chemistry from wood forming tissue under inclined treatment', *Energy Procedia*, 16(PART B), pp. 758–762. doi: 10.1016/j.egypro.2012.01.122.

Singh, D. and Wagh, A. S. (1998) 'PHOSPHATE BONDED STRUCTURAL PRODUCTS

References

FROM HIGH VOLUME WASTES'. United States of America: United States Patent.

Sinnott, R. K. (2005) *Chemical Engineering Design: Chemical Engineering Volume 6 (Chemica Engineering Series)*. Oxford: Butterworth-Heinemann.

Sluiter, a, Ruiz, R., Scarlata, C., Sluiter, J. and Templeton, D. (2005) 'Determination of Extractives in Biomass Laboratory Analytical Procedure (LAP) Issue Date : 7 / 17 / 2005 Determination of Extractives in Biomass Laboratory Analytical Procedure (LAP)', *National Renewable Energy Laboratory (NREL)*, (January), p. 12. doi: NREL/TP-510-42619.

Sluiter, A., Ruiz, R., Scarlata, C., Sluiter, J. and Templeton, D. (2008) 'Determination of Extractives in Biomass: Laboratory Analytical Procedure (LAP); Issue Date 7/17/2005 - 42619.pdf', *Technical Report NREL/TP-510-42619*, (January), pp. 1–9. doi: NREL/TP-510-42621.

Sluiter, A., Hames, B., Hyman, D., Payne, C., Ruiz, R., Scarlata, C., Sluiter, J., Templeton, D. and Nrel, J. W. (2008) 'Determination of total solids in biomass and total dissolved solids in liquid process samples', *National Renewable Energy Laboratory (NREL)*, (March), p. 9. doi: NREL/TP-510-42621.

Sluiter, A., Hames, B., Ruiz, R., Scarlata, C., Sluiter, J., Templeton, D. and Crocker, D. (2012) 'NREL/TP-510-42618 analytical procedure - Determination of structural carbohydrates and lignin in Biomass', *Laboratory Analytical Procedure (LAP)*, (April 2008), p. 17. doi: NREL/TP-510-42618.

Soucy, J., Koubaa, A., Migneault, S. and Riedl, B. (2014) 'The potential of paper mill sludge for wood-plastic composites', *Industrial Crops and Products*. Elsevier B.V., 54, pp. 248–256. doi: 10.1016/j.indcrop.2014.01.013.

Tappi, T. (2006) 'T 233 cm-06 Fiber length of pulp by projection', *Tappi*, (1), pp. 1–7.

Taramian, A., Doosthoseini, K., Mirshokraii, S. A. and Faezipour, M. (2007) 'Particleboard manufacturing: An innovative way to recycle paper sludge', *Waste Management*, 27(12), pp. 1739–1746. doi: 10.1016/j.wasman.2006.09.009.

Troschinetz, A. M. and Mihelcic, J. R. (2009) 'Sustainable recycling of municipal solid waste in developing countries', *Waste Management*. Elsevier Ltd, 29(2), pp. 915–923. doi: 10.1016/j.wasman.2008.04.016.

Turton, R., Bailie, R. C., Whiting, W. B., Shaewitz, J. A. and Bhattacharya, D. (2012) *Analysis*

References

Synthesis and Design of Chemical Processes.

Vickers, P., Barnes, S. and Jacques, M. (2019) *The concept of peak shape*. Available at: http://pd.chem.ucl.ac.uk/pdnn/peaks/peakcon.htm (Accessed: 25 October 2019).

Wagh, A. S. (2013) 'Recent Progress in Chemically Bonded Phosphate Ceramics', *ISRN Ceramics*, 2013, pp. 1–20. doi: 10.1155/2013/983731.

Wagh, A. S. and Jeong, S. Y. (2003) 'Chemically Bonded Phosphate Ceramics I A dissolution model of formation .pdf', *Journal of American Ceramic Society*, 86(11), pp. 1838–1844.

Williams, A. (2017) *THE PRODUCTION OF BIOETHANOL AND BIOGAS FROM PAPER SLUDGE*. Stellenbosch University.

World Bank (2018) *Solid Waste Management*.

Xu, B., Ma, H. and Li, Z. (2015) 'Influence of magnesia-to-phosphate molar ratio on microstructures, mechanical properties and thermal conductivity of magnesium potassium phosphate cement paste with large water-to-solid ratio', *Cement and Concrete Research*. Elsevier Ltd, 68, pp. 1–9. doi: 10.1016/j.cemconres.2014.10.019.

Xu, C. C. and Lancaster, J. (2009) 'Treatment of secondary sludge for energy recovery', *Energy Recovery*, pp. 187–212.

Yang, X., Wang, W. and Huang, H. (2015) 'Resistance of paper mill sludge / wood fiber / high-density polyethylene composites to water immersion and thermotreatment', *Journal of Applied Polymer Science*, 41655, pp. 1–7. doi: 10.1002/app.41655.

Youngquist, J. A. (1999) 'Wood-based Composites and Panel Products', *Wood Handbook—Wood as an Engineering Material*, pp. 1–31. doi: http://dx.doi.org/10.1016/B0-12-145160-7/00045-4.

Yue, L., Jia, S. and Bing, C. (2014) 'Experimental study of magnesia and M/P ratio influencing properties of magnesium phosphate cement', *Construction and Building Materials*. Elsevier Ltd, 65, pp. 177–183. doi: 10.1016/j.conbuildmat.2014.04.136.

Zheng, D. D., Ji, T., Wang, C. Q., Sun, C. J., Lin, X. J. and Hossain, K. M. A. (2016) 'Effect of the combination of fly ash and silica fume on water resistance of Magnesium-Potassium Phosphate Cement', *Construction and Building Materials*. Elsevier Ltd, 106, pp. 415–421. doi: 10.1016/j.conbuildmat.2015.12.085.

References

Zhou, X., Tan, L., Zhang, W., Lv, C., Zheng, F., Zhang, R., Du, G., Tang, B. and Liu, X. (2011) 'Enzymatic hydrolysis lignin derived from corn stover as an intrinstic binder for bio-composites manufacture: Effect of fiber moisture content and pressing temperature on boards' properties', *BioResources*, 6(1), pp. 253–264.

Chapter 7. Appendix

7.1 **Appendix A: Chapter 3**

7.1.1 Response surface plots

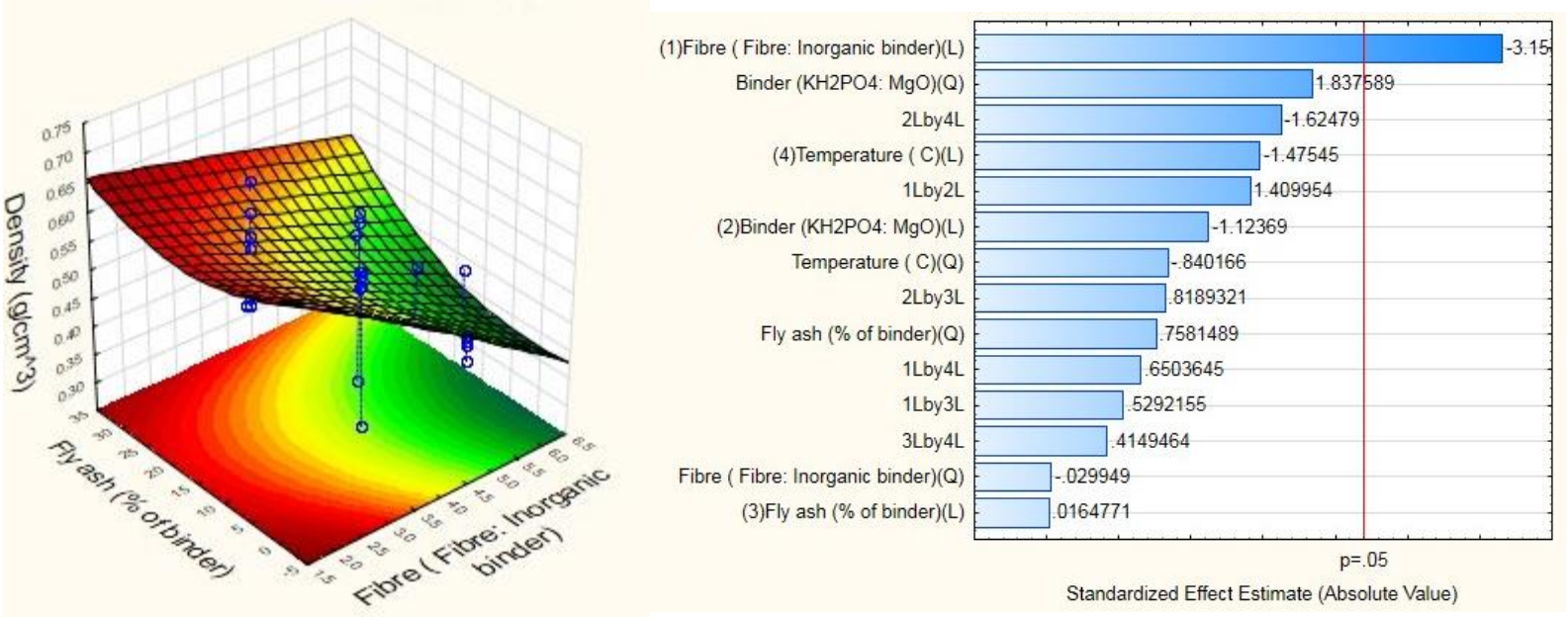

Figure 7-1: VP-PS with Fly ash Surface plots and Parento chart for Density

Appendix

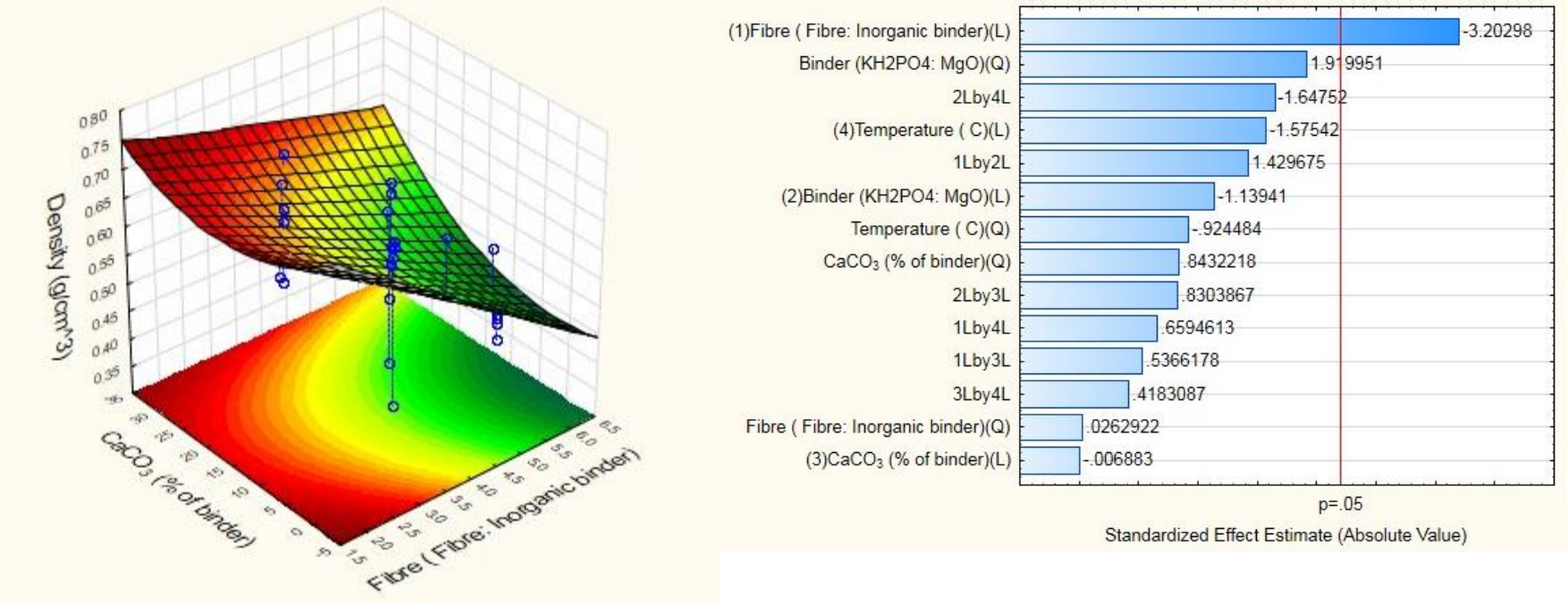

Figure 7-2:VP- PS with CaCO3 - Surface plot and Parento chart for Denstiy

Appendix

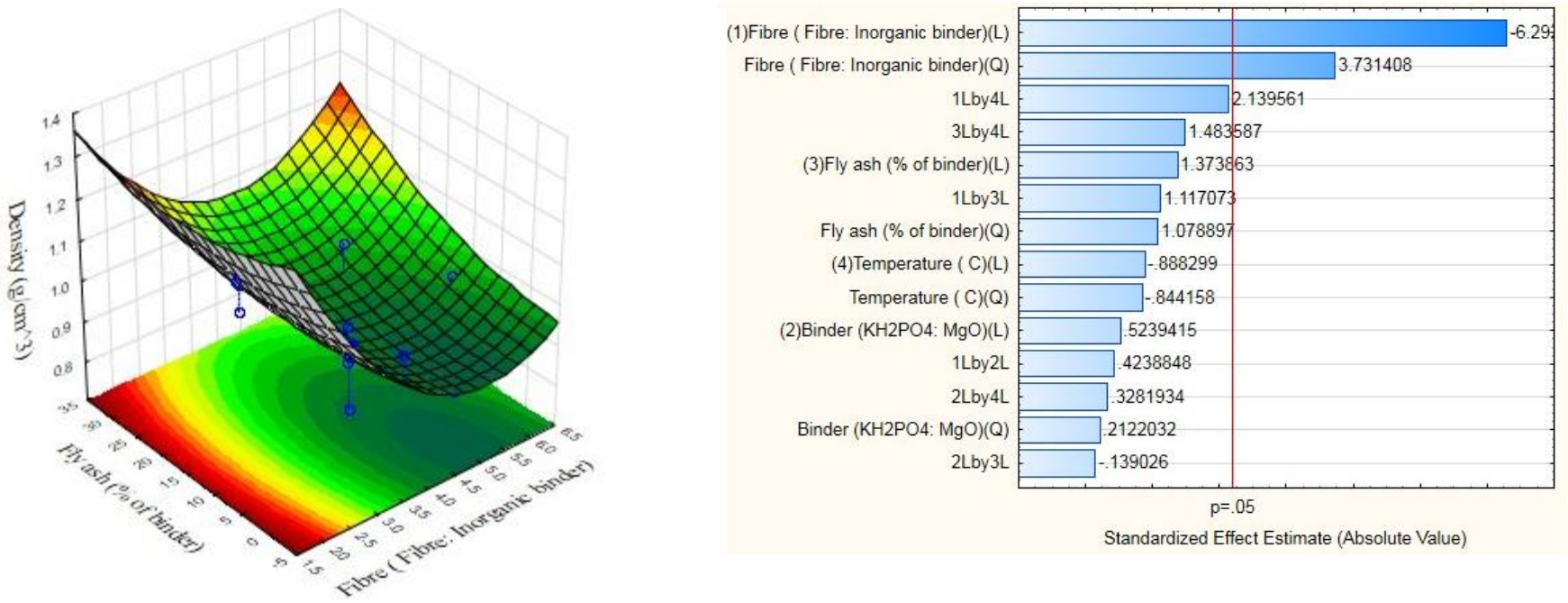

Figure 7-3: CR-PS with FA- Surface plot and parento chart for Density

Appendix

7.1.2 Response surface model parameters

$$y = x_0 + ax_1 + bx_2 + cx_3 + dx_4 + a(Q)x_1 + b(Q)x_2 + c(Q)x_3 + d(Q)x_4 + abx_1x_2 + acx_1x_3 + adx_1x_4 + bcx_2x_3 + bdx_2x_4 + cdx_3x_4$$

Table 7-1: Statistical model fitted for response variables from the independent process condition variables

	MODEL														
	Response variable	Int	a	a(Q)	b	b(Q)	c	c(Q)	d	d(Q)	ab	ac	ad	bc	bc	cd
MPACT - CC	MOE	315.00	-41.39	-3.82	33.84	-57.19	34.79	-6.95	4.62	29.21	-38.11	39.13	3.62	79.71	-4.10	-56.39
	MOR	0.47	-0.05	0.04	-0.05	0.03	0.03	0.09	0.01	0.23	-0.06	0.03	0.06	-0.02	-0.06	0.07
	WA	8.29	2.04	6.47	-2.79	4.70	1.40	1.87	-4.91	-4.32	-0.87	-1.14	0.48	-0.33	0.03	0.17
	TS	2.02	0.09	0.27	-0.75	0.31	-0.63	0.89	-0.07	1.63	0.63	0.02	-0.46	-0.79	-0.67	-0.03
	VS	7.31	-0.22	1.45	0.77	0.53	0.78	-1.57	0.52	-0.80	-0.31	1.04	0.10	-2.14	-0.39	0.07
	Density	0.90	-0.07	0.04	0.01	0.00	0.02	0.01	-0.03	0.01	-0.01	0.03	0.03	0.01	0.01	0.00
MPACT - FA	MOE	424.49	-1.83	-44.17	3.07	6.53	-17.47	44.72	1.96	-94.42	12.04	-38.93	-40.89	40.76	-15.99	37.84
	MOR	0.10	0.00	0.00	-0.01	0.00	0.00	0.00	0.00	-0.01	0.00	0.00	0.00	0.00	0.00	0.00
	WA	8.61	1.98	6.31	-2.71	4.59	1.26	2.04	-4.48	-5.42	-0.85	-1.11	0.47	-0.33	0.03	0.15
	TS	1.76	0.15	0.27	-0.66	0.32	-0.60	0.82	-0.21	2.07	0.70	-0.01	-0.46	-0.80	-0.66	-0.01
	VS	0.34	-0.73	0.93	1.62	1.74	1.68	0.79	-0.13	4.81	-0.74	-3.43	0.00	0.49	-0.01	-0.03
	Density	0.93	-0.06	0.04	0.01	0.00	0.02	0.01	-0.01	-0.02	0.01	0.01	0.03	0.00	0.00	0.02

Appendix

Table 7-2: Statistical model fitted for response variables from the independent process condition variables (Continued)

	Response variable	**Int**	**a**	**a(Q)**	**b**	**b(Q)**	**c**	**c(Q)**	**d**	**d(Q)**	**ab**	**ac**	**ad**	**bc**	**bc**	**cd**
MPACT - SF	MOE	399.34	-1.62	-44.18	2.73	0.95	-14.41	33.37	-1.63	-89.68	10.71	-34.64	-36.39	36.28	-14.23	33.81
	MOR	0.09	0.00	0.00	-0.01	0.00	0.00	0.00	0.00	-0.01	0.00	0.00	0.00	0.00	0.00	0.00
	WA	6.76	1.66	5.28	-2.28	3.83	1.14	1.52	-4.01	-3.52	-0.71	-0.93	0.39	-0.27	0.03	0.14
	TS	1.88	0.15	0.29	-0.62	0.33	-0.59	0.86	-0.05	1.54	0.68	0.00	-0.42	-0.74	-0.61	0.01
	VS	-3.17	-2.25	2.31	1.68	3.14	2.50	2.64	0.19	9.66	-3.10	-7.03	-0.73	0.74	-0.83	0.46
	Density	0.92	-0.07	0.04	0.02	0.00	0.00	0.02	-0.04	0.00	0.01	0.01	0.00	0.00	-0.01	0.01
KC - CC	MOE	366.35	-98.90	123.10	100.51	78.36	-118.88	65.66	116.30	375.29	14.64	139.06	-7.42	-4.08	9.27	-50.33
	MOR	1.28	-0.07	0.11	0.18	0.09	-0.03	0.07	0.16	0.51	0.27	0.25	0.07	-0.14	-0.01	-0.09
	WA	3.20	1.87	7.02	-2.65	5.36	1.51	2.46	-4.60	-2.01	-0.88	-1.13	0.39	-0.38	-0.03	0.13
	TS	-0.05	5.87	2.04	3.95	1.56	3.32	1.22	4.42	7.53	5.63	4.63	4.65	6.50	5.58	5.90
	VS	7.46	-0.22	1.48	0.78	0.54	0.79	-1.60	0.53	-0.81	-0.31	1.06	0.10	-2.19	-0.40	0.07
	Density	1.06	-0.06	0.01	-0.02	0.04	0.00	0.04	-0.04	-0.05	0.03	0.01	0.01	0.02	-0.04	0.01

Appendix

Table 7-3: Statistical model fitted for response variables from the independent process condition variables (Continued)

	Response variable	Int	a	a(Q)	b	b(Q)	c	c(Q)	d	d(Q)	ab	ac	ad	bc	bc	cd
KC - FA	MOE	530.27	-128.36	99.10	108.28	38.91	-107.81	7.40	142.17	272.01	-5.20	120.78	-15.36	-54.07	14.15	-14.18
	MOR	1.16	0.10	0.29	-0.12	0.25	-0.18	0.09	0.33	1.37	-0.43	0.03	0.01	-0.14	-0.01	-0.02
	WA	3.20	1.87	7.02	-2.65	5.36	1.51	2.46	-4.60	-2.01	-0.88	-1.13	0.39	-0.38	-0.03	0.13
	TS	-1.07	0.93	1.22	1.03	1.34	1.29	1.28	-0.56	4.70	-0.44	-2.94	-0.14	0.56	-0.02	-0.04
	VS	-0.90	-0.74	1.23	1.65	2.06	1.64	1.18	0.06	5.22	-0.75	-3.50	0.00	0.50	-0.01	-0.04
	Density	1.14	-0.06	-0.01	-0.03	0.03	0.00	0.02	-0.02	-0.07	0.02	0.00	0.02	0.01	-0.03	0.01
KC - SF	MOE	471.94	-114.24	88.20	96.37	34.63	-95.95	6.58	126.53	242.09	-4.63	107.49	-13.67	-48.12	12.60	-12.62
	MOR	1.03	0.09	0.26	-0.11	0.22	-0.16	0.08	0.29	1.22	-0.38	0.03	0.01	-0.12	-0.01	-0.02
	WA	7.97	1.96	6.22	-2.68	4.52	1.35	1.80	-4.72	-4.15	-0.84	-1.09	0.46	-0.32	0.03	0.16
	TS	-1.09	0.95	1.25	1.05	1.37	1.32	1.31	-0.57	4.79	-0.45	-3.00	-0.14	0.57	-0.02	-0.04
	VS	-3.23	-2.30	2.36	1.71	3.20	2.56	2.69	0.19	9.86	-3.17	-7.17	-0.74	0.75	-0.85	0.47
	Density	1.09	-0.07	-0.01	-0.02	0.02	0.01	0.00	-0.03	-0.03	0.02	0.00	0.02	-0.02	-0.03	0.01

Appendix

Table 7-4: Statistical model fitted for response variables from the independent process condition variables (Continued)

	Response variable	**Int**	**a**	**a(Q)**	**b**	**b(Q)**	**c**	**c(Q)**	**d**	**d(Q)**	**ab**	**ac**	**ad**	**bc**	**bc**	**cd**
SAPPI - CC	MOE	267.75	-35.18	-3.25	28.77	-48.61	29.57	-5.91	3.92	24.83	-32.39	33.26	3.08	67.76	-3.49	-47.93
	MOR	0.40	-0.04	0.03	-0.04	0.02	0.03	0.08	0.01	0.20	-0.05	0.02	0.05	-0.02	-0.05	0.06
	WA	6.99	1.72	5.46	-2.35	3.96	1.18	1.57	-4.14	-3.64	-0.73	-0.96	0.40	-0.28	0.03	0.14
	TS	1.94	0.09	0.26	-0.72	0.30	-0.60	0.86	-0.07	1.56	0.60	0.02	-0.44	-0.76	-0.64	-0.03
	VS	7.90	-0.24	1.57	0.83	0.57	0.84	-1.69	0.56	-0.86	-0.33	1.13	0.11	-2.32	-0.42	0.08
	Density	0.97	-0.05	0.00	-0.02	0.03	0.00	0.02	-0.03	-0.03	0.03	0.01	0.01	0.02	-0.03	0.01
SAPPI - FA	MOE	275.78	-36.24	-3.35	29.63	-50.07	30.46	-6.09	4.04	25.57	-33.37	34.26	3.17	69.79	-3.59	-49.37
	MOR	0.41	-0.04	0.03	-0.04	0.03	0.03	0.08	0.01	0.20	-0.05	0.03	0.06	-0.02	-0.05	0.07
	WA	8.13	2.00	6.34	-2.74	4.61	1.38	1.83	-4.81	-4.23	-0.85	-1.12	0.47	-0.33	0.03	0.17
	TS	1.64	0.14	0.32	-0.64	0.37	-0.62	0.93	-0.07	1.65	0.67	-0.01	-0.44	-0.77	-0.63	-0.01
	VS	-0.95	-0.79	1.30	1.75	2.18	1.74	1.25	0.07	5.53	-0.80	-3.71	0.00	0.53	-0.01	-0.04
	Density	0.90	-0.05	0.00	-0.02	0.03	0.00	0.02	-0.03	-0.02	0.03	0.01	0.01	0.02	-0.03	0.01

Appendix

Table 7-5: Statistical model fitted for response variables from the independent process condition variables (Continued)

	Response variable	**Int**	**a**	**a(Q)**	**b**	**b(Q)**	**c**	**c(Q)**	**d**	**d(Q)**	**ab**	**ac**	**ad**	**bc**	**bc**	**cd**
SAPPI - SF	MOE	200.81	-26.39	-2.44	21.57	-36.46	22.18	-4.43	2.94	18.62	-24.30	24.94	2.31	50.82	-2.62	-35.95
	MOR	0.30	-0.03	0.02	-0.03	0.02	0.02	0.06	0.01	0.15	-0.04	0.02	0.04	-0.02	-0.04	0.05
	WA	6.67	1.64	5.20	-2.24	3.78	1.13	1.50	-3.95	-3.47	-0.70	-0.91	0.39	-0.27	0.03	0.14
	TS	1.81	0.15	0.28	-0.59	0.32	-0.56	0.83	-0.05	1.48	0.66	0.00	-0.40	-0.71	-0.58	0.01
	VS	-3.43	-2.44	2.50	1.82	3.39	2.71	2.86	0.21	10.45	-3.35	-7.60	-0.79	0.80	-0.90	0.50
	Density	1.00	-0.05	0.00	-0.02	0.03	0.00	0.02	-0.03	-0.03	0.03	0.01	0.01	0.02	-0.03	0.01

7.1.3 ANOVA analysis on process conditions variables

Table 7-6: Statistical analysis using ANOVA analysis illustrating the effects of input variables on board properties for CR-PS sludge (bolded and uncerlined are $p < 0.05$ shows significant values)

	Response variable	Int	a	a(Q)	b	b(Q)	c	c(Q)	d	d(Q)	ab	ac	ad	bc	bc	cd
CR-PS - CC	MOE	**0.00**	0.30	0.56	0.74	0.74	0.13	0.54	0.98	0.88	0.85	0.83	0.98	0.33	0.52	0.31
	MOR	**0.02**	0.06	0.06	0.42	0.85	0.56	0.49	0.86	0.17	0.45	0.71	0.48	0.75	0.47	0.33
	WA	**0.00**	**0.00**	0.88	**0.01**	0.64	0.80	0.52	0.81	0.81	0.49	0.84	0.79	0.54	0.53	0.70
	TS	**0.00**	**0.00**	0.27	**0.01**	0.58	0.88	0.29	0.60	0.58	0.49	0.89	0.93	0.89	0.80	0.89
	VS	**0.00**	**0.00**	0.52	**0.03**	0.74	0.78	0.37	0.39	0.22	0.81	0.81	0.66	0.25	0.88	1.00
	Density	**0.00**	**0.00**	**0.00**	0.26	0.74	0.13	0.26	**0.01**	0.47	0.59	**0.01**	**0.04**	0.55	0.23	1.00
CR-PS - FA	MOE	**0.00**	0.35	0.74	0.92	0.97	0.67	0.41	0.92	0.07	0.75	0.32	0.26	0.30	0.67	0.33
	MOR	0.06	**0.01**	**0.02**	0.66	0.35	0.53	0.59	0.28	0.46	0.63	0.31	0.43	0.40	0.13	0.08
	WA	**0.00**	**0.00**	0.79	**0.01**	0.71	0.78	0.53	0.83	0.99	0.51	0.41	0.84	0.57	1.00	0.65
	TS	**0.01**	**0.00**	0.88	0.77	0.87	0.81	0.33	0.48	0.33	0.14	0.58	0.76	0.63	0.84	0.73
	VS	**0.00**	**0.00**	0.46	**0.03**	0.80	0.75	0.43	0.46	0.20	0.81	0.81	0.65	0.25	0.88	0.99
	Density	**0.00**	**0.00**	**0.00**	0.61	0.84	0.20	0.30	0.39	0.42	0.68	0.29	0.06	0.89	0.75	0.17
CR-PS - SF	MOE	**0.00**	0.33	0.58	0.92	0.87	0.70	0.52	0.95	**0.04**	0.74	0.30	0.25	0.28	0.66	0.31
	MOR	0.07	**0.01**	**0.02**	0.66	0.33	0.50	0.53	0.32	0.57	0.63	0.32	0.43	0.41	0.13	0.09
	WA	**0.00**	**0.00**	0.73	**0.01**	0.75	0.91	0.44	0.84	0.87	0.45	0.44	0.78	0.55	0.87	0.63
	TS	**0.01**	**0.00**	0.91	0.78	0.85	0.87	0.29	0.42	0.46	0.16	0.61	0.78	0.62	0.83	0.75
	VS	**0.00**	**0.00**	0.55	**0.02**	0.71	0.80	0.34	0.39	0.19	0.83	0.83	0.67	0.25	0.87	0.98
	Density	**0.00**	**0.00**	**0.01**	0.11	0.80	0.80	0.26	**0.01**	0.96	0.55	0.61	0.75	0.88	0.70	0.46

where , a = fibre(linear) , b = binder (linear) , c = Filler (linear) , d = Temperature (linear) , a(Q) = fibre (quadratic), b(Q) = binder ratio (quadratic) , c(Q) = filler (quadratic) , d(Q) = quadratic coefficients; ab, ac, ad, bc, bd, cd x

Appendix

Table 7-7: Statistical analysis using ANOVA analysis illustrating the effects of input variables on board properties for RN-PS sludge ($p < 0.05$ shows significant values)

	Response variable	Int	a	a(Q)	b	b(Q)	c	c(Q)	d	d(Q)	ab	ac	ad	bc	bc	cd
RN-PS - CC	MOE	**0.00**	**0.04**	0.36	**0.04**	0.51	0.49	0.06	0.67	0.20	0.97	0.65	0.45	0.65	0.62	0.09
	MOR	**0.00**	**0.00**	0.52	**0.05**	0.29	**0.05**	**0.02**	0.21	**0.00**	0.09	0.44	0.82	0.30	0.15	0.91
	WA	**0.00**	**0.00**	0.87	**0.01**	0.64	0.78	0.49	0.77	0.72	0.49	0.84	0.79	0.54	0.53	0.69
	TS	**0.00**	**0.00**	0.31	**0.02**	0.66	0.87	0.28	0.64	0.87	0.49	0.89	0.93	0.89	0.81	0.89
	VS	**0.00**	**0.00**	0.46	**0.03**	0.80	0.75	0.43	0.46	0.20	0.81	0.81	0.65	0.25	0.88	0.99
	Density	**0.00**	**0.01**	**0.03**	0.19	0.45	**0.00**	0.82	0.96	0.27	0.97	0.72	0.98	0.97	0.83	0.96
RN-PS-FA	MOE	**0.00**	**0.04**	0.43	**0.04**	0.59	0.51	**0.05**	0.58	0.17	0.97	0.65	0.45	0.64	0.62	0.08
	MOR	**0.00**	**0.00**	0.78	**0.04**	0.47	**0.03**	**0.01**	0.10	**0.00**	0.08	0.43	0.81	0.28	0.14	0.90
	WA	**0.00**	**0.00**	0.92	**0.01**	0.63	0.82	0.55	0.81	0.77	0.50	0.85	0.80	0.56	0.54	0.71
	TS	**0.00**	**0.00**	0.26	**0.01**	0.57	0.87	0.29	0.59	0.55	0.49	0.89	0.93	0.89	0.81	0.89
	VS	**0.00**	**0.00**	0.51	**0.03**	0.75	0.77	0.38	0.39	0.23	0.81	0.81	0.66	0.26	0.88	1.00
	Density	**0.00**	**0.00**	0.66	0.11	0.08	0.82	0.41	0.18	**0.02**	0.23	0.82	0.23	0.51	0.12	0.49
RN-PS-SF	MOE	**0.00**	**0.04**	0.43	**0.04**	0.59	0.51	**0.05**	0.58	0.17	0.97	0.65	0.45	0.64	0.62	0.08
	MOR	**0.00**	**0.00**	0.78	**0.04**	0.47	**0.03**	**0.01**	0.10	**0.00**	0.08	0.43	0.81	0.28	0.14	0.90
	WA	**0.00**	**0.00**	0.92	**0.01**	0.63	0.82	0.55	0.81	0.77	0.50	0.85	0.80	0.56	0.54	0.71
	TS	0.63	0.23	0.12	0.18	0.09	0.15	0.22	0.50	**0.01**	0.64	**0.01**	0.88	0.54	0.98	0.96
	VS	0.44	0.12	0.11	0.23	**0.04**	0.13	0.18	0.90	**0.00**	0.09	**0.00**	0.67	0.66	0.62	0.79
	Density	**0.00**	**0.00**	0.51	0.22	0.23	0.77	0.87	0.14	0.41	0.35	0.96	0.30	0.44	0.15	0.60

where , a = fibre(linear) , b = binder (linear) , c = Filler (linear) , d = Temperature (linear) , a(Q) = fibre (quadratic), b(Q) = binder ratio (quadratic) , c(Q) = filler (quadratic) , d(Q) = quadratic coefficients; ab, ac, ad, bc, bd, cd

Appendix

Table 7-8: Statistical analysis using ANOVA analysis illustrating the effects of input variables on board properties for VP-PS sludge ($p < 0.05$ shows significant values)

	Response variable	Int	a	a(Q)	b	b(Q)	c	c(Q)	d	d(Q)	ab	ac	ad	bc	bc	cd
VP-PS - CC	MOE	**0.00**	0.30	0.56	0.74	0.74	0.13	0.54	0.98	0.88	0.85	0.83	0.98	0.33	0.52	0.31
	MOR	**0.02**	0.06	0.06	0.42	0.85	0.56	0.49	0.86	0.17	0.45	0.71	0.48	0.75	0.47	0.33
	WA	**0.00**	0.12	0.88	0.15	0.53	0.75	0.76	0.79	0.29	0.23	0.77	0.85	0.89	0.57	0.74
	TS	**0.01**	**0.00**	0.93	0.78	0.84	0.88	0.29	0.43	0.45	0.16	0.61	0.78	0.61	0.82	0.76
	VS	**0.00**	**0.00**	0.56	**0.02**	0.69	0.82	0.32	0.39	0.18	0.83	0.83	0.67	0.25	0.86	0.97
	Density	**0.00**	**0.01**	0.98	0.28	0.08	0.99	0.42	0.14	0.38	0.18	0.60	0.52	0.42	0.13	0.68
VP-PS - FA	MOE	**0.00**	0.30	0.56	0.74	0.74	0.13	0.54	0.98	0.88	0.85	0.83	0.98	0.33	0.52	0.31
	MOR	**0.02**	0.06	0.06	0.42	0.85	0.56	0.49	0.86	0.17	0.45	0.71	0.48	0.75	0.47	0.33
	WA	**0.00**	**0.00**	0.89	**0.02**	0.54	0.96	0.51	0.86	0.94	0.49	0.54	0.79	0.61	0.79	0.64
	TS	**0.01**	**0.00**	0.82	0.78	0.94	0.86	0.29	0.41	0.50	0.16	0.61	0.78	0.61	0.81	0.75
	VS	**0.00**	**0.00**	0.44	**0.03**	0.83	0.79	0.34	0.38	0.20	0.84	0.83	0.68	0.26	0.86	0.98
	Density	**0.00**	**0.01**	0.98	0.29	0.09	0.99	0.46	0.17	0.42	0.19	0.61	0.53	0.43	0.13	0.69
VP-PS - SF	MOE	**0.00**	0.30	0.56	0.74	0.74	0.13	0.54	0.98	0.88	0.85	0.83	0.98	0.33	0.52	0.31
	MOR	**0.02**	0.06	0.06	0.42	0.85	0.56	0.49	0.86	0.17	0.45	0.71	0.48	0.75	0.47	0.33
	WA	**0.00**	**0.00**	0.76	0.09	0.53	0.33	0.61	0.91	0.55	0.63	0.44	0.82	0.73	0.18	0.77
	TS	0.22	0.76	0.57	0.23	0.51	0.32	0.22	0.93	0.12	0.28	0.99	0.50	0.24	0.34	0.99
	VS	0.44	0.12	0.11	0.23	**0.04**	0.13	0.18	0.90	**0.00**	0.09	**0.00**	0.67	0.66	0.62	0.79
	Density	**0.00**	**0.01**	0.98	0.28	0.09	0.99	0.46	0.17	0.41	0.19	0.61	0.53	0.43	0.13	0.69

7.1.4 Optimisation

Confirmation runs were performed in order to assess the accuracy of the response model developed from the CCD design.

Table 7-9: Confirmation runs from optimised process conditions comparing predicted vs actual response variable using statistical model

	Response	Predicted	Experimental results	%error	R-squared	Adjusted R-squared
RN-PS: CaCO3	MOE	1367.4	1295	6	0.72	0.36
	MOR	4.92	4.12	16	0.87	0.7
	WA	18.86	23.22	18	0.86	0.7
	TS	-2.58	1.22	NA	0.84	0.63
	VS	-0.18	1.42	NA	0.77	0.47
	Density	1.6	1.5	6	0.91	0.41
CR-PS: CaCO3	MOE	583.9	620.26	6	0.4	0
	MOR	1.55	2.1	26	0.57	0.02
	WA	21.14	26.23	19	0.87	0.7
	TS	-2.94	2.12	NA	0.84	0.64
	VS	0.36	2	NA	0.77	0.47
	Density	1.27	1.23	3	0.91	0.79
VP-PS: CaCO3	MOE	751.62	742.18	1	0.4	0
	MOR	2.29	1.95	15	0.57	0.2
	WA	16.57	30.23	45	0.46	0
	TS	-7.4	2.54	NA	0.74	0.42
	VS	0.09	4	NA	0.78	0.49
	Density	0.75	0.74	1	0.7	0.33

R^2: Coefficient of determination; R^2_{adj}: adjusted coefficient of determination

7.2 Appendix B: Chapter 4

7.2.1 RN-PS scenario

7.2.1.1 *RN-PS process mass balance*

Table 7-10: RN-PS Stream Table

Description			PS inlet to M100	Water inlet to M-101		MPP inlet to M-100		MgO inlet to M-100		CaCO3 inlet to M-		Borax inlet to M-100		Mixture after M-101		After Matt Fomation	Matt Formation	After Pre-press	Excess Water	After Hot Press	After Conditioning	Final Product	To Trimming Waste
Stream		Units	1	3	4	5	6	7	8	9	10	11	12	13	14	15	16	17	18	19	20	21	22
Tempature		°C	25	25	25	25	25	25	25	25	25	25	25	25	25	25	25	25	25	100	25	25	25
Pressure		bar	1	1	1	1	1	1	1	1	1	1	1	1	1	1	1	1	1	1	1	1	1
Vapor Frac		wt%	0	0	1	0	0	0	0	0	0	0	0	0	0	0	0	0	0	0	0	0	0
Liquid Frac		wt%	1	1	0	0	0	0	0	0	0	0	0	0	1	0	0	0	1	0	0	0	0
Solid Frac		wt%	0	0	0	1	1	1	1	1	1	1	1	1	0	1	1	1	0	1	1	1	1
Moisture Content		wt%	54%	100%	100%	0%	0%	0%	0%	0%	0%	0%	0%	55%	55%	55%	55%	55%	100%	5%	5%	5%	5%
Mass Flow		kg/hr	1630	537	537	258	258	51	51	77	77	41	41	2595	2595	2439	156	2439	1275	1165	1165	1072	93
WATER	l	kg/hr	880	537	537	0	0	0	0	0	0	0	0	1418	1418	1333	85	1333	1275	58	58	54	5
Magnesium Oxide	S	kg/hr	0	0	0	0	0	51	51	0	0	0	0	51	51	48	3	48	0	48	48	44	4
Calcium Carbonate	S	kg/hr	0	0	0	0	0	0	0	77	77	0.0	0.0	77	77	73	5	73	0	73	73	67	6
Monopotassium phosphate	S	kg/hr	0	0	0	258	258	0	0	0	0	0.0	0.0	258	258	243	15	243	0	243	243	223	19
Borox	S	kg/hr	0	0	0	0	0	0	0	0	0	40.8	40.8	41	41	38	2	38	0	38	38	35	3
Paper sludge	S	kg/hr	750	0	0	0	0	0	0	0	0	0.0	0.0	750	750	705	45	705	0	705	705	649	56
Mass fractions																							
WATER	l	-	0.54	1.00	1.00	0.00	0.00	0.00	0.00	0.00	0.00	0.0	0.0	0.55	0.55	0.55	0.55	0.55	1.00	0.05	0.05	0.05	0.05
Magnesium Oxide	S	-	0.00	0.00	0.00	0.00	0.00	1.00	1.00	0.00	0.00	0.00	0.00	0.02	0.02	0.02	0.02	0.02	0.00	0.04	0.04	0.04	0.04
Calcium Carbonate	S	-	0.00	0.00	0.00	0.00	0.00	0.00	0.00	1.00	1.00	0.00	0.00	0.03	0.03	0.03	0.03	0.03	0.00	0.06	0.06	0.06	0.06
Monopotassium phosphate	S	-	0.00	0.00	0.00	1.00	1.00	0.00	0.00	0.00	0.00	0.00	0.00	0.10	0.10	0.10	0.10	0.10	0.00	0.21	0.21	0.21	0.21
Borox	S	-	0.00	0.00	0.00	0.00	0.00	0.00	0.00	0.00	0.00	1.00	1.00	0.02	0.02	0.02	0.02	0.02	0.00	0.03	0.03	0.03	0.03
Paper sludge	S	-	0.46	0.00	0.00	0.00	0.00	0.00	0.00	0.00	0.00	0.00	0.00	0.29	0.29	0.29	0.29	0.29	0.00	0.61	0.61	0.61	0.61

7.2.1.2 *RN-PS Utility Consumption*

Table 7-11: RN-PS utility consumption cost

Utility Cost				
Equipment	**Equipment ID**	**Flowrate**	**Yearly usage**	**Cost R**
Electricity		kW	kWh	
Vibrating screens	NA			
Forming machine	NA			
prepress machine	PRESS-100			
Belt conveyor for mat boards	NA			
Loader for mat board	NA			
Hot press machine	PRESS-101			
Unloader for finished board	NA			
Overturning machine	NA			
Edge saw machine	NA			
Stacking machine	NA			
Sanding machine	T-100	2500	20000000	16800000
Industrial Air conditioner	NA			
Pumps		0.06	505	424
Screw conveyer	SC-100 (A/B)	6	44000	36960
Screw conveyer	SC-101 (A/B)	6	44000	36960
Screw conveyer	SC-102 (A/B)	6	0	0
Belt Conveyor	CV-100 (A/B)	6	44000	36960
Belt Conveyor	CV-101 (A/B)	6	44000	36960
Belt Conveyor	CV-102 (A/B)	6	44000	36960
Belt Conveyor	CV-103 (A/B)	6	44000	36960
Agitator	NA	7	52162	43816
Hot Oil		kg/hr	GJ/year	
Hot Press machine	Press-101	56	5497	1105492
			Total	18 171 492

Appendix

Sample calculation for hot oil requirement to heat up boards to optimum press temperature

Figure 7-4: Board plate system

Assumptions:

- Hot oil incoming temperature 280 C and outgoing temperature 275 C
- Steady state system i.e. the plate is already at 280 C
- No heat loss to the environment
- Perfect contact with hot oil and plates
- Assuming that capital and utility cost investment has already been completed for the hot oil generation system

Mass of 1 board = 38.7 kg

For RN-PS: Operating board press temperature = 180°C

Board initial temperature = 25°C

cp of dried sludge = 1.95 kJ/kg.C(Xu and Lancaster, 2009)

Heat energy equation: $Q_{boards} = Q_{oil}$

$Q_{board} = m_{board} \times cp_{board} \times \Delta T_{board}$ = 38.7 kg x 1.95 kJ/kg.C x (180 – 25) °C = 11 697.05 kJ per board

Q_{board} = heat energyfrom board system (J), m = m_{board} (kg), cp (specific heat kJ/kg.c) and T_{board} in °C.

Heating requirement sourced from oil

$Q_{oil} = m_{oil} \times cp_{oil} \times \Delta T_{oil}$ therefore since $Q_{boards} = Q_{oil}$

$m_{oil} = Q_{oil} / (cp_{oil} \times \Delta T_{oil})$ = 11 697.050kJ / (2.44 kJ/kg.K x ((280+273) – (275+273)))

m_{oil} = 958.78 kg per board made

mass flowrate = m_{oil} x board production per year / operating hours per year

mass flow rate (kg/hr) = (958.78 kg x 234 965 baord per year)/ 8000 hours = 28.16 kg/hr

But since the top and bottom plate is getting heated up, need twice as much

Therefore, mass flow rate = 28.16 kg/hr x 2 = 56.3 kg/hr

Q_{oil} = heat energyfrom board system (J), m = m_{oil} (kg), cp (specific heat kJ/kg.c) and T_{oil} in °C.

7.2.1.3 *RN-PS Equipment Costing*

Table 7-12: RN-PS Total Capital Investment

Equipments	Equipment Code	Purchased Cost (R) in 2004	Purchased Cost (R) in 2018	Installation Cost (R) in 2018
MDF Press Machines				
Vibrating screens	V-100			
Forming machine	MT-100			
prepress machine	PRESS-100			
Belt conveyor for mat boards	NA			
Loader for mat board	NA			
Hot press machine	PRESS-101			
Unloader for finished board	NA			
Overturning machine	NA			
Edge saw machine	NA			
Stacking machine	NA			
Sanding machine	T-100		2374984.94	2422484.64
Industrial Air conditioner	NA		2478.12	2527.68
Pumps				
Pumps	P-101 A/B	226042.52	345116.45	1069860.99
Pumps - Transport pumps from water source to storage tank		211346.44	322678.81	1000304.31
Storage Tanks				
Storage Tanks	ST-100	9590.98	12988.41	38965.24
Storage Tanks	NA	24086.47	32618.68	97856.04
Storage tanks	NA	8577.36	11615.74	34847.21
Storage tanks	NA	6851.58	9278.63	27835.89
Storage tanks	NA	3602.74	4878.94	14636.83
Storage tanks	NA	40260.18	54521.64	163564.91
Conveyor Belts				
Screw conveyer	SC-100 (A/B)		5335.48	9070.32
Screw conveyer	SC-101 (A/B)		5335.48	9070.32
Screw conveyer	SC-102 (A/B)		5335.48	9070.32
Belt Conveyor	CV-100 (A/B)			20363.46
Belt Conveyor	CV-101 (A/B)			7688.59
Belt Conveyor	CV-102 (A/B)			10801.61
Belt Conveyor	CV-103 (A/B)			6725.13
Agigator Mixer				
Mixing Vessel	M-100	87860.98	118984.18	214171.52
Agitator Mixer			297340.0885	475744.1415
Totals			**$ -**	**R 5 635 589.15**

Appendix

7.2.1.4 *RN-PS Discounted Cash Flow Sheet*

Table 7-13: RN-PS Discounted cash flow

Year	0	1	2	3	4	5	6	7	8	9	10	11	12	13	14	15
Fixed Capital Investment	R 10 721 289.39															
Land	R -															
Working Capital	R 536 064.47															
Baord Price (R/m2)	R 248.40	R 262.56	R 276.72	R 290.88	R 305.04	R 319.19	R 333.35	R 347.51	R 361.67	R 375.83	R 389.99	R 404.15	R 418.31	R 432.46	R 446.62	R 460.78
Board Production sales	R -	R 61 692 223.08	R 65 019 050.63	R 68 345 878.17	R 71 672 705.72	R 74 999 533.27	R 78 326 360.81	R 81 653 188.36	R 84 980 015.90	R 88 306 843.45	R 91 633 670.99	R 94 960 498.54	R 98 287 326.09	R 101 614 153.63	R 104 940 981.18	R 108 267 808.72
Total Annual Sales		R 43 184 556.16	R 52 015 240.50	R 61 511 290.36	R 71 672 705.72	R 74 999 533.27	R 78 326 360.81	R 81 653 188.36	R 84 980 015.90	R 88 306 843.45	R 91 633 670.99	R 94 960 498.54	R 98 287 326.09	R 101 614 153.63	R 104 940 981.18	R 108 267 808.72
Disposal Cost Saving		5574618	5892371.226	6228236.386	6583245.86	6958490.874	7355124.854	7774366.97	8217505.888	8685903.723	9181000.235	9704317.249	10257463.33	10842138.74	11460140.65	12113368.67
Total Revenue	R -	R 48 759 174.16	R 57 907 611.73	R 67 739 526.74	R 78 255 951.58	R 81 958 024.14	R 85 681 485.67	R 89 427 555.33	R 93 197 521.79	R 96 992 747.17	R 100 814 671.23	R 104 664 815.79	R 108 544 789.42	R 112 456 292.37	R 116 401 121.83	R 120 381 177.39
Annual Manufacturing Cost																
Feedstock Price ($/ ton)		R -	R -	R -	R -	R -	R -	R -	R -	R -	R -	R -	R -	R -	R -	R -
Feedstock cost		R -	R -	R -	R -	R -	R -	R -	R -	R -	R -	R -	R -	R -	R -	R -
Other Variable Costs		R 43 892 259.18	R 49 038 582.68	R 51 833 781.89	R 54 788 307.46	R 57 911 240.99	R 61 212 181.72	R 64 701 276.08	R 68 389 248.82	R 72 287 436.00	R 76 407 819.85	R 80 763 065.58	R 85 366 560.32	R 90 232 454.26	R 95 375 704.15	R 100 812 119.29
Fixed Operating Costs		R 11 254 860.73	R 12 574 481.90	R 13 291 227.36	R 14 048 827.32	R 14 849 610.48	R 15 696 038.28	R 16 590 712.46	R 17 536 383.07	R 18 535 956.91	R 19 592 506.45	R 20 709 279.32	R 21 889 708.24	R 23 137 421.61	R 24 456 254.64	R 25 850 261.16
Total Product Cost	R -	R 55 147 119.91	R 61 613 064.58	R 65 125 009.26	R 68 837 134.78	R 72 760 851.47	R 76 908 220.00	R 81 291 988.54	R 85 925 631.89	R 90 823 392.91	R 96 000 326.30	R 101 472 344.90	R 107 256 268.56	R 113 369 875.87	R 119 831 958.79	R 126 662 380.44
Annual Depreciation																
Plant Writedown		0.20	0.20	0.20	0.20	0.20										
Depreciation Charge		R 2 144 257.88	R 2 144 257.88	R 2 144 257.88	R 2 144 257.88	R 2 144 257.88	R -	R -	R -	R -	R -	R -	R -	R -	R -	R -
Remaining Value		R 8 577 031.51	R 6 432 773.63	R 4 288 515.75	R 2 144 257.88	R -	R -	R -	R -	R -	R -	R -	R -	R -	R -	R -
Net Revenue	R -10 185 224.92	R -106 050 551.95	R -121 664 934.18	R -135 008 793.88	R -149 237 344.24	R -156 863 133.48	R -162 589 705.67	R -170 719 543.87	R -179 123 153.68	R -187 816 140.08	R -196 814 997.53	R -206 137 160.69	R -215 801 057.98	R -225 826 168.24	R -236 233 080.62	R -247 043 557.83
Losses Forward			R -106 050 551.95	R -227 715 486.13	R -362 724 280.01	R -511 961 624.25	R -668 824 757.74	R -831 414 463.40	R -1 002 134 007.27	R -1 181 257 160.95	R -1 369 073 301.03	R -1 565 888 298.56	R -1 772 025 459.25	R -1 987 826 517.23	R -2 213 652 685.47	R -2 449 885 766.09
Taxable Income		R -106 050 551.95	R -227 715 486.13	R -362 724 280.01	R -511 961 624.25	R -668 824 757.74	R -831 414 463.40	R -1 002 134 007.27	R -1 181 257 160.95	R -1 369 073 301.03	R -1 565 888 298.56	R -1 772 025 459.25	R -1 987 826 517.23	R -2 213 652 685.47	R -2 449 885 766.09	R -2 696 929 323.92
Income Tax		R -	R -	R -	R -	R -	R -	R -	R -	R -	R -	R -	R -	R -	R -	R -
Net Present Worth	R -715 503.23															
Gross Proft		(R6 387 946)	(R3 705 453)	R2 614 517.49	R9 418 816.80	R9 197 172.67	R8 773 265.66	R8 135 566.79	R7 271 889.90	R6 169 354.27	R4 814 344.93	R3 192 470.89	R1 288 520.86	(R913 583)	(R3 430 837)	(R6 281 203)
Net Profit		(R8 532 204)	(R5 849 711)	R470 259.61	R7 274 558.92	R7 052 914.80	R8 773 265.66	R8 135 566.79	R7 271 889.90	R6 169 354.27	R4 814 344.93	R3 192 470.89	R1 288 520.86	(R913 583)	(R3 430 837)	(R6 281 203)
Cash Flow	(R10 185 225)	(R6 387 946)	(R3 705 453)	R2 614 517.49	R9 418 816.80	R9 197 172.67	R8 773 265.66	R8 135 566.79	R7 271 889.90	R6 169 354.27	R4 814 344.93	R3 192 470.89	R1 288 520.86	(R913 583)	(R3 430 837)	(R6 281 203)
Discounted Cash Flow	(R10 185 225)	(R5 323 288)	(R2 573 231)	R1 513 030.95	R4 542 253.47	R3 696 137.42	R2 938 148.92	R2 270 487.38	R1 691 209.18	R1 195 662.19	R777 543.58	R429 668.23	R144 516.19	(R85 387)	(R267 216)	(R407 684)
Cumualtive Cash Flow	(R10 185 225)	(R16 573 171)	(R20 278 624)	(R17 664 106)	(R8 245 289)	R951 883.44	R9 725 149.10	R17 860 715.89	R25 132 605.79	R31 301 960.06	R36 116 304.98	R39 308 775.87	R40 597 296.73	R39 683 713.24	R36 252 876.27	R29 971 673.22
Discounted Cumulative Cash Flow	(R10 185 225)	(R15 508 513)	(R18 081 744)	(R16 568 713)	(R12 026 460)	(R8 330 322)	(R5 392 173)	(R3 121 686)	(R1 430 477)	(R234 815)	R542 728.91	R972 397.13	R1 116 913.32	R1 031 526.26	R764 310.15	R356 625.71

7.2.1.5 *RN-PS Cumulative Cash Flow*

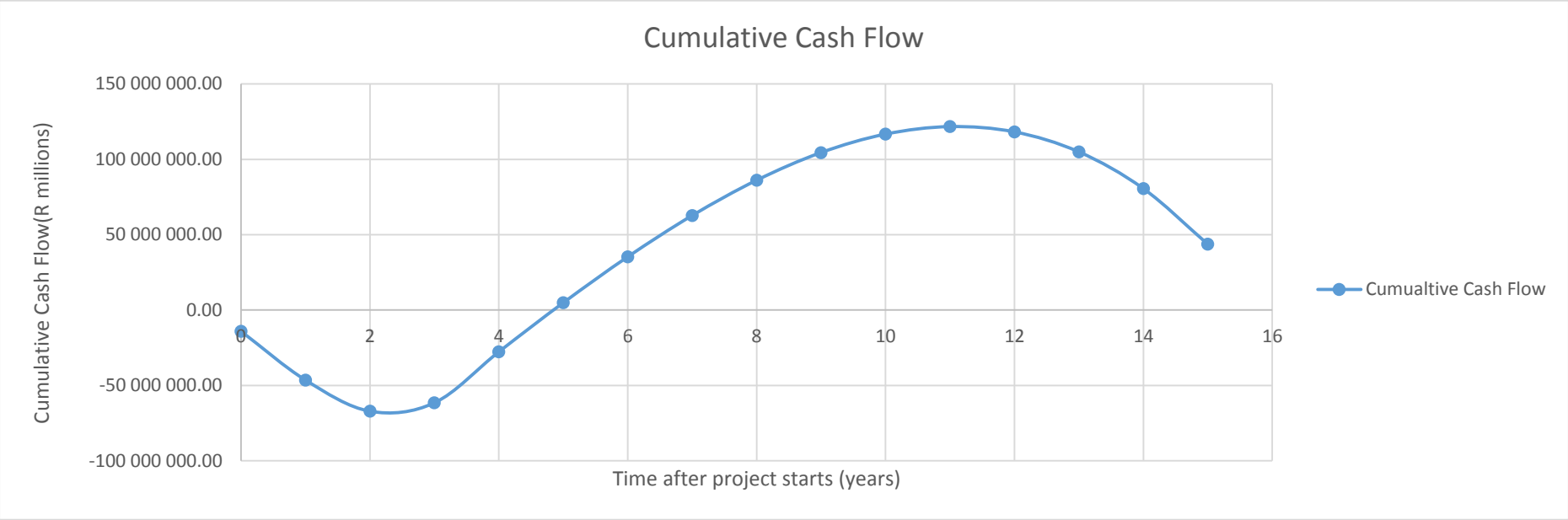

Figure 7-5: RN-PS Cumulative Cash Flow

7.2.2 CR-PS scenario

7.2.2.1 *CR-PS process mass balance*

Table 7-14: CR-PS Stream Table

Description			PS inlet to M100	Water inlet to M-101		MPP inlet to M-100		MgO inlet to M-100		CaCO3 inlet to M-100		Borax inlet to M-100		Mixture after M-101		After Matt Fomation	Matt Formation Reject	After Pre-press	Excess Water	After Hot Press	After Conditioning	Final Product	To Trimming Waste
Stream		Units	1	3	4	5	6	7	8	9	10	11	12	13	14	15	16	17	18	19	20	21	22
Tempature		°c	25	25	25	25	25	25	25	25	25	25	25	25	25	25	25	25	25	25	25	25	25
Pressure		bar	1	1	1	1	1	1	1	1	1	1	1	1	1	1	1	1	1	1	1	1	1
Vapor Frac		wt%	0	0	1	0	0	0	0	0	0	0	0	0	0	0	0	0	0	0	0	0	0
Liquid Frac		wt%	1	1	0	0	0	0	0	0	0	0	0	0	1	0	0	0	1	0	0	0	0
Solid Frac		wt%	0	0	0	1	1	1	1	1	1	1	1	1	0	1	1	1	0	1	1	1	1
Moisture Content		wt%	80%	100%	100%	0%	0%	0%	0%	0%	0%	0%	0%	75%	75%	75%	75%	75%	100%	5%	5%	5%	5%
Mass Flow		kg/hr	6875	823	823	459	459	90	90	159	159	72	72	8480	8480	7971	509	7971	5837	2133	2133	1963	171
WATER	l	kg/hr	5500	823	823	0	0	0	0	0	0	0	0	6323	6323	5944	379	5944	5837	107	107	98	9
Magnesium Oxide	S	kg/hr	0	0	0	0	0	90	90	0	0	0	0	90	90	85	5	85	0	85	85	78	7
Calcium Carbonate	S	kg/hr	0	0	0	0	0	0	0	159	159	0.0	0.0	159	159	150	10	150	0	150	150	138	12
Monopotassium phosphate	S	kg/hr	0	0	0	459	459	0	0	0	0	0.0	0.0	459	459	431	28	431	0	431	431	397	35
Borox	S	kg/hr	0	0	0	0	0	0	0	0	0	72.4	72.4	72	72	68	4	68	0	68	68	63	5
Paper sludge	S	kg/hr	1375	0	0	0	0	0	0	0	0	0.0	0.0	1375	1375	1293	83	1293	0	1293	1293	1189	103
Mass fractions																							
WATER	l	-	0.80	1.00	1.00	0.00	0.00	0.00	0.00	0.00	0.00	0.0	0.0	0.75	0.75	0.75	0.75	0.75	1.00	0.05	0.05	0.05	0.05
Magnesium Oxide	S	-	0.00	0.00	0.00	0.00	0.00	1.00	1.00	0.00	0.00	0.00	0.00	0.01	0.01	0.01	0.01	0.01	0.00	0.04	0.04	0.04	0.04
Calcium Carbonate	S	-	0.00	0.00	0.00	0.00	0.00	0.00	0.00	1.00	1.00	0.00	0.00	0.02	0.02	0.02	0.02	0.02	0.00	0.07	0.07	0.07	0.07
Monopotassium phosphate	S	-	0.00	0.00	0.00	1.00	1.00	0.00	0.00	0.00	0.00	0.00	0.00	0.05	0.05	0.05	0.05	0.05	0.00	0.20	0.20	0.20	0.20
Borox	S	-	0.00	0.00	0.00	0.00	0.00	0.00	0.00	0.00	0.00	1.00	1.00	0.01	0.01	0.01	0.01	0.01	0.00	0.03	0.03	0.03	0.03
Paper sludge	S	-	0.20	0.00	0.00	0.00	0.00	0.00	0.00	0.00	0.00	0.00	0.00	0.16	0.16	0.16	0.16	0.16	0.00	0.61	0.61	0.61	0.61

7.2.2.2 *CR-PS Utility Consumption*

Table 7-15: CR-PS utility consumption cost

Utility Cost				
Equipment	**Equipment ID**	**Flowrate**	**Yeary usage**	**Cost R**
Electricity		kW	kWh	
Vibrating screens	NA			
Forming machine	NA			
prepress machine	PRESS-100			
Belt conveyor for mat boards	NA			
Loader for mat board	NA			
Hot press machine	PRESS-101			
Unloader for finished board	NA			
Overturning machine	NA			
Edge saw machine	NA			
Stacking machine	NA			
Sanding machine	T-100	2500	20000000	16800000
Industrial Air conditioner	NA			
Pumps		0	790	663
Screw conveyer	SC-100 (A/B)	6	44000	36960
Screw conveyer	SC-101 (A/B)	6	44000	36960
Screw conveyer	SC-102 (A/B)	6	0	0
Belt Conveyor	CV-100 (A/B)	6	44000	36960
Belt Conveyor	CV-101 (A/B)	6	44000	36960
Belt Conveyor	CV-102 (A/B)	6	44000	36960
Belt Conveyor	CV-103 (A/B)	6	44000	36960
Agitator	NA	21	170432	143163
Hot Oil		kg/hr	GJ/year	
Hot Press machine	Press-101	43	4226	849921
			Total	18015507

Appendix

Sample calculation for hot oil requirement to heat up boards to optimum press temperature

Figure 7-6: Board plate system

Assumptions:

- Hot oil incoming temperature 280 C and outgoing temperature 275 C
- Steady state system i.e. the plate is already at 280 C
- No heat loss to the environment
- Perfect contact with hot oil and plates
- Assuming that capital and utility cost investment has already been completed for the hot oil generation system

Mass of 1 board = 38.7 kg

For RN-PS: Operating board press temperature = 90°C

Board initial temperature = 25°C

cp of dried sludge = 1.95 kJ/kg.C (Xu and Lancaster, 2009)

Heat energy equation: $Q_{boards} = Q_{oil}$

$Q_{board} = m_{board} \times cp_{board} \times \Delta T_{board} = 38.7 \text{ kg} \times 1.95 \text{ kJ/kg.C} \times (90 - 25)\ ^\circ\text{C} = 4905 \text{ kJ per board}$

Q_{board} = heat energyfrom board system (J), m = m_{board} (kg), cp (specific heat kJ/kg.c) and T_{board} in °C.

Heating requirement sourced from oil

$Q_{oil} = m_{oil} \times cp_{oil} \times \Delta T_{oil}$ therefore since $Q_{boards} = Q_{oil}$

$m_{oil} = Q_{oil} / (cp_{oil} \times \Delta T_{oil}) = 4\,905 \text{kJ} / (2.44 \text{ kJ/kg.K} \times ((280+273) - (275+273)))$

$m_{oil} = 402.1$ kg per board made

mass flowrate = m_{oil} x board production per year / operating hours per year

mass flow rate (kg/hr) = (402.1 kg x 430 770baord per year)/ 8000 hours = 21.6 kg/hr

But since the top and bottom plate is getting heated up, need twice as much

Therefore, mass flow rate = 21.6 kg/hr x 2 = 43.3 kg/hr

Q_{oil} = heat energyfrom board system (J), m = m_{oil} (kg), cp (specific heat kJ/kg.c) and T_{oil} in °C.

7.2.2.3 *CR-PS Equipment Costing*

Table 7-16: CR-PS Total Capital Investment

Equipments	Equipment Code	Purchased Cost (R) in 2004	Purchased Cost (R) in 2018	Installation Cost (R) in 2018
MDF Press Machines				
Vibrating screens	V-100			
Forming machine	MT-100			
prepress machine	PRESS-100			
Belt conveyor for mat boards	NA			
Loader for mat board	NA			
Hot press machine	PRESS-101			
Unloader for finished board	NA			
Overturning machine	NA			
Edge saw machine	NA			
Stacking machine	NA			
Sanding machine	T-100		2374984.94	2422484.64
Industrial Air conditioner	NA		2478.12	2527.68
Pumps				
Pumps	P-101 A/B	226042.52	345116.45	1069860.99
Pumps - Transport pumps from water source to storage tank		211346.44	322678.81	1000304.31
Storage Tanks				
Storage Tanks	ST-100	9590.98	12988.41	38965.24
Storage Tanks	NA	24086.47	32618.68	97856.04
Storage tanks	NA	8577.36	11615.74	34847.21
Storage tanks	NA	6851.58	9278.63	27835.89
Storage tanks	NA	3602.74	4878.94	14636.83
Storage tanks	NA	40260.18	54521.64	163564.91
Conveyor Belts				
Screw conveyer	SC-100 (A/B)		5335.48	9070.32
Screw conveyer	SC-101 (A/B)		5335.48	9070.32
Screw conveyer	SC-102 (A/B)		5335.48	9070.32
Belt Conveyor	CV-100 (A/B)			20363.46
Belt Conveyor	CV-101 (A/B)			7688.59
Belt Conveyor	CV-102 (A/B)			10801.61
Belt Conveyor	CV-103 (A/B)			6725.13
Agigator Mixer				
Mixing Vessel	M-100	87860.98	118984.18	214171.52
Agitator Mixer			297340.0885	475744.1415
Totals			**$ -**	**R 5 635 589.15**

7.2.2.4 *CR-PS Discounted Cash Flow Sheet*

Table 7-17:Cash flow sheet for CR-PS

Year	0	1	2	3	4	5	6	7	8	9	10	11	12	13	14	15
Fixed Capital Investment	R 10 594 907.60															
Land	R -															
Working Capital	R 529 745.38															
Baord Price (R/m2)	R 177.08	R 187.17	R 197.27	R 207.36	R 217.45	R 227.55	R 237.64	R 247.73	R 257.83	R 267.92	R 278.02	R 288.11	R 298.20	R 308.30	R 318.39	R 328.48
Board Production sales	R -	R 80 628 722.16	R 84 976 723.26	R 89 324 724.36	R 93 672 725.46	R 98 020 726.56	R 102 368 727.66	R 106 716 728.76	R 111 064 729.86	R 115 412 730.96	R 119 760 732.06	R 124 108 733.16	R 128 456 734.26	R 132 804 735.36	R 137 152 736.46	R 141 500 737.56
Total Annual Sales		R 56 440 105.51	R 67 981 378.60	R 80 392 251.92	R 93 672 725.46	R 98 020 726.56	R 102 368 727.66	R 106 716 728.76	R 111 064 729.86	R 115 412 730.96	R 119 760 732.06	R 124 108 733.16	R 128 456 734.26	R 132 804 735.36	R 137 152 736.46	R 141 500 737.56
Disposal Cost Saving		10220133	10802680.58	11418433.37	12069284.08	12757233.27	13484395.57	14253006.11	15065427.46	15924156.83	16831833.77	17791248.29	18805349.44	19877254.36	21010257.86	22207842.56
Total Revenue	R -	R 66 660 238.51	R 78 784 059.19	R 91 810 685.29	R 105 742 009.53	R 110 777 959.82	R 115 853 123.22	R 120 969 734.87	R 126 130 157.32	R 131 336 887.78	R 136 592 565.82	R 141 899 981.45	R 147 262 083.70	R 152 681 989.72	R 158 162 994.32	R 163 708 580.11
Annual Manufacturing Cost																
Feedstock Price ($/ ton)		R -	R -	R -	R -	R -	R -	R -	R -	R -	R -	R -	R -	R -	R -	R -
Feedstock cost		R -	R -	R -	R -	R -	R -	R -	R -	R -	R -	R -	R -	R -	R -	R -
Other Variable Costs		R 64 155 366.57	R 71 677 519.15	R 75 763 137.74	R 80 081 636.59	R 84 646 289.88	R 89 471 128.40	R 94 570 982.72	R 99 961 528.74	R 105 659 335.87	R 111 681 918.02	R 118 047 787.35	R 124 776 511.22	R 131 888 772.36	R 139 406 432.39	R 147 352 599.04
Fixed Operating Costs		R 11 251 959.33	R 12 571 240.31	R 13 287 801.00	R 14 045 205.66	R 14 845 782.38	R 15 691 991.98	R 16 586 435.52	R 17 531 862.35	R 18 531 178.50	R 19 587 455.68	R 20 703 940.65	R 21 884 065.27	R 23 131 456.99	R 24 449 950.04	R 25 843 597.19
Total Product Cost	R -	R 75 407 325.90	R 84 248 759.46	R 89 050 938.75	R 94 126 842.25	R 99 492 072.26	R 105 163 120.38	R 111 157 418.24	R 117 493 391.08	R 124 190 514.38	R 131 269 373.70	R 138 751 728.00	R 146 660 576.49	R 155 020 229.35	R 163 856 382.42	R 173 196 196.22
Annual Depreciation																
Plant Writedown		0.20	0.20	0.20	0.20	0.20										
Depreciation Charge		R 2 118 981.52	R 2 118 981.52	R 2 118 981.52	R 2 118 981.52	R 2 118 981.52	R -	R -	R -	R -	R -	R -	R -	R -	R -	R -
Remaining Value		R 8 475 926.08	R 6 356 944.56	R 4 237 963.04	R 2 118 981.52	R -	R -	R -	R -	R -	R -	R -	R -	R -	R -	R -
Net Revenue	R -10 065 162.22	R -144 186 545.93	R -165 151 800.16	R -182 980 605.56	R -201 987 833.31	R -212 389 013.61	R -221 016 243.60	R -232 127 153.11	R -243 623 548.40	R -255 527 402.16	R -267 861 939.52	R -280 651 709.44	R -293 922 660.19	R -307 702 219.07	R -322 019 376.74	R -336 904 776.34
Losses Forward			R -144 186 545.93	R -309 338 346.09	R -492 318 951.65	R -694 306 784.96	R -906 695 798.57	R -1 127 712 042.17	R -1 359 839 195.28	R -1 603 462 743.68	R -1 858 990 145.84	R -2 126 852 085.36	R -2 407 503 794.80	R -2 701 426 454.99	R -3 009 128 674.06	R -3 331 148 050.80
Taxable Income		R -144 186 545.93	R -309 338 346.09	R -492 318 951.65	R -694 306 784.96	R -906 695 798.57	R -1 127 712 042.17	R -1 359 839 195.28	R -1 603 462 743.68	R -1 858 990 145.84	R -2 126 852 085.36	R -2 407 503 794.80	R -2 701 426 454.99	R -3 009 128 674.06	R -3 331 148 050.80	R -3 668 052 827.14
Income Tax		R -	R -	R -	R -	R -	R -	R -	R -	R -	R -	R -	R -	R -	R -	R -
Gross Proft		(R8 747 087)	(R5 464 700)	R2 759 746.55	R11 615 167.28	R11 285 887.56	R10 690 002.84	R9 812 316.62	R8 636 766.23	R7 146 373.41	R5 323 192.13	R3 148 253.45	R601 507.21	(R2 338 240)	(R5 693 388)	(R9 487 616)
Net Profit		(R10 866 069)	(R7 583 682)	R640 765.03	R9 496 185.76	R9 166 906.04	R10 690 002.84	R9 812 316.62	R8 636 766.23	R7 146 373.41	R5 323 192.13	R3 148 253.45	R601 507.21	(R2 338 240)	(R5 693 388)	(R9 487 616)
Cash Flow	(R10 065 162)	(R8 747 087)	(R5 464 700)	R2 759 746.55	R11 615 167.28	R11 285 887.56	R10 690 002.84	R9 812 316.62	R8 636 766.23	R7 146 373.41	R5 323 192.13	R3 148 253.45	R601 507.21	(R2 338 240)	(R5 693 388)	(R9 487 616)
Discounted Cash Flow	(R10 065 162)	(R7 289 239)	(R3 794 931)	R1 597 075.55	R5 601 450.27	R4 535 545.09	R3 580 060.32	R2 738 437.49	R2 008 635.79	R1 385 015.04	R859 725.25	R423 717.09	R67 463.04	(R218 541)	(R443 438)	(R615 798)
Cumualtive Cash Flow	(R10 065 162)	(R18 812 250)	(R24 276 950)	(R21 517 203)	(R9 902 036)	R1 383 851.50	R12 073 854.34	R21 886 170.96	R30 522 937.19	R37 669 310.60	R42 992 502.73	R46 140 756.18	R46 742 263.38	R44 404 023.75	R38 710 635.64	R29 223 019.53
Discounted Cumulative Cash Flow	(R10 065 162)	(R17 354 402)	(R21 149 332)	(R19 552 257)	(R13 950 807)	(R9 415 262)	(R5 835 201)	(R3 096 764)	(R1 088 128)	R296 887.09	R1 156 612.33	R1 580 329.42	R1 647 792.46	R1 429 251.51	R985 813.07	R370 014.87

7.2.2.5 *CR-PS Cumulative Cash Flow*

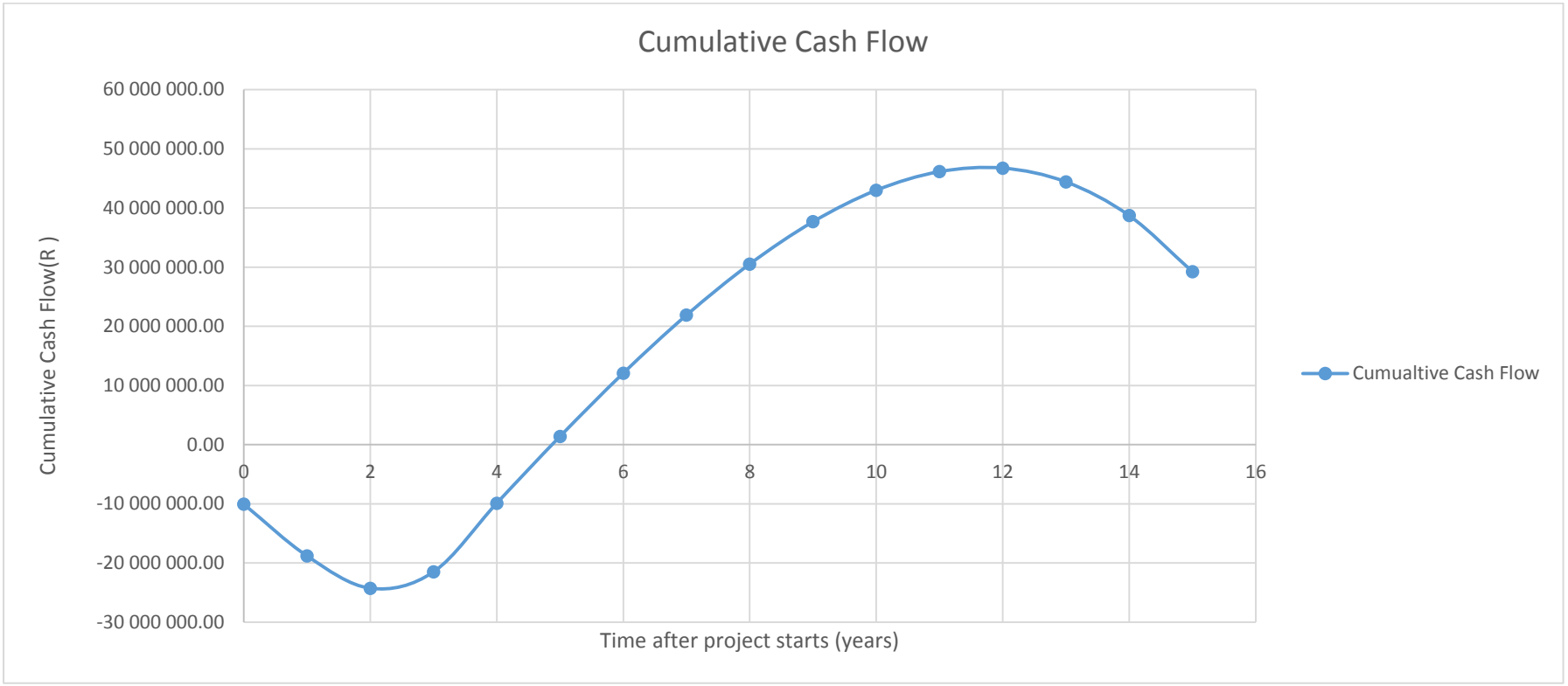

Figure 7-7: CR-PS Cumulative Cash Flow

7.2.3 VP-PS scenario

7.2.3.1 *VP-PS process mass balance*

Table 7-18: VP-PS Stream Table

Description			PS inlet to M100	Water inlet to M-101		MPP inlet to M-100		MgO inlet to M-100		CaCO3 inlet to M-100		Borax inlet to M-100		Mixture after M-101		After Matt Fomation	Matt Formation Reject	After Pre-press	Excess Water	After Hot Press	After Conditioning	Final Product	To Trimming Waste
Stream		Units	1	3	4	5	6	7	8	9	10	11	12	13	14	15	16	17	18	19	20	21	22
Tempature		°c	25	25	25	25	25	25	25	25	25	25	25	25	25	25	25	25	25	100	25	25	25
Pressure		bar	1	1	1	1	1	1	1	1	1	1	1	1	1	1	1	1	1	1	1	1	1
Vapor Frac		wt%	0	0	1	0	0	0	0	0	0	0	0	0	0	0	0	0	0	0	0	0	0
Liquid Frac		wt%	1	1	0	0	0	0	0	0	0	0	0	0	1	0	0	0	1	0	0	0	0
Solid Frac		wt%	0	0	0	1	1	1	1	1	1	1	1	1	0	1	1	1	0	1	1	1	1
Moisture Content		wt%	80%	100%	100%	0%	0%	0%	0%	0%	0%	0%	0%	75%	75%	75%	75%	75%	100%	5%	5%	5%	5%
Mass Flow		kg/hr	9375	1123	1123	686	686	136	136	145	145	109	109	11573	11573	10878	694	10878	7959	2919	2919	2686	234
WATER	l	kg/hr	7500	1123	1123	0	0	0	0	0	0	0	0	8623	8623	8105	517	8105	7959	146	146	134	12
Magnesium Oxide	S	kg/hr	0	0	0	0	0	136	136	0	0	0	0	136	136	128	8	128	0	128	128	117	10
Calcium Carbonate	S	kg/hr	0	0	0	0	0	0	0	145	145	0.0	0.0	145	145	136	9	136	0	136	136	125	11
Monopotassium phosphate	S	kg/hr	0	0	0	686	686	0	0	0	0	0.0	0.0	686	686	645	41	645	0	645	645	593	52
Borox	S	kg/hr	0	0	0	0	0	0	0	0	0	108.6	108.6	109	109	102	7	102	0	102	102	94	8
Paper sludge	S	kg/hr	1875	0	0	0	0	0	0	0	0	0.0	0.0	1875	1875	1763	113	1763	0	1763	1763	1622	141
Mass fractions																							
WATER	l	-	0.80	1.00	1.00	0.00	0.00	0.00	0.00	0.00	0.00	0.0	0.0	0.75	0.75	0.75	0.75	0.75	1.00	0.05	0.05	0.05	0.05
Magnesium Oxide	S	-	0.00	0.00	0.00	0.00	0.00	1.00	1.00	0.00	0.00	0.00	0.00	0.01	0.01	0.01	0.01	0.01	0.00	0.04	0.04	0.04	0.04
Calcium Carbonate	S	-	0.00	0.00	0.00	0.00	0.00	0.00	0.00	1.00	1.00	0.00	0.00	0.01	0.01	0.01	0.01	0.01	0.00	0.05	0.05	0.05	0.05
Monopotassium phosphate	S	-	0.00	0.00	0.00	1.00	1.00	0.00	0.00	0.00	0.00	0.00	0.00	0.06	0.06	0.06	0.06	0.06	0.00	0.22	0.22	0.22	0.22
Borox	S	-	0.00	0.00	0.00	0.00	0.00	0.00	0.00	0.00	0.00	1.00	1.00	0.01	0.01	0.01	0.01	0.01	0.00	0.03	0.03	0.03	0.03
Paper sludge	S	-	0.20	0.00	0.00	0.00	0.00	0.00	0.00	0.00	0.00	0.00	0.00	0.16	0.16	0.16	0.16	0.16	0.00	0.60	0.60	0.60	0.60

7.2.3.2 *VP-PS Utility Consumption*

Table 7-19: VP-PS utility consumption cost

Utility Cost				
Equipment	**Equipment ID**	**Flowrate**	**Yeary usage**	**Cost R**
Electricity		kW	kWh	
Vibrating screens	NA			
Forming machine	NA			
prepress machine	PRESS-100			
Belt conveyor for mat boards	NA			
Loader for mat board	NA			
Hot press machine	PRESS-101			
Unloader for finished board	NA			
Overturning machine	NA			
Edge saw machine	NA			
Stacking machine	NA			
Sanding machine	T-100	2500	20000000	16800000
Industrial Air conditioner	NA			
Pumps		0	1080	907
Screw conveyer	SC-100 (A/B)	6	44000	36960
Screw conveyer	SC-101 (A/B)	6	44000	36960
Screw conveyer	SC-102 (A/B)	6	0	0
Belt Conveyor	CV-100 (A/B)	6	44000	36960
Belt Conveyor	CV-101 (A/B)	6	44000	36960
Belt Conveyor	CV-102 (A/B)	6	44000	36960
Belt Conveyor	CV-103 (A/B)	6	44000	36960
Agitator	NA	29	232606	195389
Hot Oil		kg/hr	GJ/year	
Hot Press machine	Press-101	0	0	0
			Total	17218056

7.2.3.3 *VP-PS Equipment Costing*

Table 7-20: VP-PS Total Capital Investment

Equipments	Equipment Code	Purchased Cost (R) in 2004	Purchased Cost (R) in 2018	Installation Cost (R) in 2018
MDF Press Machines				
Vibrating screens	V-100			
Forming machine	MT-100			
prepress machine	PRESS-100			
Belt conveyor for mat boards	NA			
Loader for mat board	NA			
Hot press machine	PRESS-101			
Unloader for finished board	NA			
Overturning machine	NA			
Edge saw machine	NA			
Stacking machine	NA			
Sanding machine	T-100		2374984.94	2422484.64
Industrial Air conditioner	NA		2478.12	2527.68
Pumps				
Pumps	P-101 A/B	194729.62	297308.64	921656.77
Pumps - Transport pumps from water source to storage tank		180434.40	275483.02	853997.37
Storage Tanks				
Storage Tanks	ST-100	11990.74	16238.24	48714.73
Storage Tanks	NA	30113.15	40780.20	122340.61
Storage tanks	NA	11455.58	15513.51	46540.54
Storage tanks	NA	9176.77	12427.48	37282.45
Storage tanks	NA	3363.80	4555.36	13666.09
Storage tanks	NA	53923.13	73024.44	219073.32
Conveyor Belts				
Screw conveyer	SC-100 (A/B)		5335.48	9070.32
Screw conveyer	SC-101 (A/B)		5335.48	9070.32
Screw conveyer	SC-102 (A/B)		5335.48	9070.32
Belt Conveyor	CV-100 (A/B)			25916.19
Belt Conveyor	CV-101 (A/B)			9808.36
Belt Conveyor	CV-102 (A/B)			10201.24
Belt Conveyor	CV-103 (A/B)			8579.27
Agigator Mixer				
Mixing Vessel	M-100	109912.46	148847.00	267924.61
Agitator Mixer			351715.601	562744.9616
Totals			**$ -**	**R 5 600 669.79**

7.2.3.4 *VP-PS Discounted Cash Flow Sheet*

Table 7-21: Cash flow sheet for VP-PS

Year	0	1	2	3	4	5	6	7	8	9	10	11	12	13	14	15
Fixed Capital Investment	R 10 594 907.60															
Land	R -															
Working Capital	R 529 745.38															
Baord Price (R/m2)	R 177.08	R 187.17	R 197.27	R 207.36	R 217.45	R 227.55	R 237.64	R 247.73	R 257.83	R 267.92	R 278.02	R 288.11	R 298.20	R 308.30	R 318.39	R 328.48
Board Production sales	R -	R 80 628 722.16	R 84 976 723.26	R 89 324 724.36	R 93 672 725.46	R 98 020 726.56	R 102 368 727.66	R 106 716 728.76	R 111 064 729.86	R 115 412 730.96	R 119 760 732.06	R 124 108 733.16	R 128 456 734.26	R 132 804 735.36	R 137 152 736.46	R 141 500 737.56
Total Annual Sales		R 56 440 105.51	R 67 981 378.60	R 80 392 251.92	R 93 672 725.46	R 98 020 726.56	R 102 368 727.66	R 106 716 728.76	R 111 064 729.86	R 115 412 730.96	R 119 760 732.06	R 124 108 733.16	R 128 456 734.26	R 132 804 735.36	R 137 152 736.46	R 141 500 737.56
Disposal Cost Saving		10220133	10802680.58	11418433.37	12069284.08	12757233.27	13484395.57	14253006.11	15065427.46	15924156.83	16831833.77	17791248.29	18805349.44	19877254.36	21010257.86	22207842.56
Total Revenue	R -	R 66 660 238.51	R 78 784 059.19	R 91 810 685.29	R 105 742 009.53	R 110 777 959.82	R 115 853 123.22	R 120 969 734.87	R 126 130 157.32	R 131 336 887.78	R 136 592 565.82	R 141 899 981.45	R 147 262 083.70	R 152 681 989.72	R 158 162 994.32	R 163 708 580.11
Annual Manufacturing Cost																
Feedstock Price ($/ ton)		R -	R -	R -	R -	R -	R -	R -	R -	R -	R -	R -	R -	R -	R -	R -
Feedstock cost		R -	R -	R -	R -	R -	R -	R -	R -	R -	R -	R -	R -	R -	R -	R -
Other Variable Costs		R 64 155 366.57	R 71 677 519.15	R 75 763 137.74	R 80 081 636.59	R 84 646 289.88	R 89 471 128.40	R 94 570 982.72	R 99 961 528.74	R 105 659 335.87	R 111 681 918.02	R 118 047 787.35	R 124 776 511.22	R 131 888 772.36	R 139 406 432.39	R 147 352 599.04
Fixed Operating Costs		R 11 251 959.33	R 12 571 240.31	R 13 287 801.00	R 14 045 205.66	R 14 845 782.38	R 15 691 991.98	R 16 586 435.52	R 17 531 862.35	R 18 531 178.50	R 19 587 455.68	R 20 703 940.65	R 21 884 065.27	R 23 131 456.99	R 24 449 950.04	R 25 843 597.19
Total Product Cost	R -	R 75 407 325.90	R 84 248 759.46	R 89 050 938.75	R 94 126 842.25	R 99 492 072.26	R 105 163 120.38	R 111 157 418.24	R 117 493 391.08	R 124 190 514.38	R 131 269 373.70	R 138 751 728.00	R 146 660 576.49	R 155 020 229.35	R 163 856 382.42	R 173 196 196.22
Annual Depreciation																
Plant Writedown		0.20	0.20	0.20	0.20	0.20										
Depreciation Charge		R 2 118 981.52	R 2 118 981.52	R 2 118 981.52	R 2 118 981.52	R 2 118 981.52	R -	R -	R -	R -	R -	R -	R -	R -	R -	R -
Remaining Value		R 8 475 926.08	R 6 356 944.56	R 4 237 963.04	R 2 118 981.52	R -	R -	R -	R -	R -	R -	R -	R -	R -	R -	R -
Net Revenue	R -10 065 162.22	R -144 186 545.93	R -165 151 800.16	R -182 980 605.56	R -201 987 833.31	R -212 389 013.61	R -221 016 243.60	R -232 127 153.11	R -243 623 548.40	R -255 527 402.16	R -267 861 939.52	R -280 651 709.44	R -293 922 660.19	R -307 702 219.07	R -322 019 376.74	R -336 904 776.34
Losses Forward			R -144 186 545.93	R -309 338 346.09	R -492 318 951.65	R -694 306 784.96	R -906 695 798.57	R -1 127 712 042.17	R -1 359 839 195.28	R -1 603 462 743.68	R -1 858 990 145.84	R -2 126 852 085.36	R -2 407 503 794.80	R -2 701 426 454.99	R -3 009 128 674.06	R -3 331 148 050.80
Taxable Income		R -144 186 545.93	R -309 338 346.09	R -492 318 951.65	R -694 306 784.96	R -906 695 798.57	R -1 127 712 042.17	R -1 359 839 195.28	R -1 603 462 743.68	R -1 858 990 145.84	R -2 126 852 085.36	R -2 407 503 794.80	R -2 701 426 454.99	R -3 009 128 674.06	R -3 331 148 050.80	R -3 668 052 827.14
Income Tax		R -	R -	R -	R -	R -	R -	R -	R -	R -	R -	R -	R -	R -	R -	R -
Gross Proft		(R8 747 087)	(R5 464 700)	R2 759 746.55	R11 615 167.28	R11 285 887.56	R10 690 002.84	R9 812 316.62	R8 636 766.23	R7 146 373.41	R5 323 192.13	R3 148 253.45	R601 507.21	(R2 338 240)	(R5 693 388)	(R9 487 616)
Net Profit		(R10 866 069)	(R7 583 682)	R640 765.03	R9 496 185.76	R9 166 906.04	R10 690 002.84	R9 812 316.62	R8 636 766.23	R7 146 373.41	R5 323 192.13	R3 148 253.45	R601 507.21	(R2 338 240)	(R5 693 388)	(R9 487 616)
Cash Flow	(R10 065 162)	(R8 747 087)	(R5 464 700)	R2 759 746.55	R11 615 167.28	R11 285 887.56	R10 690 002.84	R9 812 316.62	R8 636 766.23	R7 146 373.41	R5 323 192.13	R3 148 253.45	R601 507.21	(R2 338 240)	(R5 693 388)	(R9 487 616)
Discounted Cash Flow	(R10 065 162)	(R7 289 239)	(R3 794 931)	R1 597 075.55	R5 601 450.27	R4 535 545.09	R3 580 060.32	R2 738 437.49	R2 008 635.79	R1 385 015.04	R859 725.25	R423 717.09	R67 463.04	(R218 541)	(R443 438)	(R615 798)
Cumualtive Cash Flow	(R10 065 162)	(R18 812 250)	(R24 276 950)	(R21 517 203)	(R9 902 036)	R1 383 851.50	R12 073 854.34	R21 886 170.96	R30 522 937.19	R37 669 310.60	R42 992 502.73	R46 140 756.18	R46 742 263.38	R44 404 023.75	R38 710 635.64	R29 223 019.53
Discounted Cumulative Cash Flow	(R10 065 162)	(R17 354 402)	(R21 149 332)	(R19 552 257)	(R13 950 807)	(R9 415 262)	(R5 835 201)	(R3 096 764)	(R1 088 128)	R296 887.09	R1 156 612.33	R1 580 329.42	R1 647 792.46	R1 429 251.51	R985 813.07	R370 014.87

7.2.3.5 *VP-PS Cumulative Cash Flow*

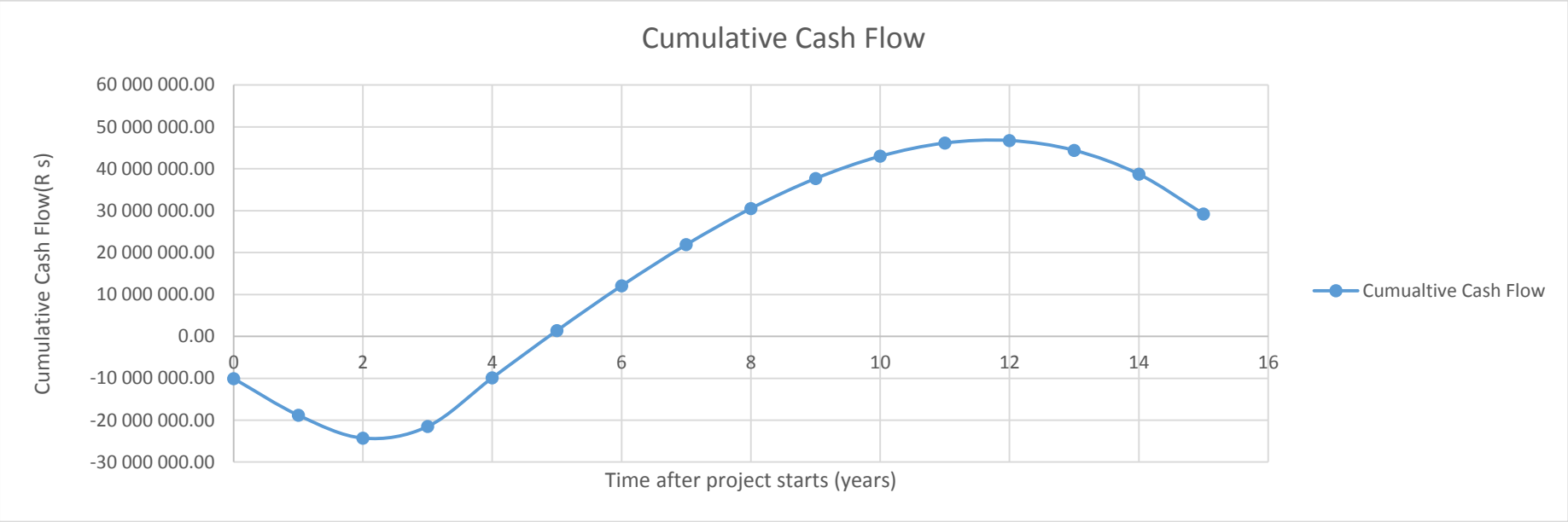

Figure 7-8: VP-PS Cumulative Cash Flow

7.2.4 Combined scenario

7.2.4.1 *Combined process mass balance*

Table 7-22: Combined Stream Table

Description			PS inlet to M100	Water inlet to M-101		MPP inlet to M-100		MgO inlet to M-100		CaCO3 inlet to M-100		Borax inlet to M-100		Mixture after M-101		After Matt Fomation	Matt Formation Reject	After Pre-press	Excess Water	After Hot Press	After Conditioning	Final Product	To Trimming Waste
Stream		Units	1	3	4	5	6	7	8	9	10	11	12	13	14	15	16	17	18	19	20	21	22
Tempature		°C	25	25	25	25	25	25	25	25	25	25	25	25	25	25	25	25	25	100	25	25	25
Pressure		bar	1	1	1	1	1	1	1	1	1	1	1	1	1	1	1	1	1	1	1	1	1
Vapor Frac		wt%	0	0	1	0	0	0	0	0	0	0	0	0	0	0	0	0	0	0	0	0	0
Liquid Frac		wt%	1	1	0	0	0	0	0	0	0	0	0	0	1	0	0	0	1	0	0	0	0
Solid Frac		wt%	0	0	0	1	1	1	1	1	1	1	1	1	0	1	1	1	0	1	1	1	1
Moisture Content		wt%	67%	100%	100%	0%	0%	0%	0%	0%	0%	0%	0%	63%	63%	63%	63%	63%	100%	5%	5%	5%	5%
Mass Flow		kg/hr	6439	1447	1447	731	731	145	145	219	219	116	116	9097	9097	8552	546	8552	5251	3301	3301	3037	264
WATER	l	kg/hr	4314	1447	1447	0	0	0	0	0	0	0	0	5761	5761	5416	346	5416	5251	165	165	152	13
Magnesium Oxide	S	kg/hr	0	0	0	0	0	145	145	0	0	0	0	145	145	136	9	136	0	136	136	125	11
Calcium Carbonate	S	kg/hr	0	0	0	0	0	0	0	219	219	0.0	0.0	219	219	206	13	206	0	206	206	189	16
Monopotassium phosphate	S	kg/hr	0	0	0	731	731	0	0	0	0	0.0	0.0	731	731	688	44	688	0	688	688	633	55
Borox	S	kg/hr	0	0	0	0	0	0	0	0	0	115.9	115.9	116	116	109	7	109	0	109	109	100	9
Paper sludge	S	kg/hr	2125	0	0	0	0	0	0	0	0	0.0	0.0	2125	2125	1998	128	1998	0	1998	1998	1838	160
Mass fractions																							
WATER	l	-	0.67	1.00	1.00	0.00	0.00	0.00	0.00	0.00	0.00	0.0	0.0	0.63	0.63	0.63	0.00	0.00	1.00	0.05	0.00	0.05	0.05
Magnesium Oxide	S	-	0.00	0.00	0.00	0.00	0.00	1.00	1.00	0.00	0.00	0.00	0.00	0.02	0.02	0.02	1.00	1.00	0.00	0.00	0.00	0.04	0.04
Calcium Carbonate	S	-	0.00	0.00	0.00	0.00	0.00	0.00	0.00	1.00	1.00	0.00	0.00	0.02	0.02	0.02	0.00	0.00	0.00	0.07	0.07	0.06	0.06
Monopotassium phosphate	S	-	0.00	0.00	0.00	1.00	1.00	0.00	0.00	0.00	0.00	0.00	0.00	0.08	0.08	0.08	0.00	0.00	0.00	0.00	0.00	0.21	0.21
Borox	S	-	0.00	0.00	0.00	0.00	0.00	0.00	0.00	0.00	0.00	1.00	1.00	0.01	0.01	0.01	0.01	0.01	0.00	0.03	0.03	0.03	0.03
Paper sludge	S	-	0.33	0.00	0.00	0.00	0.00	0.00	0.00	0.00	0.00	0.00	0.00	0.23	0.23	0.23	0.23	0.23	0.00	0.61	0.61	0.61	0.61

7.2.4.2 *Combined Utility Consumption*

Table 7-23: Combined utility consumption cost

Utility Cost				
Equipment	**Equipment ID**	**Flowrate**	**Yeary usage**	**Cost R**
Electricity		kW	kWh	
Vibrating screens	NA			
Forming machine	NA			
prepress machine	PRESS-100			
Belt conveyor for mat boards	NA			
Loader for mat board	NA			
Hot press machine	PRESS-101			
Unloader for finished board	NA			
Overturning machine	NA			
Edge saw machine	NA			
Stacking machine	NA			
Sanding machine	T-100	2500	20000000	16800000
Industrial Air conditioner	NA			
Pumps		0	1392	1169
Screw conveyer	SC-100 (A/B)	6	44000	36960
Screw conveyer	SC-101 (A/B)	6	44000	36960
Screw conveyer	SC-102 (A/B)	6	0	0
Belt Conveyor	CV-100 (A/B)	6	44000	36960
Belt Conveyor	CV-101 (A/B)	6	44000	36960
Belt Conveyor	CV-102 (A/B)	6	44000	36960
Belt Conveyor	CV-103 (A/B)	6	44000	36960
Agitator	NA	23	182852	153596
Hot Oil		kg/hr	GJ/year	
Hot Press machine	Press-101	67	6531	1313515
			Total	18 490 040

Appendix

Sample calculation for hot oil requirement to heat up boards to optimum press temperature

Figure 7-9: Board plate system

Assumptions:

- Hot oil incoming temperature 280 C and outgoing temperature 275 C
- Steady state system i.e. the plate is already at 280 C
- No heat loss to the environment
- Perfect contact with hot oil and plates
- Assuming that capital and utility cost investment has already been completed for the hot oil generation system

Mass of 1 board = 38.7 kg

For RN-PS: Operating board press temperature = 90°C

Board initial temperature = 25°C

cp of dried sludge = 1.95 kJ/kg.C(Xu and Lancaster, 2009)

Heat energy equation: $Q_{boards} = Q_{oil}$

$Q_{board} = m_{board} \times cp_{board} \times \Delta T_{board} = 38.7\ kg \times 1.95\ kJ/kg.C \times (90 - 25)\ °C = 4\ 905\ kJ$ per board

Q_{board} = heat energyfrom board system (J), m = m_{board} (kg), cp (specific heat kJ/kg.c) and T_{board} in °C.

Heating requirement sourced from oil

$Q_{oil} = m_{oil} \times cp_{oil} \times \Delta T_{oil}$ therefore since $Q_{boards} = Q_{oil}$

$m_{oil} = Q_{oil} / (cp_{oil} \times \Delta T_{oil}) = 4\ 905kJ / (2.44\ kJ/kg.K \times ((280+273) - (275+273)))$

$m_{oil} = 402.1kg$ per board made

mass flowrate = m_{oil} x board production per year / operating hours per year

mass flow rate (kg/hr) = (958.78 kg x 665 735 baord per year)/ 8000 hours = 33.5 kg/hr

But since the top and bottom plate is getting heated up, need twice as much

Therefore, mass flow rate = 28.16 kg/hr x 2 = 66.9 kg/hr

Q_{oil} = heat energyfrom board system (J), m = m_{oil} (kg), cp (specific heat kJ/kg.c) and T_{oil} in °C.

7.2.4.3 *Combined Equipment Costing*

Table 7-24: Combined Total Capital Investment

Equipments	Equipment Code	Purchased Cost (R) in 2004	Purchased Cost (R) in 2018	Installation Cost (R) in 2018
MDF Press Machines				
Vibrating screens	V-100			
Forming machine	MT-100			
prepress machine	PRESS-100			
Belt conveyor for mat boards	NA			
Loader for mat board	NA			
Hot press machine	PRESS-101			
Unloader for finished board	NA			
Overturning machine	NA			
Edge saw machine	NA			
Stacking machine	NA			
Sanding machine	T-100		2374984.94	2422484.64
Industrial Air conditioner	NA		2478.12	2527.68
Pumps				
Pumps	P-101 A/B	265912.14	405988.45	1258564.19
Pumps - Transport pumps from water source to storage tank		216491.70	330534.47	1024656.86
Storage Tanks				
Storage Tanks	ST-100	13121.50	17769.55	53308.66
Storage Tanks	NA	36145.78	48949.78	146849.33
Storage tanks	NA	12000.45	16251.40	48754.21
Storage tanks	NA	9613.26	13018.59	39055.77
Storage tanks	NA	4528.18	6132.20	18396.61
Storage tanks	NA	56487.94	76497.80	229493.39
Conveyor Belts				
Screw conveyer	SC-100 (A/B)		5335.48	9070.32
Screw conveyer	SC-101 (A/B)		5335.48	9070.32
Screw conveyer	SC-102 (A/B)		5335.48	9070.32
Belt Conveyor	CV-100 (A/B)			26939.43
Belt Conveyor	CV-101 (A/B)			10195.62
Belt Conveyor	CV-102 (A/B)			13068.65
Belt Conveyor	CV-103 (A/B)			8918.00
Agigator Mixer				
Mixing Vessel	M-100	92425.60	125165.73	225298.31
Agitator Mixer			308852.1552	494163.4483
Totals			**$ -**	**R 6 049 885.75**

Appendix

7.2.4.4 *Combined scenario Discounted Cash Flow Sheet*

Table 7-25: Cash flow sheet for Combined Scenario

Year	0	1	2	3	4	5	6	7	8	9	10	11	12	13	14	15
Fixed Capital Investment	R 11 373 785.20															
Land	R -															
Working Capital	R 568 689.26															
Baord Price (R/m2)	R 157.10	R 166.05	R 175.01	R 183.96	R 192.92	R 201.87	R 210.83	R 219.78	R 228.74	R 237.69	R 246.65	R 255.60	R 264.56	R 273.51	R 282.47	R 291.42
Board Production sales	R -	R 110 548 456.92	R 116 509 915.80	R 122 471 374.69	R 128 432 833.58	R 134 394 292.47	R 140 355 751.36	R 146 317 210.24	R 152 278 669.13	R 158 240 128.02	R 164 201 586.91	R 170 163 045.79	R 176 124 504.68	R 182 085 963.57	R 188 047 422.46	R 194 008 881.34
Total Annual Sales		R 77 383 919.84	R 93 207 932.64	R 110 224 237.22	R 128 432 833.58	R 134 394 292.47	R 140 355 751.36	R 146 317 210.24	R 152 278 669.13	R 158 240 128.02	R 164 201 586.91	R 170 163 045.79	R 176 124 504.68	R 182 085 963.57	R 188 047 422.46	R 194 008 881.34
Disposal Cost Saving		15794751	16695051.81	17646669.76	18652529.94	19715724.14	20839520.42	22027373.08	23282933.35	24610060.55	26012834	27495565.54	29062812.77	30719393.1	32470398.51	34321211.22
Total Revenue	R -	R 93 178 670.84	R 109 902 984.45	R 127 870 906.98	R 147 085 363.52	R 154 110 016.61	R 161 195 271.77	R 168 344 583.33	R 175 561 602.48	R 182 850 188.57	R 190 214 420.91	R 197 658 611.33	R 205 187 317.46	R 212 805 356.67	R 220 517 820.97	R 228 330 092.57
Annual Manufacturing Cost																
Feedstock Price ($/ ton)		R -	R -	R -	R -	R -	R -	R -	R -	R -	R -	R -	R -	R -	R -	R -
Feedstock cost		R -	R -	R -	R -	R -	R -	R -	R -	R -	R -	R -	R -	R -	R -	R -
Other Variable Costs		R 94 318 161.18	R 105 376 871.26	R 111 383 352.93	R 117 732 204.04	R 124 442 939.67	R 131 536 187.23	R 139 033 749.91	R 146 958 673.65	R 155 335 318.05	R 164 189 431.18	R 173 548 228.75	R 183 440 477.79	R 193 896 585.03	R 204 948 690.37	R 216 630 765.73
Fixed Operating Costs		R 11 269 840.37	R 12 591 217.88	R 13 308 917.30	R 14 067 525.59	R 14 869 374.55	R 15 716 928.90	R 16 612 793.84	R 17 559 723.09	R 18 560 627.31	R 19 618 583.06	R 20 736 842.30	R 21 918 842.31	R 23 168 216.32	R 24 488 804.65	R 25 884 666.52
Total Product Cost	R -	R 105 588 001.55	R 117 968 089.15	R 124 692 270.23	R 131 799 729.63	R 139 312 314.22	R 147 253 116.13	R 155 646 543.75	R 164 518 396.74	R 173 895 945.36	R 183 808 014.24	R 194 285 071.05	R 205 359 320.10	R 217 064 801.35	R 229 437 495.03	R 242 515 432.24
Annual Depreciation																
Plant Writedown		0.20	0.20	0.20	0.20	0.20										
Depreciation Charge		R 2 274 757.04	R 2 274 757.04	R 2 274 757.04	R 2 274 757.04	R 2 274 757.04	R -	R -	R -	R -	R -	R -	R -	R -	R -	R -
Remaining Value		R 9 099 028.16	R 6 824 271.12	R 4 549 514.08	R 2 274 757.04	R -	R -	R -	R -	R -	R -	R -	R -	R -	R -	R -
Taxable Income		R -201 041 429.43	R -431 187 260.07	R -686 025 194.32	R -967 185 044.51	R -1 262 882 132.37	R -1 571 330 520.28	R -1 895 321 647.35	R -2 235 401 646.57	R -2 592 147 780.50	R -2 966 170 215.64	R -3 358 113 898.03	R -3 768 660 535.59	R -4 198 530 693.61	R -4 648 486 009.60	R -5 119 331 534.41
Income Tax		R -	R -	R -	R -	R -	R -	R -	R -	R -	R -	R -	R -	R -	R -	R -
Gross Profit		(R12 409 331)	(R8 065 105)	R3 178 636.76	R15 285 633.89	R14 797 702.39	R13 942 155.65	R12 698 039.58	R11 043 205.74	R8 954 243.21	R6 406 406.67	R3 373 540.28	(R172 003)	(R4 259 445)	(R8 919 674)	(R14 185 340)
Net Profit		(R14 684 088)	(R10 339 862)	R903 879.72	R13 010 876.85	R12 522 945.35	R13 942 155.65	R12 698 039.58	R11 043 205.74	R8 954 243.21	R6 406 406.67	R3 373 540.28	(R172 003)	(R4 259 445)	(R8 919 674)	(R14 185 340)
Cash Flow	(R10 805 096)	(R12 409 331)	(R8 065 105)	R3 178 636.76	R15 285 633.89	R14 797 702.39	R13 942 155.65	R12 698 039.58	R11 043 205.74	R8 954 243.21	R6 406 406.67	R3 373 540.28	(R172 003)	(R4 259 445)	(R8 919 674)	(R14 185 340)
Discounted Cash Flow	(R10 805 096)	(R10 341 109)	(R5 600 767)	R1 839 488.86	R7 371 544.12	R5 946 864.71	R4 669 199.72	R3 543 789.80	R2 568 296.71	R1 735 392.32	R1 034 670.44	R454 037.99	(R19 291)	(R398 104)	(R694 723)	(R920 706)
Cumualtive Cash Flow	(R10 805 096)	(R23 214 427)	(R31 279 531)	(R28 100 895)	(R12 815 261)	R1 982 441.69	R15 924 597.34	R28 622 636.91	R39 665 842.65	R48 620 085.86	R55 026 492.53	R58 400 032.81	R58 228 030.16	R53 968 585.48	R45 048 911.42	R30 863 571.75
Discounted Cumulative Cash Flow	(R10 805 096)	(R21 146 205)	(R26 746 972)	(R24 907 483)	(R17 535 939)	(R11 589 074)	(R6 919 875)	(R3 376 085)	(R807 788)	R927 604.23	R1 962 274.67	R2 416 312.66	R2 397 021.42	R1 998 917.20	R1 304 194.41	R383 488.25

7.2.4.5 *Combined scenario Cumulative Cash Flow*

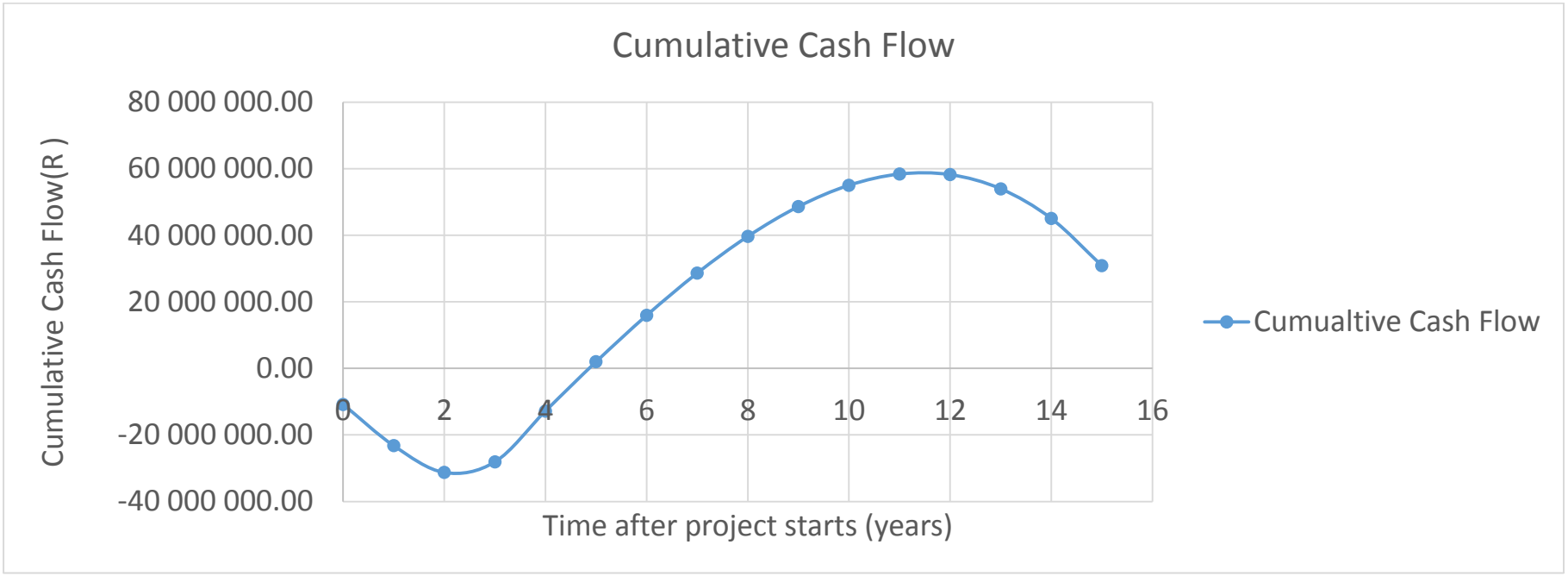

Figure 7-10: Combined scenario Cumulative Cash Flow

7.2.5 Equipment Size

7.2.5.1 *Pumps*

Table 7-26: Pump sizing

Pump			RN-PS	CR-PS	VP-PS	Combined
Water pump from storage tank	P-101 A/B	Type	Centrifugral Pump	Centrifugral Pump	Centrifugral Pump	Centrifugral Pump
		Capacity (m3/hr)	0.59	0.91	1.24	1.59
		Duty (kW)	0.03	0.04	0.05	0.07
		Inlet flow (kg/hr)	537	823	1123	1447
		Head (m)	11.4	11.4	11.1	10.7
		Quantity	2	2	2	2
Water Pump to storage tank		Type	Centrifugral Pump	Centrifugral Pump	Centrifugral Pump	Centrifugral Pump
		Capacity (m3/hr)	0.59	0.91	1.24	1.59
		Duty (kW)	0.04	0.06	0.08	0.11
		Inlet flow (kg/hr)	537	823	1123	1447
		Head (m)	15.92	16.49	16.95	17.37
		Quantity	2	2	2	2

7.2.5.2 *Conveyors*

Table 7-27: Conveyors sizing

Conveyors			RN-PS	CR-PS	VP-PS	Combined
Monopotasssium Phosphate Conveyor	CV-100(A/B)	Mass flow (kg/hr)	258	459	686	731
		Length (m)	3	3	3	3
		Quantity (m)	2	2	2	2
		Power (kW)	5.5	5.5	5.5	5.5
MgO Conveyor	CV-101(A/B)	Mass flow (kg/hr)	51	90	136	145
		Length (m)	3	3	3	3
		Quantity (m)	2	2	2	2
		Power (kW)	5.5	5.5	5.5	5.5
CaCO3 Conveyor	CV-102(A/B)	Mass flow (kg/hr)	77	159	145	219
		Length (m)	3	3	3	3
		Quantity (m)	2	2	2	2
		Power (kW)	5.5	5.5	5.5	5.5
Borax Conveyor	CV-103(A/B)	Mass flow (kg/hr)	40.8	72.4	108.6	115.9
		Length (m)	3	3	3	3
		Quantity (m)	2	2	2	2
		Power (kW)	5.5	5.5	5.5	5.5
PS screw Conveyor	SC-100(A/B)	Mass flow (kg/hr)	1630	6875	9375	6439
		Length (m)	3	3	3	3
		Quantity (m)	2	2	2	2
		Power (kW)	5.5	5.5	5.5	5.5
Matt formation screw conveyor	SC-101(A/B)	Mass flow (kg/hr)	2439	7971	10878	8552
		Length (m)	3	3	3	3
		Quantity (m)	2	2	2	2
		Power (kW)	5.5	5.5	5.5	5.5
Press Feed conveyor	SC-102(A/B)	Mass flow (kg/hr)	2439	7971	10878	8552
		Length (m)	3	3	3	3
		Quantity (m)	2	2	2	2
		Power (kW)	5.5	5.5	5.5	5.5

7.2.5.3 *Storage tanks*

Table 7-28: Storage tank sizing

Storage tanks		RN-PS	CR-PS	VP-PS	Combined
Paper sludge	Orientation	Vertical Tanks	Vertical Tanks	Vertical Tanks	Vertical Tanks
	Volume (m3)	3.33	6.11	8.33	9.44
	Length (m)	2.28	2.79	3.09	3.22
	Diameter (m)	1.37	1.67	1.85	1.93
	Feed Flow rate (kg/hr)	750.00	1375.00	1875.00	2125.00
	Residence time (hr)	4	4	4	4
	MOC	Carbon Steel	Carbon Steel	Carbon Steel	Carbon Steel
Water	Orientation	Vertical Tanks	Vertical Tanks	Vertical Tanks	Vertical Tanks
	Volume (m3)	14.3	22.0	29.9	38.6
	Length (m)	3.70	4.27	4.73	5.15
	Diameter (m)	2.22	2.56	2.84	3.09
	Feed Flow rate (kg/hr)	537	823	1123	1447
	Residence time (hr)	24	24	24	24
	MOC	Carbon stell	Carbon Steel	Carbon Steel	Carbon Steel
Monopotassium Phosphate	Orientation	Vertical Tanks	Vertical Tanks	Vertical Tanks	Vertical Tanks
	Volume (m3)	2.95	5.23	7.82	8.34
	Length (m)	2.18	2.65	3.02	3.09
	Diameter (m)	1.31	1.59	1.81	1.85
	Feed Flow rate (kg/hr)	258	459	686	731
	Residence time (hr)	24	24	24	24
	MOC	Carbon Steel	Carbon Steel	Carbon Steel	Carbon Steel
MgO	Orientation	Vertical Tanks	Vertical Tanks	Vertical Tanks	Vertical Tanks
	Volume (m3)	2.16	3.83	5.75	6.13
	Length (m)	1.97	2.38	2.73	2.79
	Diameter (m)	1.18	1.43	1.64	1.67

	Feed Flow rate (kg/hr)	50.95	90.49	135.79	144.84
	Residence time (hr)	24	24	24	24
	MOC	Carbon Steel	Carbon Steel	Carbon Steel	Carbon Steel
CaCO3	Orientation	Horizontal Tanks	Horizontal Tanks	Horizontal Tanks	Horizontal Tanks
	Volume (m3)	0.76	1.57	1.43	2.15
	Length (m)	1.39	1.77	1.71	1.97
	Diameter (m)	0.83	1.06	1.03	1.18
	Feed Flow rate (kg/hr)	77.32	159.47	144.97	219.07
	Residence time (hr)	24	24	24	24
	MOC	Carbon Steel	Carbon Steel	Carbon Steel	Carbon Steel
Borax	Orientation	Horizontal tanks	Horizontal tanks	Horizontal tanks	Horizontal tanks
	Volume (m3)	0.63	1.12	1.67	1.79
	Length (m)	1.30	1.58	1.81	1.85
	Diameter (m)	0.78	0.95	1.09	1.11
	Feed Flow rate (kg/hr)	40.76	72.39	108.63	115.87
	Residence time (hr)	24	24	24	24
	MOC	Carbon Steel	Carbon Steel	Carbon Steel	Carbon Steel

7.2.5.4 *Agitator,mixer and press*

Mixer and Agitator			RN-PS	CR-PS	VP-PS	Combined
Mixer vessel	M-100	Orientation	Vertical	Vertical	Vertical	Vertical
		Volume (m3)	3.68	12.02	16.40	12.89
		Length (m)	2.35	3.49	3.87	3.57
		Diameter (m)	1.41	2.09	2.32	2.14
		Feed Flow rate (kg/hr)	2595.21	8479.50	11572.87	9097.47
		Residence time (hr)	2	2	2	2
		MOC	Stainless steel	Stainless steel	Stainless steel	Stainless steel
		Power (kW)	6.52	21.30	29.08	22.86
Press Machine			RN-PS	CR-PS	VP-PS	Combined
	Press-101	Type	Multi-layered	Multi-layered	Multi-layered	Multi-layered
		MOC	Stainless steel	Stainless steel	Stainless steel	Stainless steel
		Dimensions	2.7mx1.56mx0.1m	2.7mx1.56mx0.1m	2.7mx1.56mx0.1m	2.7mx1.56mx0.1m
		No of slots	10	10	10	10
		Service fluid	Hot oil	Hot oil		Hot oil
		Operating temperature C	180	90	25	90
		Mass flow (kg/hr)	56.3	43.3	0.0	66.9